USGS
science for a changing world

In cooperation with the Texas Department of Transportation

Potential for Bed-Material Entrainment in Selected Streams of the Edwards Plateau—Edwards, Kimble, and Real Counties, Texas, and Vicinity

Scientific Investigations Report 2008–5017
(TxDOT Research Report 0–4695–4)

U.S. Department of the Interior
U.S. Geological Survey

—Technical Report Documentation Page—

1. Report No. FHWA/TX–08/0–4695–4	2. Government Accession No.	3. Recipient's Catalog No.	
4. Title and Subtitle Potential for Bed-Material Entrainment in Selected Streams of the Edwards Plateau—Edwards, Kimble, and Real Counties, Texas, and Vicinity		5. Report Date June 2008 6. Performing Organization Code	
7. Author(s) Franklin T. Heitmuller and William H. Asquith		8. Performing Organization Report No. USGS SIR 2008–5017	
9. Performing Organization Name and Address U.S. Geological Survey Water Resources Division 8027 Exchange Drive Austin, Texas 78754		10. Work Unit No. (TRAIS) 11. Contract or Grant No. Project 0–4695	
12. Sponsoring Agency Name and Address Texas Department of Transportation Research and Technology Implementation Office P.O. Box 5080 Austin, Texas 78731		13. Type of Report and Period Covered Technical report on research from 2003 to 2008 14. Sponsoring Agency Code	
15. Supplementary Notes Project conducted in cooperation with the Texas Department of Transportation and the Federal Highway Administration.			
16. Abstract The Texas Department of Transportation spends considerable money for maintenance and replacement of low-water crossings of streams in the Edwards Plateau in Central Texas as a result of damages caused in part by the transport of cobble- and gravel-sized bed material. An investigation of the problem at low-water crossings was made by the U.S. Geological Survey in cooperation with the Texas Department of Transportation, and in collaboration with Texas Tech University, Lamar University, and the University of Houston. The bed-material entrainment problem for low-water crossings occurs at two spatial scales—watershed scale and channel-reach scale. First, the relative abundance and activity of cobble- and gravel-sized bed material along a given channel reach becomes greater with increasingly steeper watershed slopes. Second, the stresses required to mobilize bed material at a location can be attributed to reach-scale hydraulic factors, including channel geometry and particle size. The frequency of entrainment generally increases with downstream distance, as a result of decreasing particle size and increased flood magnitudes. An average of 1 year occurs between flows that initially entrain bed material as large as the median particle size, and an average of 1.5 years occurs between flows that completely entrain bed material as large as the median particle size. The Froude numbers associated with initial and complete entrainment of bed material up to the median particle size approximately are 0.40 and 0.45, respectively.			
17. Key Words Bed-material entrainment, Edwards Plateau, gravel transport, low-water crossings, Texas		18. Distribution Statement No restrictions. This document is available to the public through the National Technical Information Service, Springfield Virginia, 22161, www.ntis.gov	
19. Security Classif. (of report) Unclassified	20. Security Classif. (of this page) Unclassified	21. No. of pages 76	22. Price

Form DOT F 1700.7 (8-72) Reproduction of completed page authorized

Cover: Yates Crossing of the Llano River along Ranch Road 385 in Kimble County, Texas, following the November 2000 flood. Photo courtesy of the Texas Department of Transportation (TxDOT).

Potential for Bed-Material Entrainment in Selected Streams of the Edwards Plateau—Edwards, Kimble, and Real Counties, Texas, and Vicinity

By Franklin T. Heitmuller and William H. Asquith

In cooperation with the Texas Department of Transportation

Scientific Investigations Report 2008–5017
(TxDOT Research Report 0–4695–4)

U.S. Department of the Interior
U.S. Geological Survey

U.S. Department of the Interior
DIRK KEMPTHORNE, Secretary

U.S. Geological Survey
Mark D. Myers, Director

U.S. Geological Survey, Reston, Virginia: 2008

For product and ordering information:
World Wide Web: http://www.usgs.gov/pubprod
Telephone: 1-888-ASK-USGS

For more information on the USGS—the Federal source for science about the Earth, its natural and living resources, natural hazards, and the environment:
World Wide Web: http://www.usgs.gov
Telephone: 1-888-ASK-USGS

Suggested citation:
Heitmuller, F.T., and Asquith, W.H., 2008, Potential for bed-material entrainment in selected streams of the Edwards Plateau—Edwards, Kimble, and Real Counties, Texas, and vicinity: U.S. Geological Survey Scientific Investigations Report 2008–5017, 76 p.

Contents

Figures

Tables

Conversion Factors

Inch/Pound to SI

Multiply	By	To obtain
	Length	
foot (ft)	0.3048	meter (m)
mile (mi)	1.609	kilometer (km)
	Area	
square foot (ft^2)	0.09290	square meter (m^2)
square mile (mi^2)	2.590	square kilometer (km^2)
	Flow rate	
cubic foot per second (ft^3/s)	0.02832	cubic meter per second (m^3/s)
	Density	
pound per cubic foot (lb/ft^3)	16.02	kilogram per cubic meter (kg/m^3)
pound per cubic foot (lb/ft^3)	0.01602	gram per cubic centimeter (g/cm^3)

Temperature in degrees Celsius (°C) may be converted to degrees Fahrenheit (°F) as follows:

$°F=(1.8×°C)+32$

Vertical coordinate information is referenced to the North American Vertical Datum of 1988 (NAVD 88).

Horizontal coordinate information is referenced to the North American Datum of 1983 (NAD 83).

SI to Inch/Pound

Multiply	By	To obtain
	Length	
centimeter (cm)	0.3937	inch (in.)
millimeter (mm)	0.03937	inch (in.)
meter (m)	3.281	foot (ft)
kilometer (km)	0.6214	mile (mi)
	Area	
square kilometer (km^2)	247.1	acre
square meter (m^2)	10.76	square foot (ft^2)
square kilometer (km^2)	0.3861	square mile (mi^2)
	Flow rate	
cubic meter per second (m^3/s)	70.07	acre-foot per day (acre-ft/d)
meter per second (m/s)	3.281	foot per second (ft/s)
cubic meter per second (m^3/s)	35.31	cubic foot per second (ft^3/s)
cubic meter per second (m^3/s)	22.83	million gallons per day (Mgal/d)
	Force	
newton (N) ($(kg×m)/s^2$)	0.225	pound (lb)

Blank Page

Potential for Bed-Material Entrainment in Selected Streams of the Edwards Plateau—Edwards, Kimble, and Real Counties, Texas, and Vicinity

By Franklin T. Heitmuller and William H. Asquith

Abstract

The Texas Department of Transportation spends considerable money for maintenance and replacement of low-water crossings of streams in the Edwards Plateau in Central Texas as a result of damages caused in part by the transport of cobble- and gravel-sized bed material. An investigation of the problem at low-water crossings was made by the U.S. Geological Survey in cooperation with the Texas Department of Transportation, and in collaboration with Texas Tech University, Lamar University, and the University of Houston. The bed-material entrainment problem for low-water crossings occurs at two spatial scales—watershed scale and channel-reach scale. First, the relative abundance and activity of cobble- and gravel-sized bed material along a given channel reach becomes greater with increasingly steeper watershed slopes. Second, the stresses required to mobilize bed material at a location can be attributed to reach-scale hydraulic factors, including channel geometry and particle size. The frequency of entrainment generally increases with downstream distance, as a result of decreasing particle size and increased flood magnitudes. An average of 1 year occurs between flows that initially entrain bed material as large as the median particle size, and an average of 1.5 years occurs between flows that completely entrain bed material as large as the median particle size. The Froude numbers associated with initial and complete entrainment of bed material up to the median particle size approximately are 0.40 and 0.45, respectively.

Introduction

The Texas Department of Transportation (TxDOT) commonly builds and maintains low-water crossings (LWCs) over streams (fig. 1) in the Edwards Plateau in Central Texas. LWCs are low-height structures, typically constructed of concrete and asphalt, that provide acceptable passage over seasonal rivers or streams with relatively low normal-depth flow and are designed to accommodate high-flow events by roadway overtopping. The streams of the Edwards Plateau are characterized by cobble- and gravel-sized bed material and highly variable flow regimes. Low base-flow conditions occurring most of the time occasionally are interrupted by severe floods. The floods entrain and transport substantial loads of bed material in the stream channels (Baker, 1977). As a result, LWCs in the Edwards Plateau are bombarded and abraded by bed material during high-flow events and periodically must be maintained or even replaced.

TxDOT spends considerable money for maintenance and replacement of LWCs on relatively low-traffic-volume highways in the Edwards Plateau. Based on a review of selected TxDOT internal budget reports in San Angelo, Texas, in 2004, on average as much as $1 million per year is spent on maintenance and repair of LWCs. TxDOT commonly must reconstruct LWCs because of site-specific constraints against bridging the stream, which might be the optimum solution. As a compromise for maintenance and repair, some LWCs are constructed more elaborately than others. Structural failure or maintenance of LWCs as a result of high-flow-induced bed-material transport has occurred as recently as the November

Figure 1. Flatrock Crossing of the South Llano River in Kimble County, Texas.

2000, July 2002, June 2004, and March 2007 floods on the Edwards Plateau.

This research study, done by the U.S. Geological Survey (USGS), in cooperation with TxDOT, and in collaboration with Texas Tech University, Lamar University, and the University of Houston, was designed to quantify the potential for bed-material entrainment in selected streams in the Edwards Plateau as part of TxDOT Research Project 0–4695: Guidance for Design in Areas of Extreme Bed-Load Mobility. The study included Geographic Information System (GIS) analyses, flood-frequency analyses, field investigations, and computations of bed-material entrainment. The results of the current (2008) study are expected to complement numerical and physical modeling of bed-material mobility done by Texas Tech University, Lamar University, and the University of Houston, and to facilitate LWC design and assignation of risk to channel reaches subject to bed-material mobility.

Purpose and Scope

The purpose of this report is to assess the potential for bed-material entrainment in selected streams of the Edwards Plateau in a study area comprising Edwards, Kimble, and Real Counties and vicinity. The methods used to address bed-material entrainment in the report are (1) GIS analyses of drainage area and slopes, (2) partial-duration flood-frequency analyses, (3) site reconnaissance, and (4) field surveys of channel geometry and bed-material particle size. Using data generated by these methods, computations of bed-material entrainment are given for selected sites, and the results are generalized for the study area.

Description of Study Area

The study area for this report comprises Edwards, Kimble, and Real Counties and some parts of adjacent counties in south-central Texas (fig. 2); however, the bed-material entrainment problem in the LWC context extends to other counties in the Edwards Plateau. An investigation of the potential for cobble- and gravel-bed entrainment could be focused anywhere in the Edwards Plateau, but the research team, in conjunction with TxDOT personnel involved in the project, decided on the three counties. The three-county study area contains a number of streams appropriate for bed-material entrainment research, including the Llano River, Frio River, Nueces River, and tributaries. The streams originate in relatively western and southern parts of the Edwards Plateau, an elevated lower-Cretaceous limestone and dolomite tableland. The streams in the study area are incised into the plateau, resulting in the removal of considerable amounts of lower-Cretaceous carbonate rock. Much of this material has been transported downstream toward the Gulf of Mexico, but large quantities remain and some of this material occurs as valley fill and bed material in the streams of the plateau.

The history of sediment transport and sedimentation in the Edwards Plateau is important to understanding the contemporary rates and processes of bed-material entrainment in the study area. Blum and Valastro (1989, 1992), Blum and others (1994), and Mear (1995) document episodes of fluvial geomorphic development and sedimentation in the Edwards Plateau for the last 20,000 years.

In summary, flood regimes were more moderate and frequent during the last glacial maximum (about 20,000 to 14,000 years ago), and soil formation in the uplands was accompanied by lateral migration of stream channels and storage of sediment in floodplains. The end of the Pleistocene Epoch (about 14,000 to 10,500 years ago) was characterized by less humid conditions. Streams removed sediment from valleys, became incised into bedrock, and caused upland soil erosion (Cooke and others, 2003). Complete upland soil erosion and an episode of valley widening and gradual aggradation occurred during the early- to middle-Holocene Epoch (about 10,500 to 5,000 years ago). The period from about 5,000 to 2,500 years ago was characterized by the driest conditions across the Edwards Plateau during the last 20,000 years. The supply of sediment exceeded the capacity of streams to transport the material, and a decrease in floods resulted in relatively little floodplain activity. More humid conditions and frequent floods characterized the period from about 2,500 to 1,000 years ago. Broad, shallow stream channels continued to fill with coarse sediment during this period. Finally, conditions during the last 1,000 years have been comparatively dry, but are punctuated by extreme floods. Stream channels are incised into the alluvium, and older floodplains are abandoned and stranded as inactive terrace deposits.

The present study area is in a climatic transition area between semiarid conditions in the west and subhumid conditions in the east (Larkin and Bomar, 1983). More importantly for bed-material entrainment, however, is that the study area is characterized by a high flash-flood potential (Beard, 1975; Caran and Baker, 1986).

Flash floods in the Edwards Plateau are generated by diverse climatic mechanisms. Convergent low-pressure troughs or cut-off systems have the potential to intercept moist air masses from either the Pacific Ocean to the southwest or the Gulf of Mexico to the southeast. Additionally, tropical disturbances and hurricanes from the Gulf of Mexico can result in widespread, intense rainfall. As a result of steep slopes and shallow soils incapable of absorbing much rainfall, streams in the study area rapidly respond to intense rainfall, and flash floods are common.

The study area is mostly rural ranchland that supports hunting leases and limited grazing. The absence of thick upland soils constrains minor irrigated agriculture to wide valley reaches. Vegetation is characterized by oak and juniper woods in the uplands and open to wooded groves of mesquite, oak, pecan, cypress, and cottonwood trees in the river valleys. Steep slopes are common throughout the study area, especially along the walls adjacent to alluvial valleys.

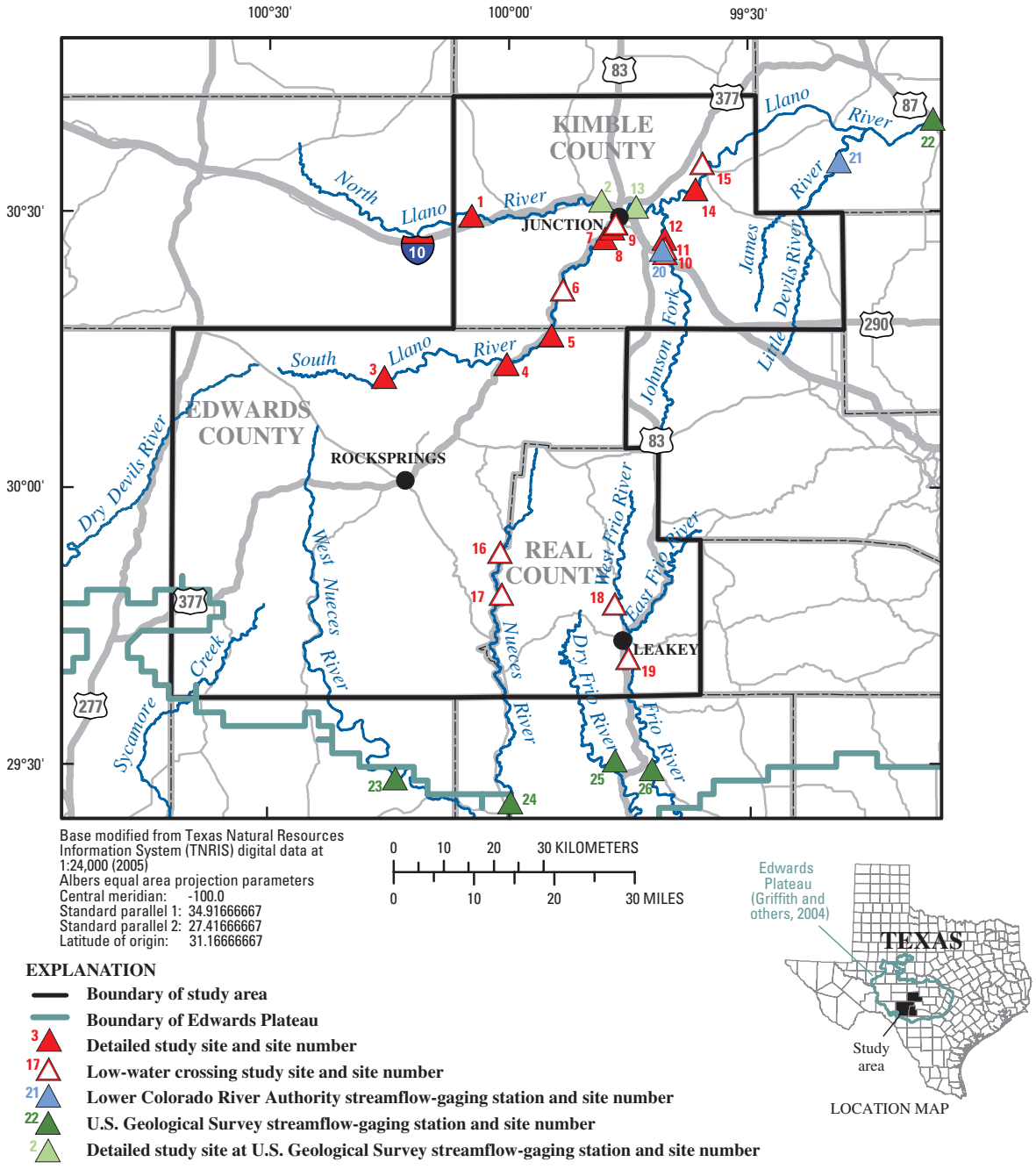

Site number (table 1)	Site name
1	North Llano River near Roosevelt
2	08148500 North Llano River near Junction
3	South Llano River at Baker Ranch
4	South Llano River at U.S. Highway 377 near Rocksprings
5	South Llano River at 700 Springs Ranch
6	South Llano River at First Crossing
7	South Llano River at South Llano River State Park
8	South Llano River at Texas Tech University–Junction
9	South Llano River at Flatrock Crossing
10	Johnson Fork at Guzman Crossing
11	Johnson Fork at Paks Crossing
12	Johnson Fork at Lowlands Crossing
13	08150000 Llano River near Junction
14	Llano River near Ivy Chapel
15	Llano River at Yates Crossing
16	Nueces River at Ben Williams Crossing
17	Nueces River at Vance Crossing
18	Cedar Creek at Ranch Road 336
19	Frio River at Upper Ranch Road 1120 Crossing
20	Johnson Fork near Junction
21	James River near Mason
22	08150700 Llano River near Mason
23	08190500 West Nueces River near Brackettville
24	08190000 Nueces River at Laguna
25	08196000 Dry Frio River near Reagan Wells
26	08195000 Frio River at Concan

Figure 2. Location of study area—Edwards, Kimble, and Real Counties, Texas, and vicinity.

Only one small reservoir is located in the study area and occurs on the South Llano River, in Junction. Although both floods and base flows spill over the top of the control structure, the impoundment effectively traps coarse bed material. The ubiquitous presence of cobble and gravel bars just downstream, however, shows that the North Llano River supplies sufficient sediment to the main-stem Llano River.

The study sites (fig. 2) primarily were chosen to characterize downstream changes in channel geometry and bed-entrainment potential, contrasting with an alternative approach to compare separate drainage basins. For this reason, all detailed study sites are in the Llano River Basin, chosen because most of the problematic LWCs identified by TxDOT personnel are located there. A summary of the study sites is provided:

- South Llano River at Baker Ranch (site 3) represents an ephemeral, upper headwater channel. The channel occurs in relatively fine-grained valley fill and is a sequence of water-filled pools that connect during storms that produce runoff.
- South Llano River at U.S. Highway 377 near Rocksprings (site 4) is a larger, bedrock, ephemeral channel just downstream from the incision point into the plateau.
- South Llano River at 700 Springs Ranch (site 5) and North Llano River near Roosevelt (site 1) represent channels with mixed bedrock and cobble and gravel beds, each having disconnected floodplain units between the channel and valley wall.
- South Llano River at South Llano River State Park (site 7) and at Texas Tech University–Junction (site 8) have a meandering channel within a Holocene floodplain containing lenses of cobble- and gravel-sized material wedged between relatively fine-grained sediment. The Holocene floodplain occurs within a larger, elevated late Pleistocene or early Holocene terrace containing cobble- and gravel-sized material, commonly cemented by calcite near the surface.
- North Llano River near Junction (site 2) is relatively straight and has a cobble and gravel bed. The channel is closely bounded by the late Pleistocene or early Holocene terrace, with a few areas of recent floodplain deposits.
- Johnson Fork at Lowlands Crossing (site 12) is similar to North Llano River near Junction (site 2), except the meander bends are enlarged as a result of Holocene hydrologic change and contemporary decreased rates of lateral migration (Blum and Valastro, 1989).
- Llano River near Junction (site 13) and near Ivy Chapel (site 14) also have enlarged meanders and gradual transitions between the older terrace deposits and modern floodplain units.

Additional study sites shown in figure 2 were not surveyed in detail and are not used in computations of bed-material entrainment. A summary of these sites is provided:

- Nueces River at Ben Williams Crossing (site 16) and at Vance Crossing (site 17) is a cobble- and gravel-choked meandering channel within Holocene floodplain units between the channel and valley wall. Cedar Creek at Ranch Road 336 (site 18) is similar to the Nueces River but at a smaller scale.
- Frio River at the Upper Ranch Road 1120 Crossing (site 19) is a meandering, cypress-tree-lined, cobble- to gravel-bed channel within a Holocene floodplain.
- South Llano River at First Crossing (site 6), South Llano River at Flatrock Crossing (site 9), Johnson Fork at Guzman Crossing (site 10), Johnson Fork at Paks Crossing (site 11), and Llano River at Yates Crossing (site 15) only were visited to document and inspect the LWC structure.

Review of Existing Data

The topic of bed-material entrainment and bedload transport of gravel-bed streams has received considerable attention. Heitmuller and others (2005), an earlier product of TxDOT research project 0–4695, serves as a literature review for this project. The literature associated with sediment transport in gravel-bed streams and application of theory to stream management is extensive, global, and multidisciplinary. Investigations focus on data derived from natural channels or experimental flumes, and approaches vary from deterministic to empirical. A variety of methods are used to study gravel-bed stream characteristics, including surveying channel geometry, particle tracking, bed-material and bedload sampling, and developing sediment-discharge rating curves, among others. Regardless of the method implemented to understand the sediment regime of gravel-bed streams, a thorough knowledge of watershed characteristics, local processes controlling the transport, and collection of data characterizing sediment mobility are essential for the success of any management practice. Heitmuller and others (2005) conclude that an investigation of bed-material mobility needs to include robust geographic, field, and laboratory assessments. For other studies on bed-material entrainment, refer to Gustavson (1978) and Elliott (2002).

Acknowledgments

The authors acknowledge the following colleagues of TxDOT for their considerable professional and technical support of this work and their critical feedback on study direction: The authors also thank Julia Brown (0–4695 Program Coordinator, 2007–2008), Lewis Nowlin (0–4695 Project Director, 2007–2008), George R. Herrmann (0–4695 Project Advisor), and Walter McCullough (0–4695 Project Advisor), and others.

Table 1. List of study sites and estimates of drainage area and slope of site-specific watersheds in the study area, Edwards, Kimble, and Real Counties, Texas, and vicinity.

[Drainage area and slope estimates were derived from a Geographic Information System; mi^2, square miles; km^2, square kilometers; LCRA, Lower Colorado River Authority; --, not computed]

Study site number (fig. 2)	Study site identifier or USGS station number and identifier	Purpose of site for bed-entrainment project[1]	Drainage area [km^2 (mi^2)]	Mean and standard deviation of watershed slope (percent)
1	North Llano River near Roosevelt	Survey	1,145 (442)	4.06; 3.87
2	08148500 North Llano River near Junction	Flood frequency and survey	2,335 (902)	5.35; 5.78
3	South Llano River at Baker Ranch	Survey	417 (161)	2.63; 1.92
4	South Llano River at U.S. Highway 377 near Rocksprings	Survey	1,134 (438)	3.88; 3.33
5	South Llano River at 700 Springs Ranch	Survey	1,352 (522)	4.46; 4.19
6	South Llano River at First Crossing	Low-water crossing survey	2,040 (788)	4.95; 4.76
7	South Llano River at South Llano River State Park	Survey	2,256 (871)	5.36; 5.50
8	South Llano River at Texas Tech University–Junction	Survey	2,271 (877)	5.41; 5.64
9	South Llano River at Flatrock Crossing	Low-water crossing survey	2,279 (880)	5.45; 5.72
20	Johnson Fork near Junction (LCRA)	Flood frequency	758 (293)	--;--
10	Johnson Fork at Guzman Crossing	Qualitative channel-bed observation only[2]	-- (--)	--;--
11	Johnson Fork at Paks Crossing	Qualitative channel-bed observation only[2]	-- (--)	--;--
12	Johnson Fork at Lowlands Crossing	Survey	778 (300)	5.30; 5.82
13	08150000 Llano River near Junction	Flood frequency and survey	4,815 (1,859)	5.50; 5.98
14	Llano River near Ivy Chapel	Survey	5,939 (2,293)	5.68; 6.38
15	Llano River at Yates Crossing	Low-water crossing survey	6,078 (2,347)	5.74; 6.47
22	08150700 Llano River near Mason	Flood frequency	8,410 (3,247)	--;--
21	James River near Mason (LCRA)	Flood frequency	845 (326)	--;--
16	Nueces River at Ben Williams Crossing	Qualitative channel-bed observation only	578 (223)	15.3; 13.3
17	Nueces River at Vance Crossing	Qualitative channel-bed observation only	642 (248)	16.4; 14.2
24	08190000 Nueces River at Laguna	Flood frequency	1,908 (737)	--;--
23	08190500 West Nueces River near Brackettville	Flood frequency	1,800 (695)	--;--
18	Cedar Creek at Ranch Road 336 Crossing	Qualitative channel-bed observation only	30.5 (11.8)	31.4; 18.6
19	Frio River at Upper Ranch Road 1120 Crossing	Qualitative channel-bed observation only	620 (239)	19.8; 17.1
26	08195000 Frio River at Concan	Flood frequency	1,009 (390)	--;--
25	08196000 Dry Frio River near Reagan Wells	Flood frequency	327 (126)	--;--

[1] Surveys include cross-sectional channel geometry and bed-material particle-size analyses. Low-water crossing surveys include only cross-sectional depictions of the roadway surface. Flood-frequency analyses were made at sites with gaging stations. Qualitative channel-bed observations were made at sites to assess bed-material abundance and activity.

[2] These sites were not included in bed-material abundance and activity analyses, because of proximity to Johnson Fork at Lowlands Crossing, which was used.

The authors are indebted to our research colleagues Theodore G. Cleveland (University of Houston), Xing Fang (Lamar University), David B. Thompson (Texas Tech University), and Keh-Han Wang (University of Houston) for their collaboration. Additionally, the authors recognize Kyle E. Juracek (USGS) for helpful reviews. Finally, we thank those who provided access to public and private properties in the study area, without which the work would not have been possible.

Methods

The methods used to obtain data necessary for computation of bed-material entrainment potential can be categorized under four headings: (1) GIS analyses, (2) flood-frequency analyses, (3) site reconnaissance, and (4) field surveys. Multiple sites for data collection are included in the study (fig. 2; table 1), and the specific methods used at each individual site varied. GIS mapping software was used to delineate watersheds, determine drainage areas, and model watershed and channel slopes. Partial-duration flood-frequency analyses were done to estimate the return period of floods for USGS and Lower Colorado River Authority (LCRA) gaging stations in the study area. Regional regression equations were used to estimate flood frequency at ungaged study sites (Asquith and Slade, 2007). Site reconnaissance was done with assistance from TxDOT personnel knowledgeable about the locations of sites with extreme bed-material mobility and damage to transportation infrastructure. Finally, field surveys were designed to obtain the parameters needed to apply equations to compute bed-material entrainment potential. Field surveys included measurements of channel geometry, LWC geometry, and bed-material particle sizes.

GIS Analysis

Watersheds

Watersheds are important when accounting for factors that contribute to surface-water hydraulics or sediment transport at spatial scales greater than the channel reach. Watersheds were delineated for all sites in the study area using ESRI ArcGIS 9.1 (Maidment, 2002). Before GIS analysis, 10-meter digital elevation models (DEMs) of the study area were downloaded from the USGS Seamless Data Distribution System (U.S. Geological Survey, 2005). Using GIS, the individual DEM panels were tiled into one raster dataset. The DEM mosaic subsequently was adjusted for sinks to ensure that the model would have continuous flow from higher to lower elevations appropriate for dendritic drainage networks. Next, the filled DEM was processed into flow-direction and flow-accumulation raster datasets. Pour points at study sites were located on the flow-accumulation raster dataset, and watersheds were constructed using the flow-direction raster dataset. Finally, individual watershed raster datasets were converted to vector polygon feature classes, reprojected from a geographic coordinate system to the Albers equal area coordinate system, and drainage areas (table 1) were computed.

Watershed and Channel Slopes

Mean watershed slope, determined by DEM-analysis and defined here as the average of all land-surface slopes in a drainage basin regardless of directional orientation, is considered an important parameter for understanding the potential for sediment delivery to stream channels in the study area. Theoretically, for watersheds of similar size, shape, and land-cover characteristics, greater mean watershed slopes will promote increased rates of hillslope erosion and subsequent delivery of sediment to channel networks. For the purpose of this investigation, mean watershed slope acts as a surrogate for the variety of processes occurring at spatial scales larger than the channel reach. Mean watershed slope was computed using GIS. The previously mentioned 10-meter DEM mosaic was used to generate a percentage-slope raster dataset. The percentage-slope raster dataset subsequently was reprojected from a geographic coordinate system to the Albers coordinate system. Using watershed polygons, zonal statistics were applied in GIS to calculate mean watershed slope (table 1) from the percentage-slope raster dataset.

Visualization of the distribution of channel slopes (conceptually distinct from mean watershed slope) is an important tool for TxDOT engineers and other practitioners operating at watershed and channel-reach scales. For this reason, channel slopes were mapped in the study area using GIS. First, high-resolution hydrography data for subbasins in the study area were downloaded from the USGS National Hydrography Dataset (NHD) (U.S. Geological Survey, 2006). Hydrography data were reprojected from a geographic coordinate system to the Albers coordinate system. Mean channel slopes were assigned to individual flowline segments using zonal statistics applied to the aforementioned percentage-slope raster dataset. Visualization is maximized because NHD flowline data originally are divided into small vector lengths. The final maps for NHD subbasins in the study area are presented in figures 3 through 10.

An alternative method for visualization of channel slope is through the creation of longitudinal profiles. A longitudinal profile is a graph of channel-bed elevation with downstream distance and is limited to one channel. Longitudinal profiles can be used to (1) estimate channel slope for reaches that were not surveyed in the field or (2) locate relatively steep channel reaches where greater energy conditions exist for sediment entrainment and transport. Longitudinal profiles for selected streams in the study area were created using GIS. Individual channel reaches, beginning at the headwaters, were selected by feature name from NHD high-resolution datasets of subbasins in the study area and were merged into one continuous line segment. The channel-reach line segment was converted to a three-dimensional (3-D) feature class using the filled 10-meter DEM mosaic. Next, the 3-D channel-reach feature class was converted to a route feature class that stores downstream

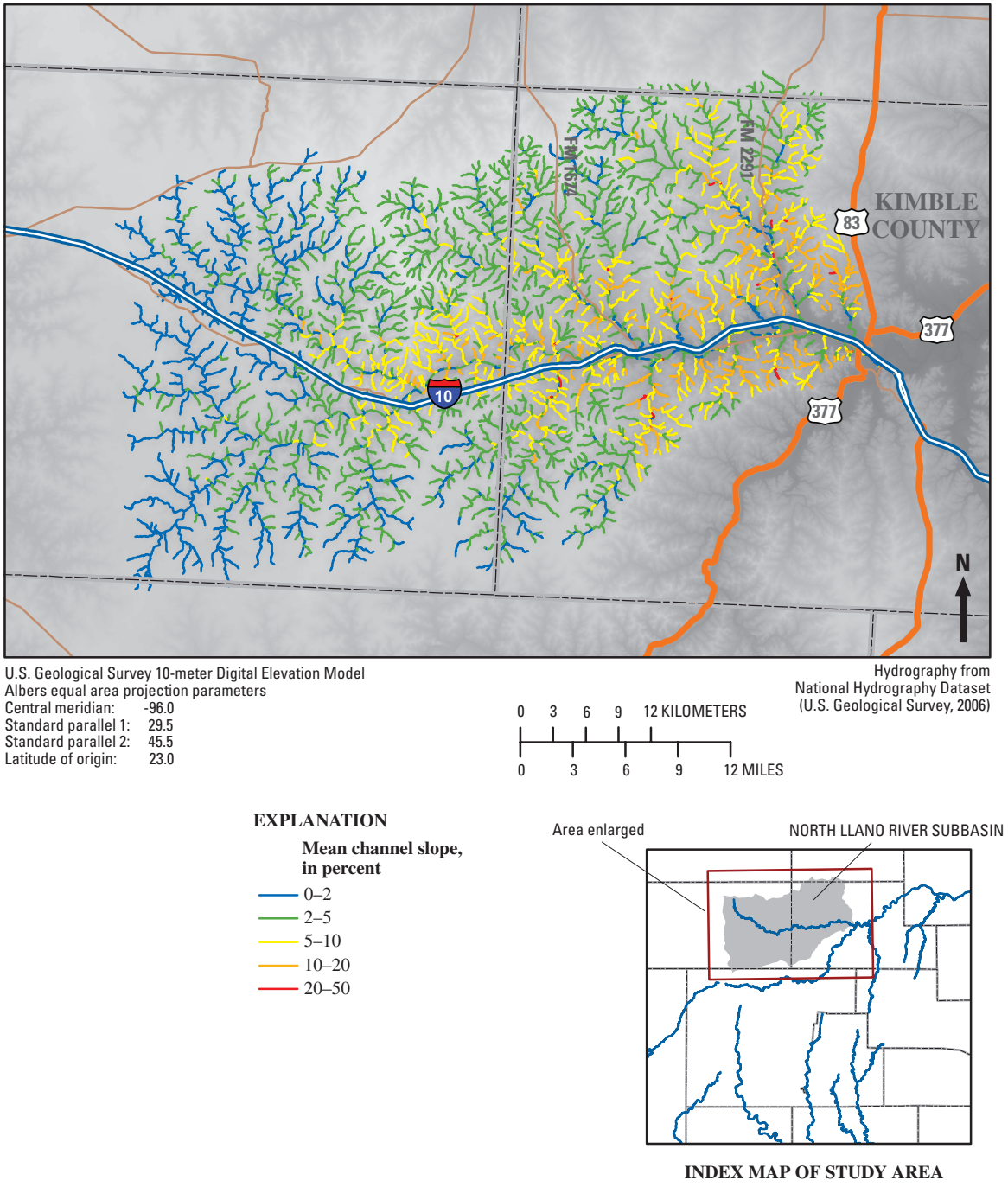

Figure 3. Channel slope of the North Llano River Subbasin, Kimble County, Texas, and vicinity.

distance. The route feature class line segment was converted into equidistant points separated by 500 meters of downstream distance, and the points were used to extract downstream distance from the route feature class. Finally, elevations were extracted to the points using the filled 10-meter DEM. Some points were selectively removed if discrepancies in the DEM caused downstream elevations to be higher than upstream elevations. Longitudinal profiles are presented in figures 11 through 23.

Flood-Frequency Analysis

The potential for bed-material entrainment can be computed for a site using GIS- and field-collected data. However, the only way to estimate the temporal frequency of bed-material entrainment is through association with flood frequency. For this reason, partial-duration flood-frequency analyses were done for USGS and LCRA gaging stations in the study area (table 2). The partial-duration series uses discharges

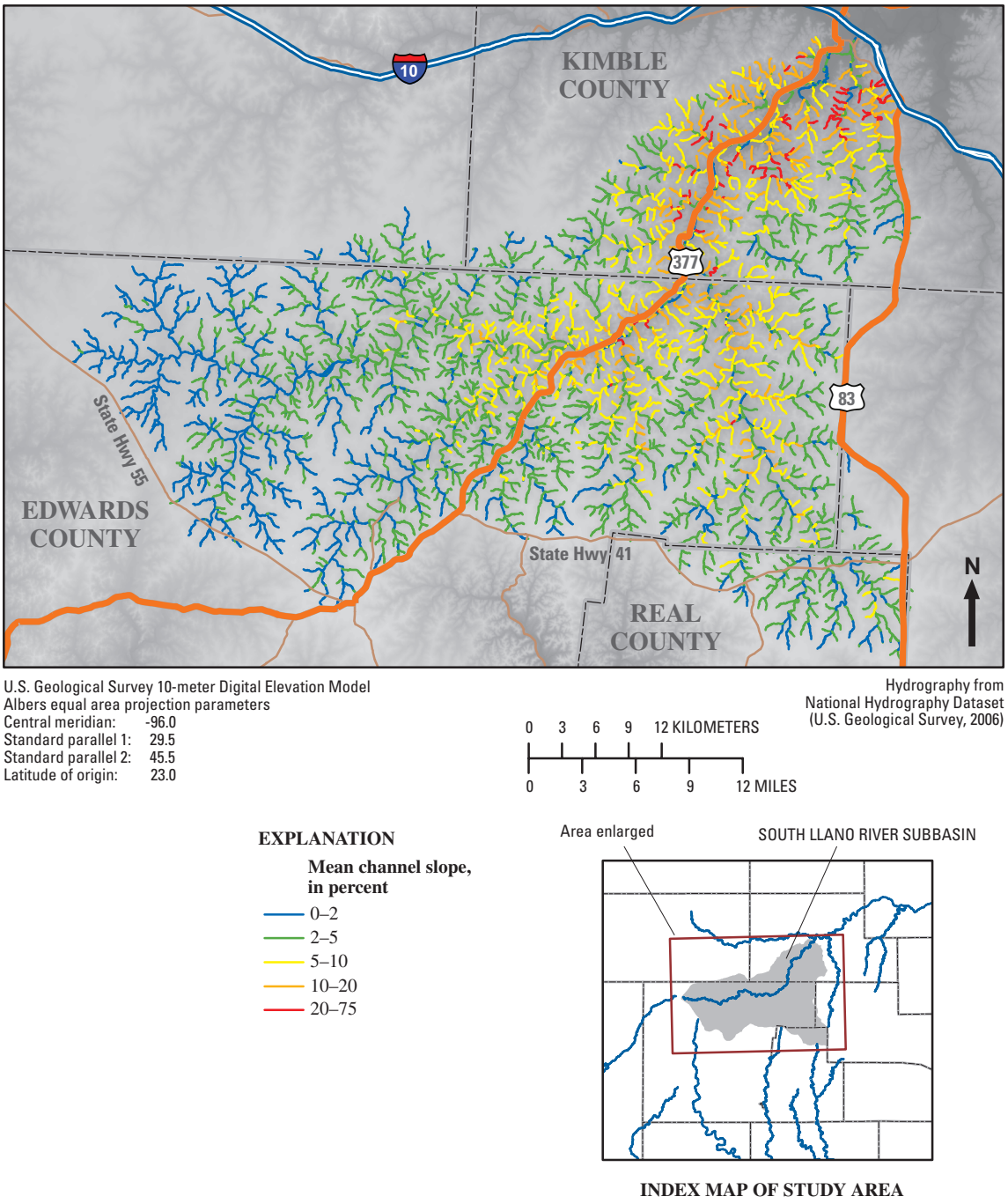

Figure 4. Channel slope of the South Llano River Subbasin, Edwards, Kimble, and Real Counties, Texas, and vicinity.

of measured and estimated flood peaks above a designated threshold (referred to as the base discharge).

Partial-duration series are preferred over annual-maximum series to estimate flood frequency of relatively small or moderate events (1- to 10-year return period) or for gaging stations with a relatively short period of record (Soong and others, 2004). This advantage is particularly important to estimate the frequency of bed-material entrainment, because sediment commonly is mobilized by moderate events, even those below bankfull stage. Additionally, the episodic nature of floods in the study area causes the annual-maximum series to have low outliers for dry years, whereas the partial-duration series avoids low outliers.

Base discharges for USGS gaging stations are published in annual water-data reports; for example U.S. Geological Survey (2007). Some published base discharges have either increased or decreased over time. As a result, some early-record peaks above base are missing for gaging stations with

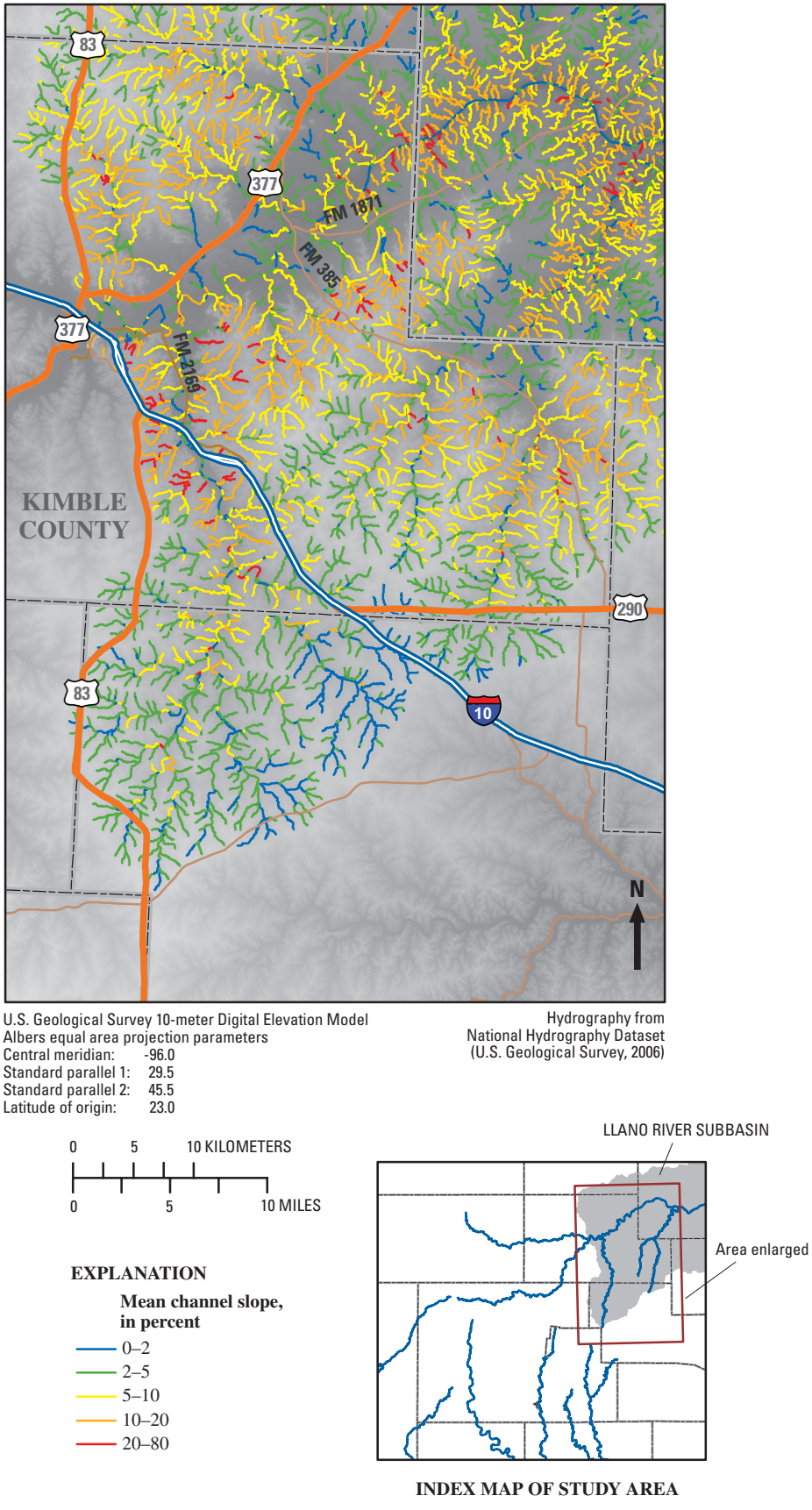

Figure 5. Channel slope of the Llano River Subbasin, Kimble County, Texas, and vicinity.

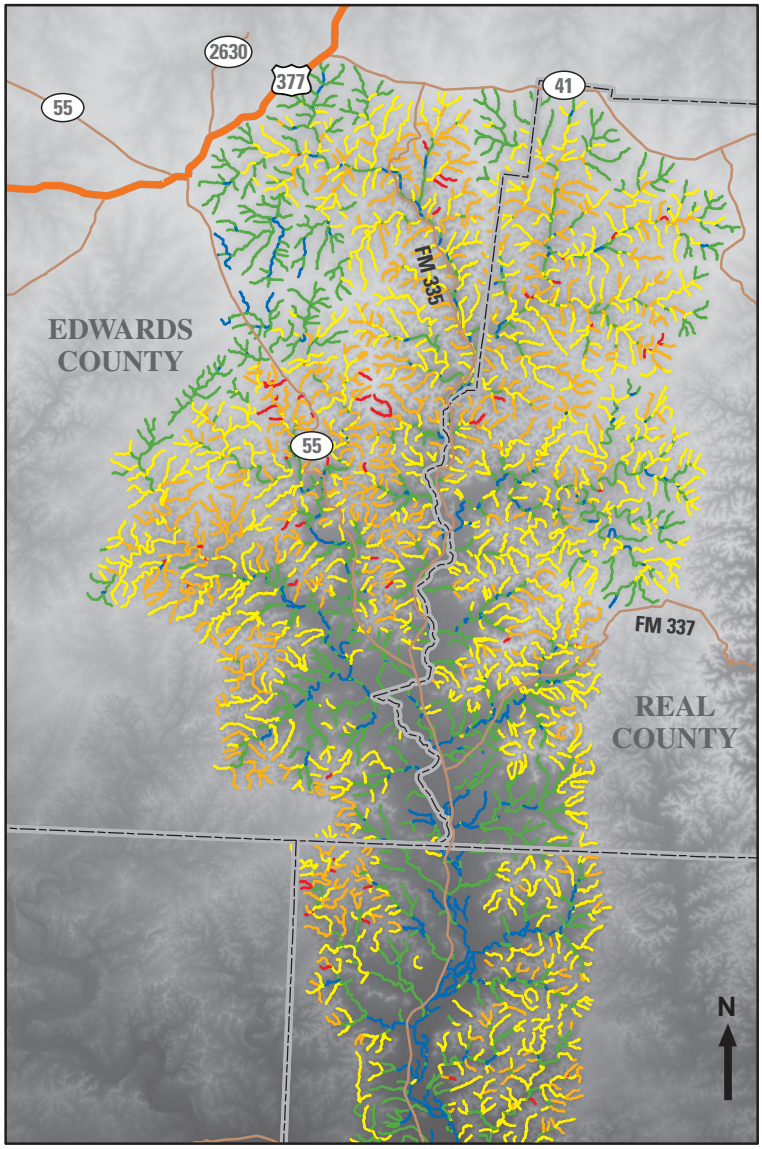

Figure 6. Channel slope of the Nueces Headwaters Subbasin, Edwards and Real Counties, Texas, and vicinity.

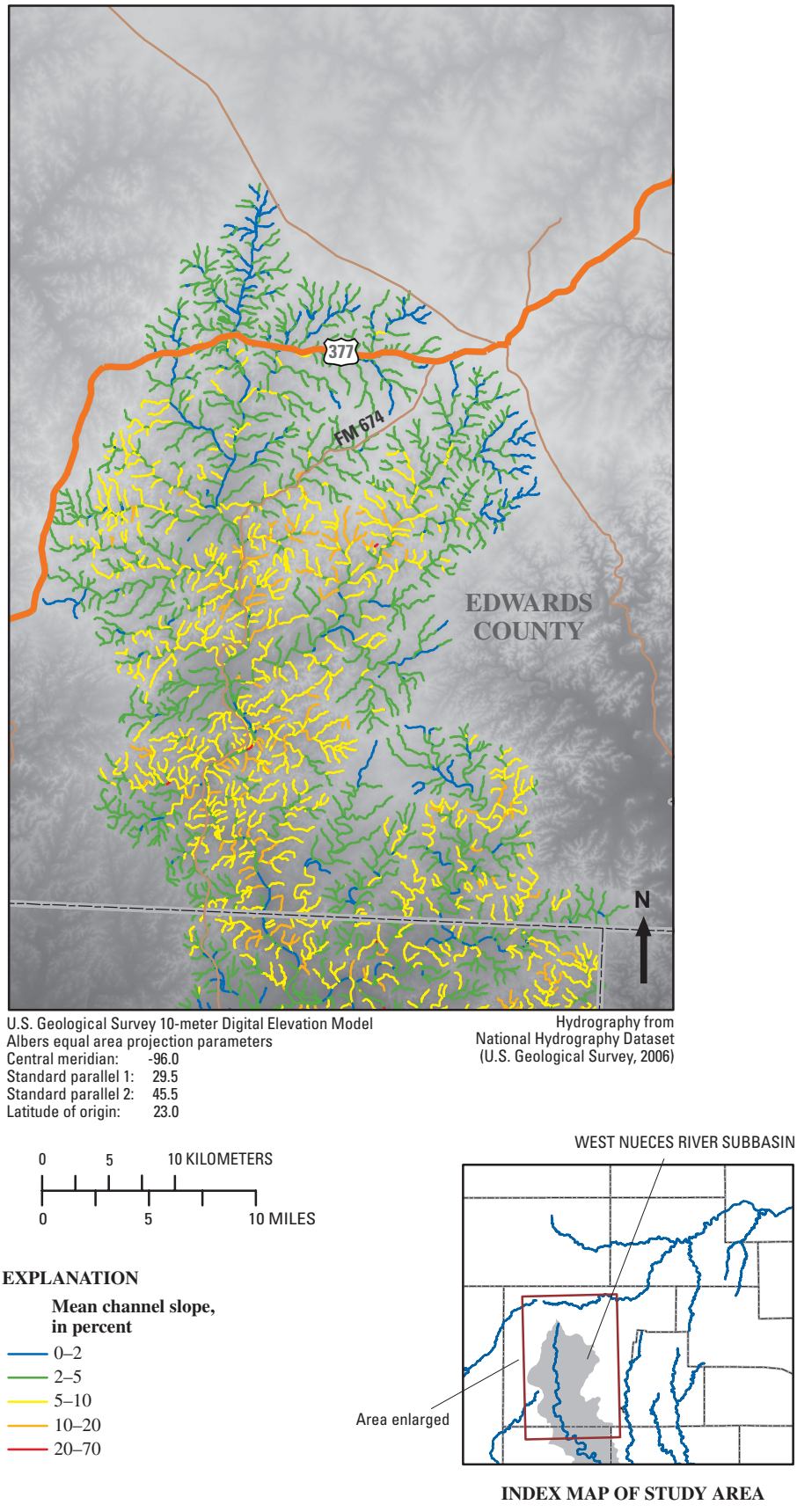

Figure 7. Channel slope of the West Nueces River Subbasin, Edwards County, Texas, and vicinity.

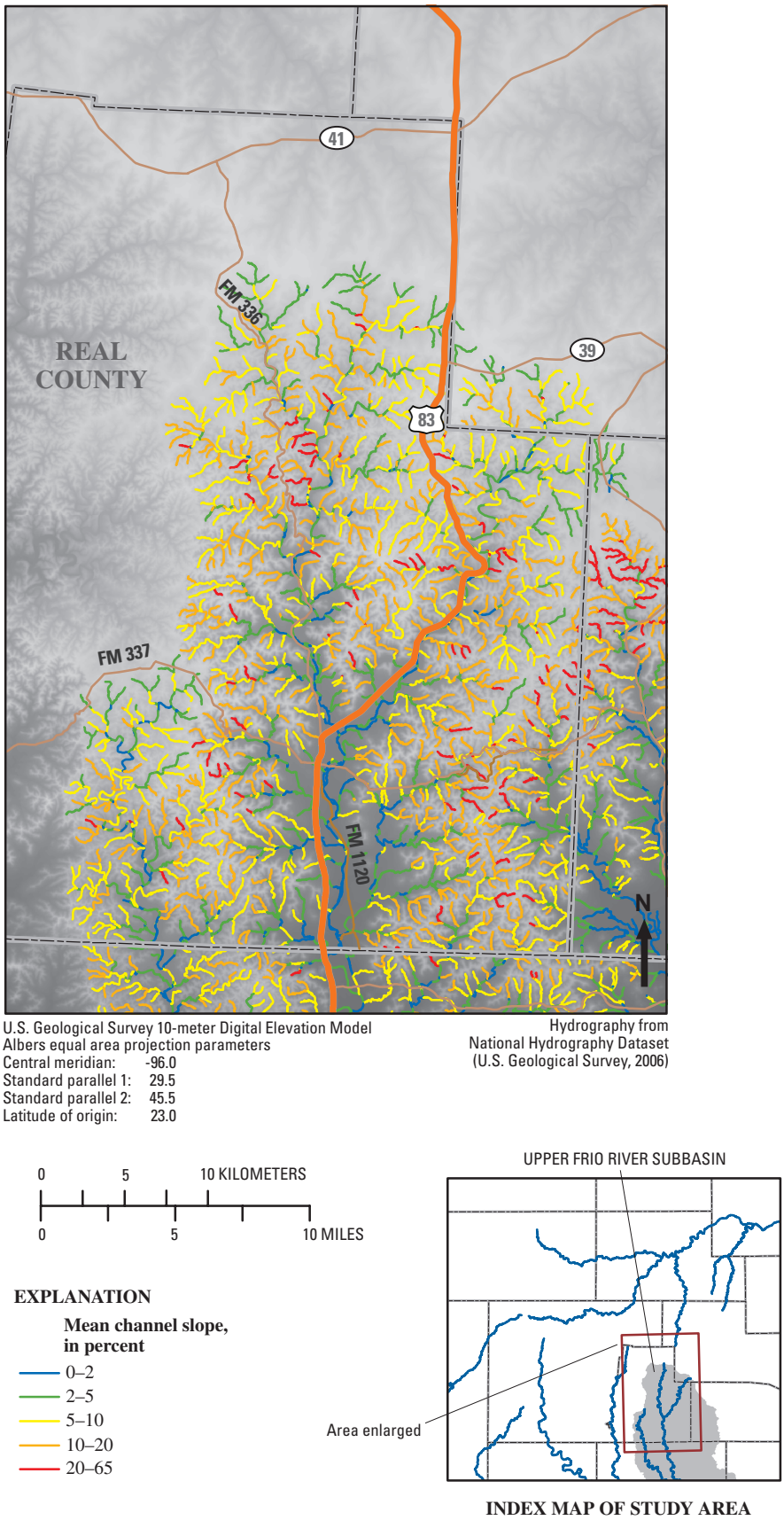

Figure 8. Channel slope of the upper Frio River Subbasin, Real County, Texas, and vicinity.

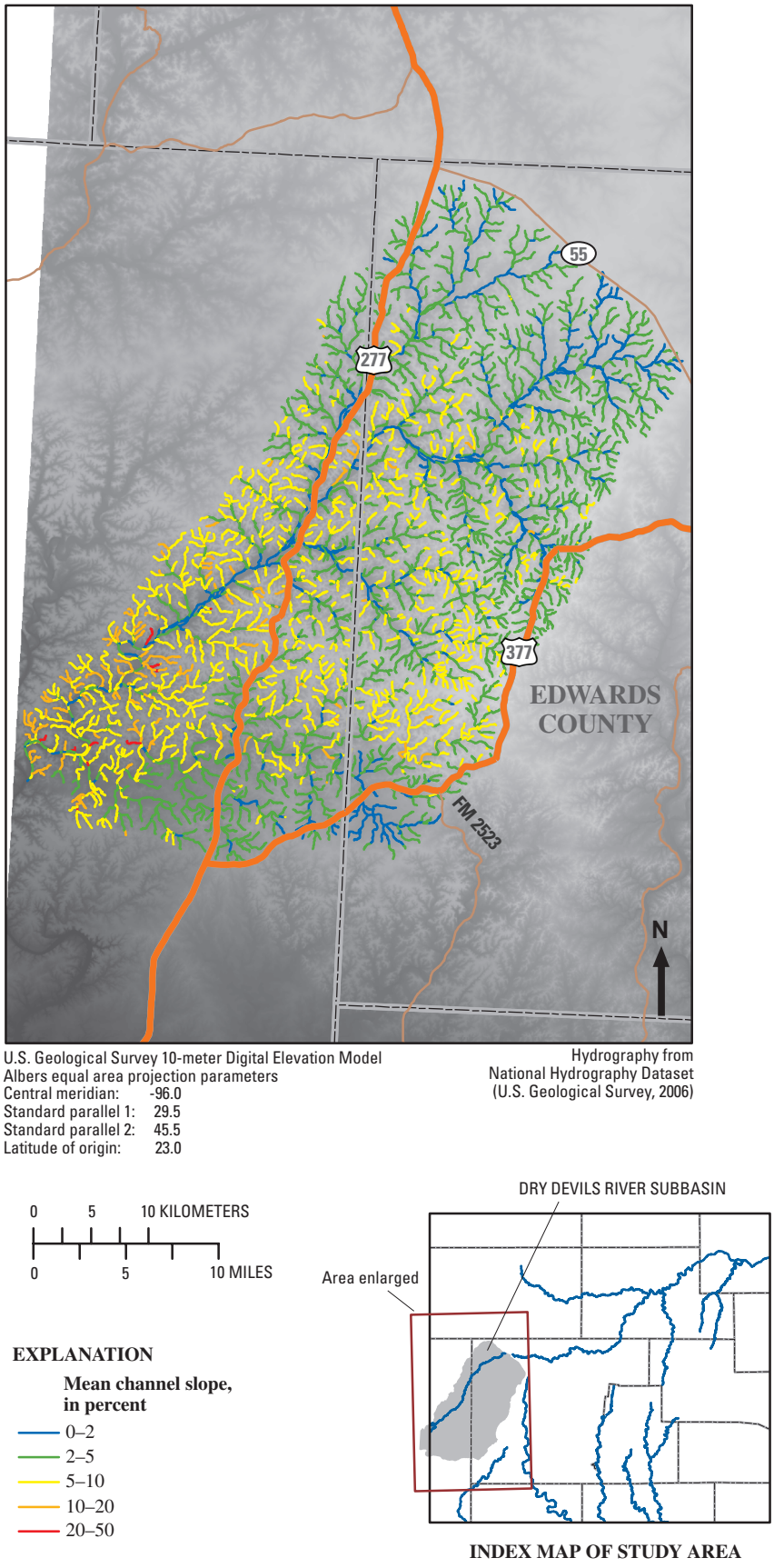

Figure 9. Channel slope of the Dry Devils River Subbasin, Edwards County, Texas, and vicinity.

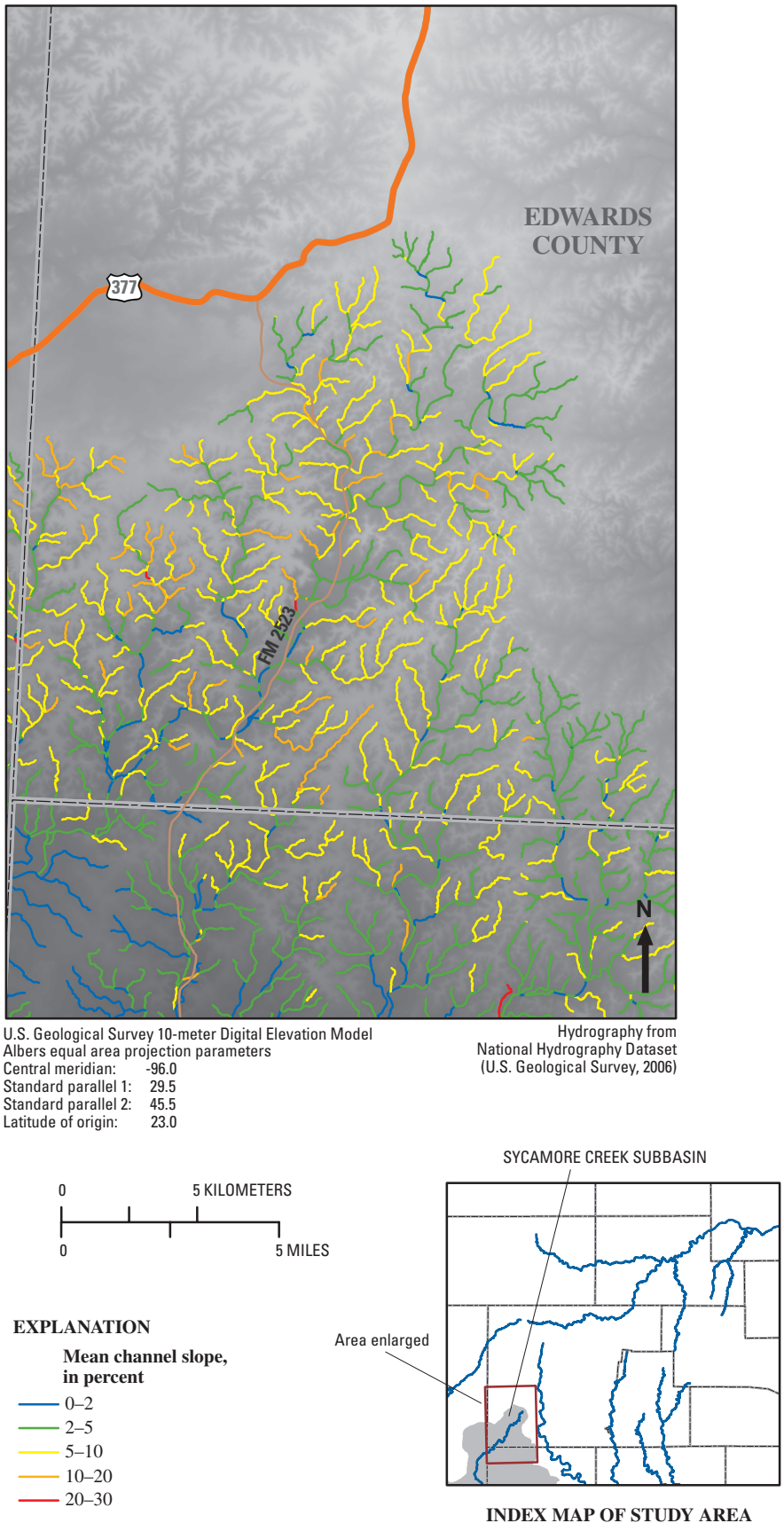

Figure 10. Channel slope of the Sycamore Creek Subbasin, Edwards County, Texas, and vicinity.

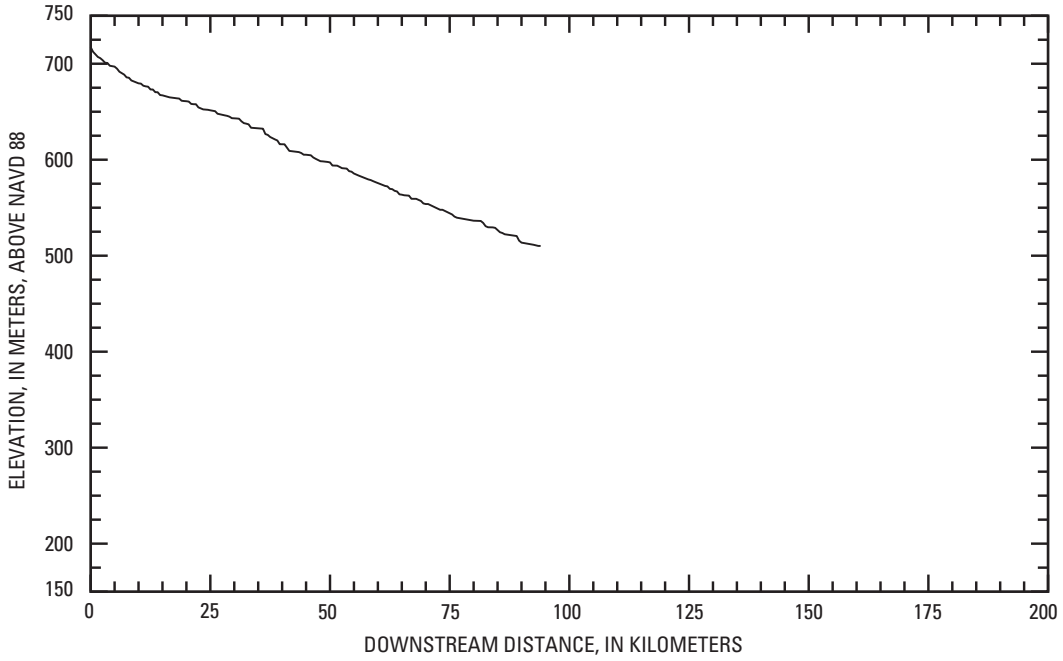

Figure 11. Longitudinal profile of the North Llano River, Kimble County, Texas, and vicinity.

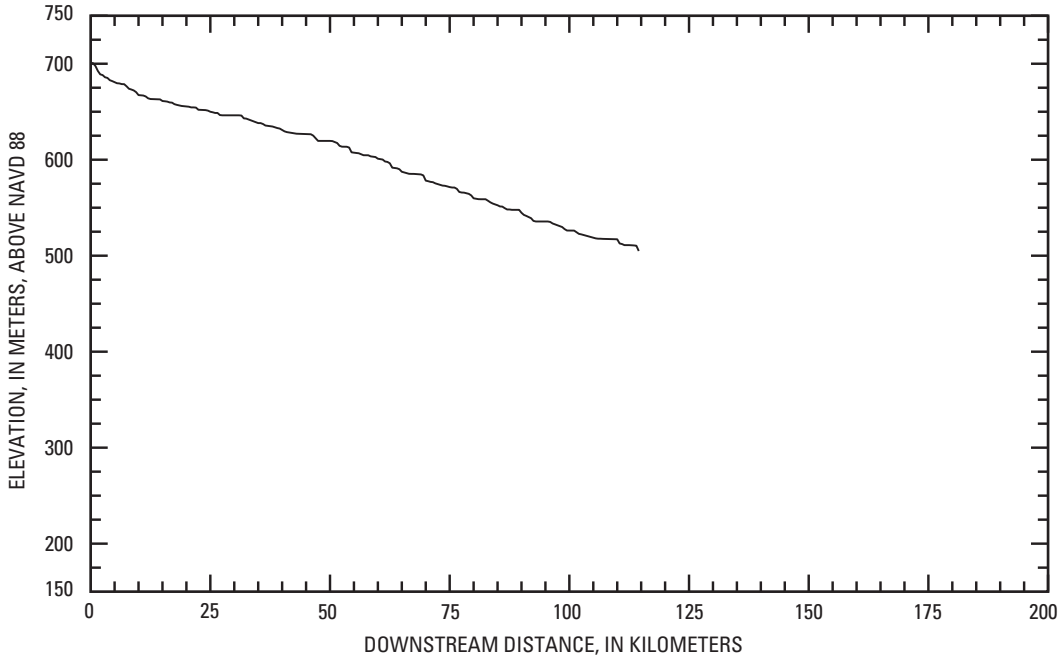

Figure 12. Longitudinal profile of the South Llano River, Edwards and Kimble Counties, Texas.

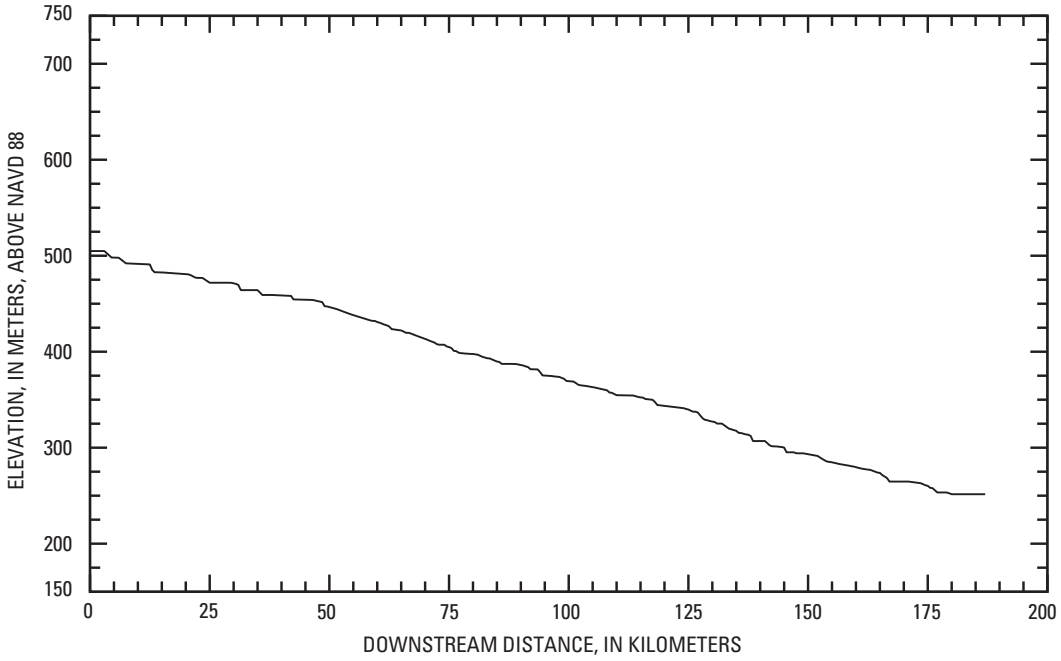

Figure 13. Longitudinal profile of the Llano River, Kimble County, Texas, and vicinity.

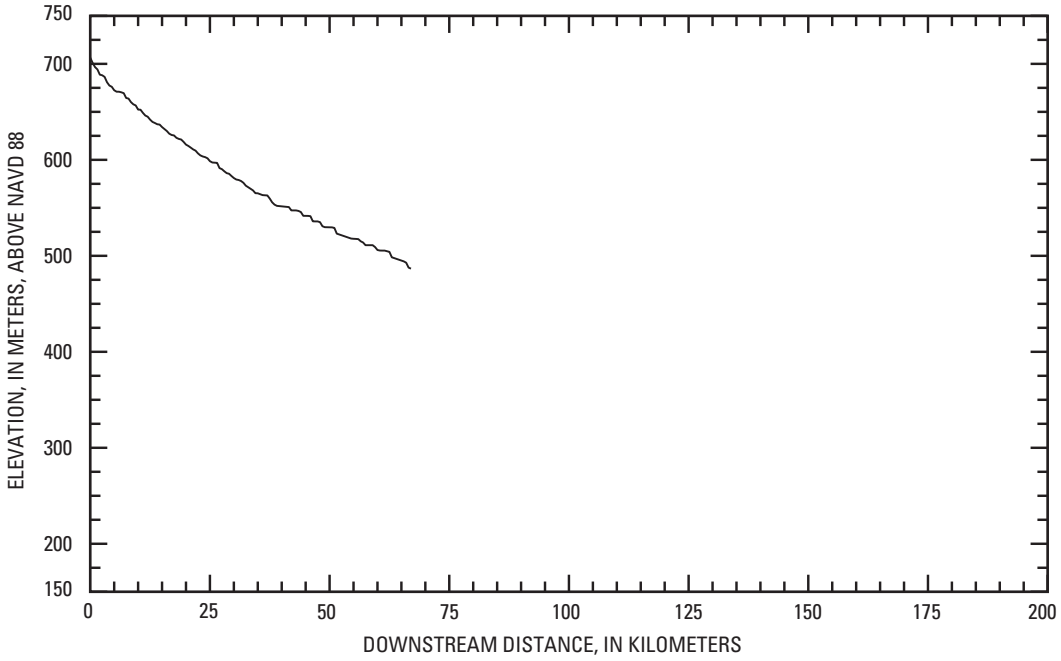

Figure 14. Longitudinal profile of Johnson Fork, Kimble County, Texas, and vicinity.

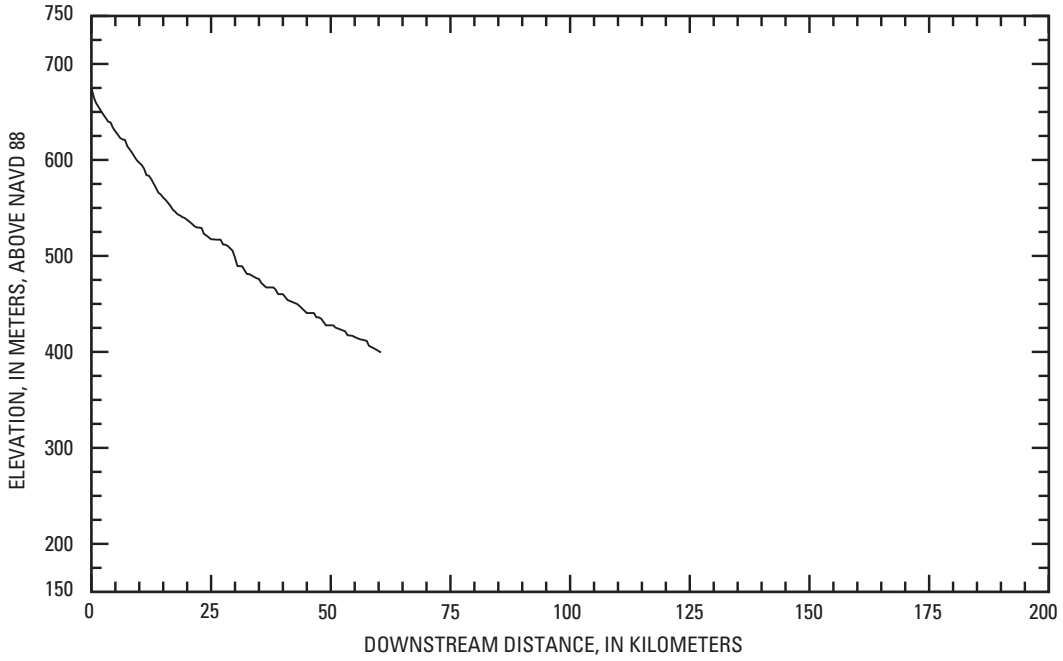

Figure 15. Longitudinal profile of the James River, Kimble County, Texas, and vicinity.

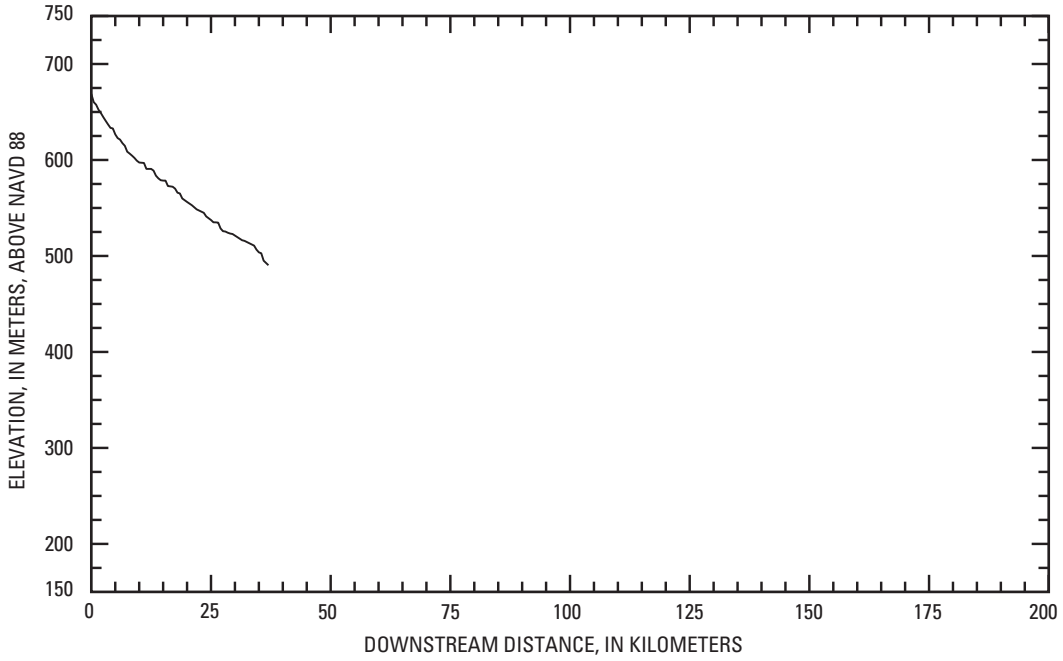

Figure 16. Longitudinal profile of the Little Devils River, Kimble County, Texas, and vicinity.

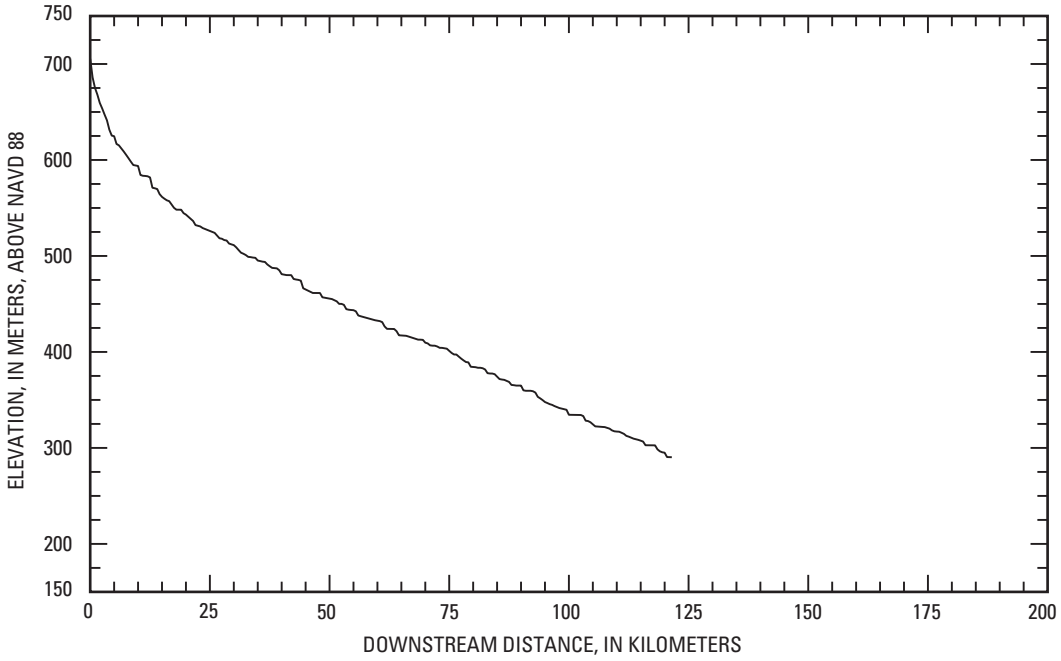

Figure 17. Longitudinal profile of the Nueces River, Edwards and Real Counties, Texas, and vicinity.

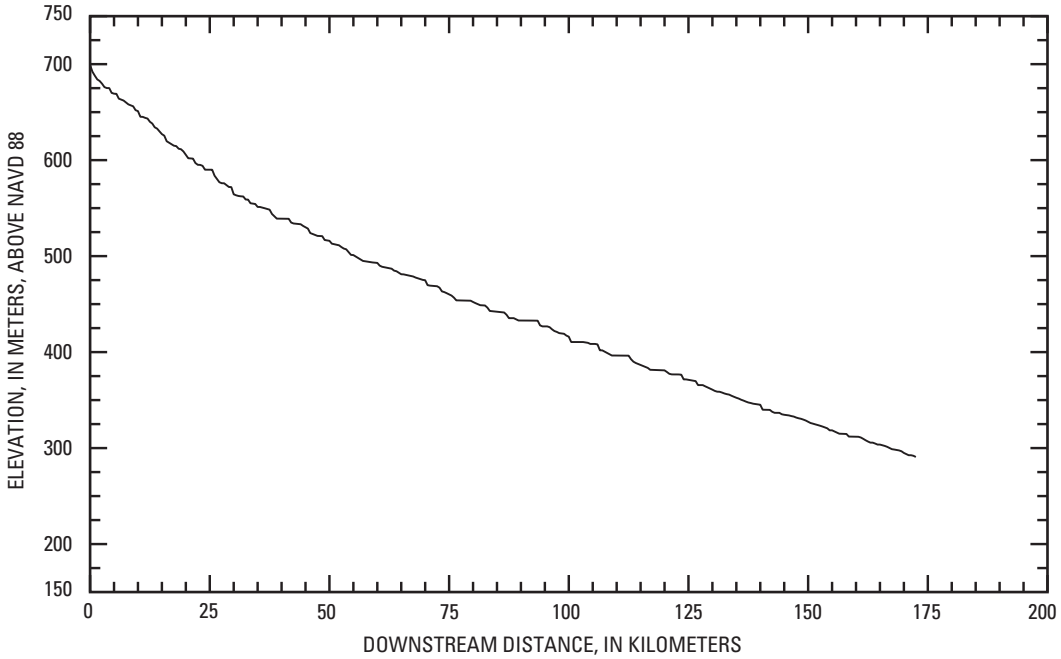

Figure 18. Longitudinal profile of the West Nueces River, Edwards County, Texas, and vicinity.

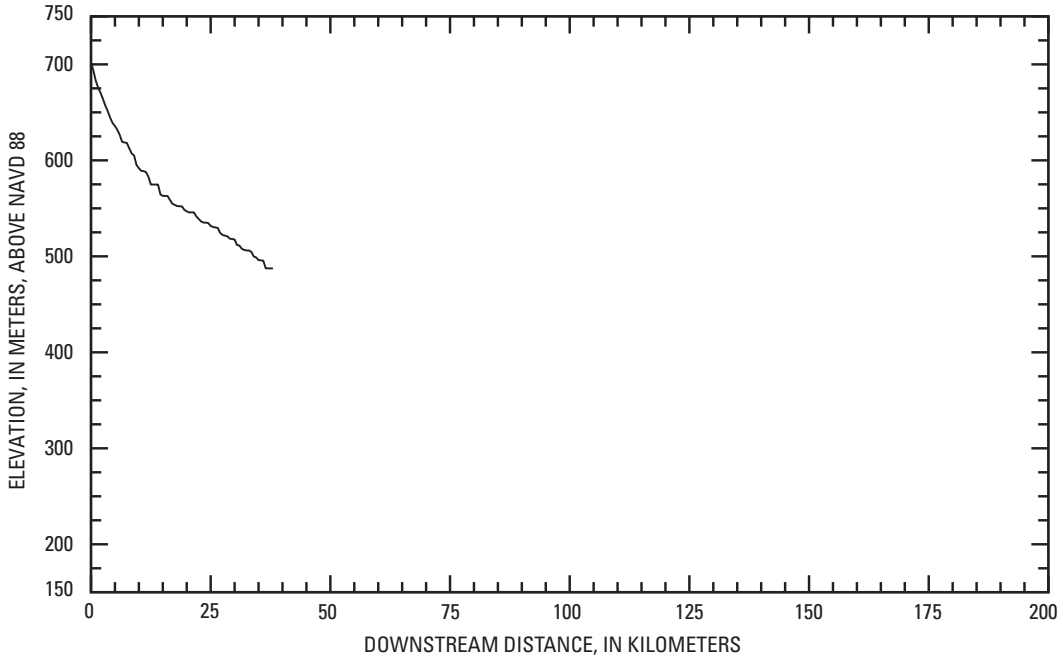

Figure 19. Longitudinal profile of the West Frio River, Real County, Texas.

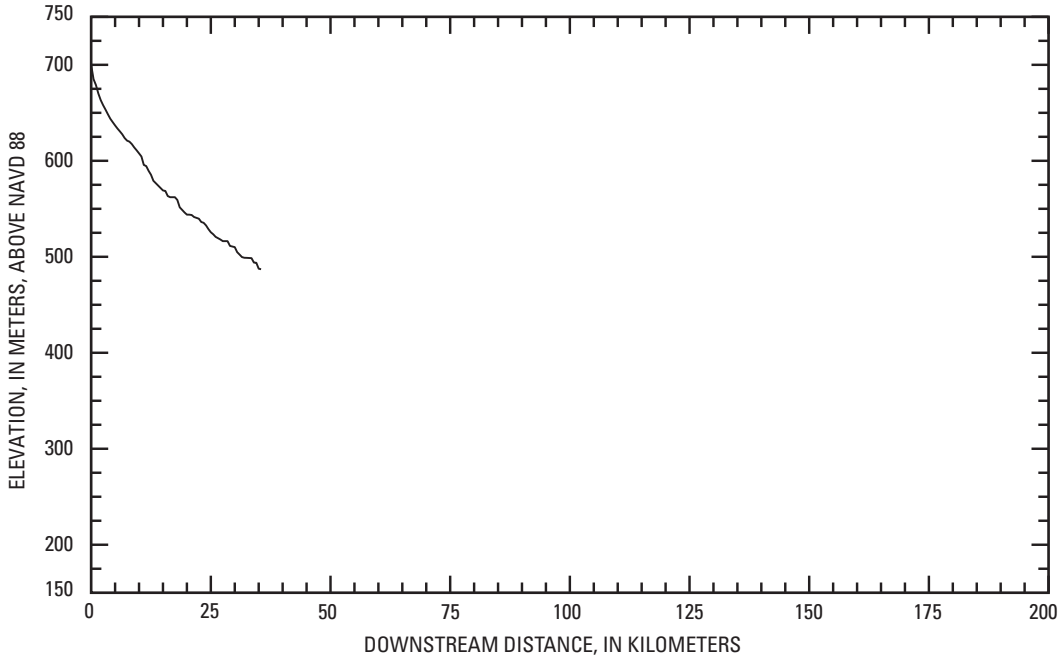

Figure 20. Longitudinal profile of the East Frio River, Real County, Texas, and vicinity.

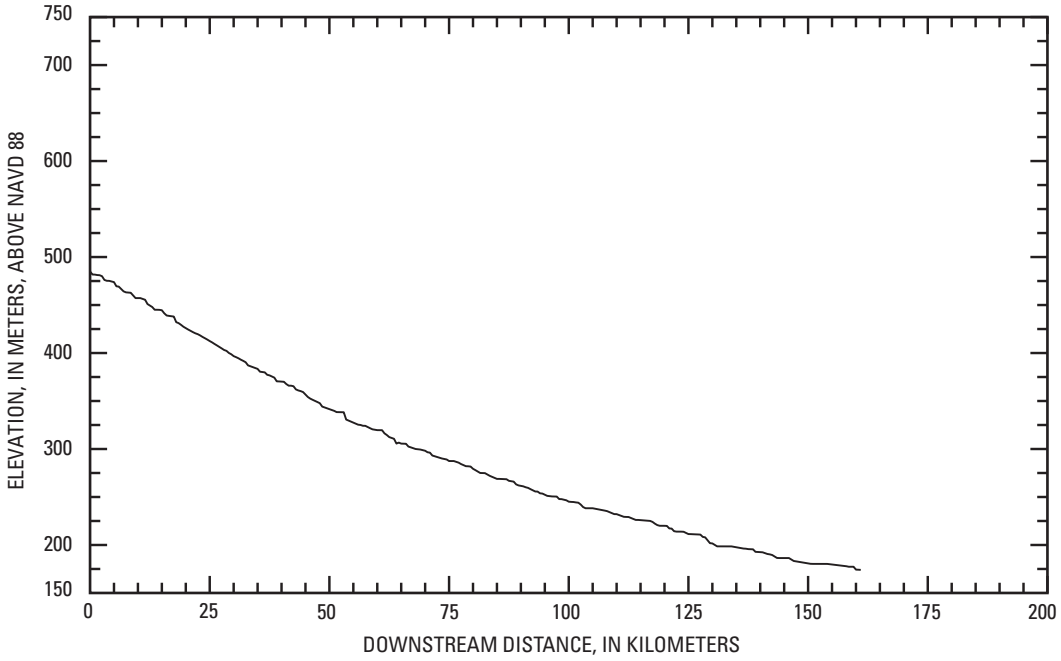

Figure 21. Longitudinal profile of the Frio River, Real County, Texas, and vicinity.

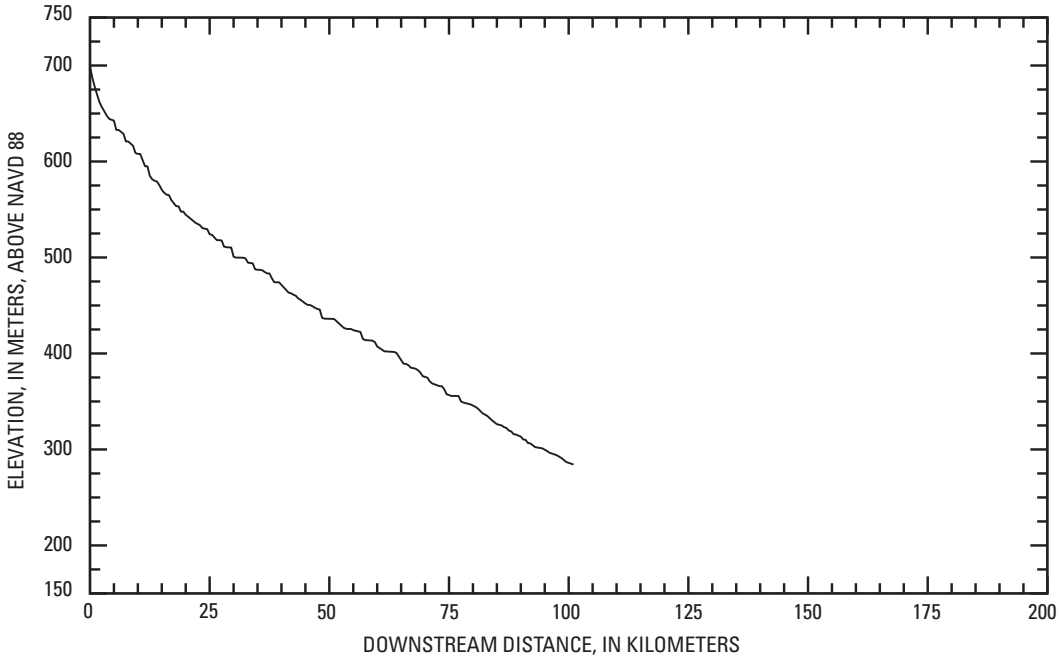

Figure 22. Longitudinal profile of the Dry Frio River, Real County, Texas, and vicinity.

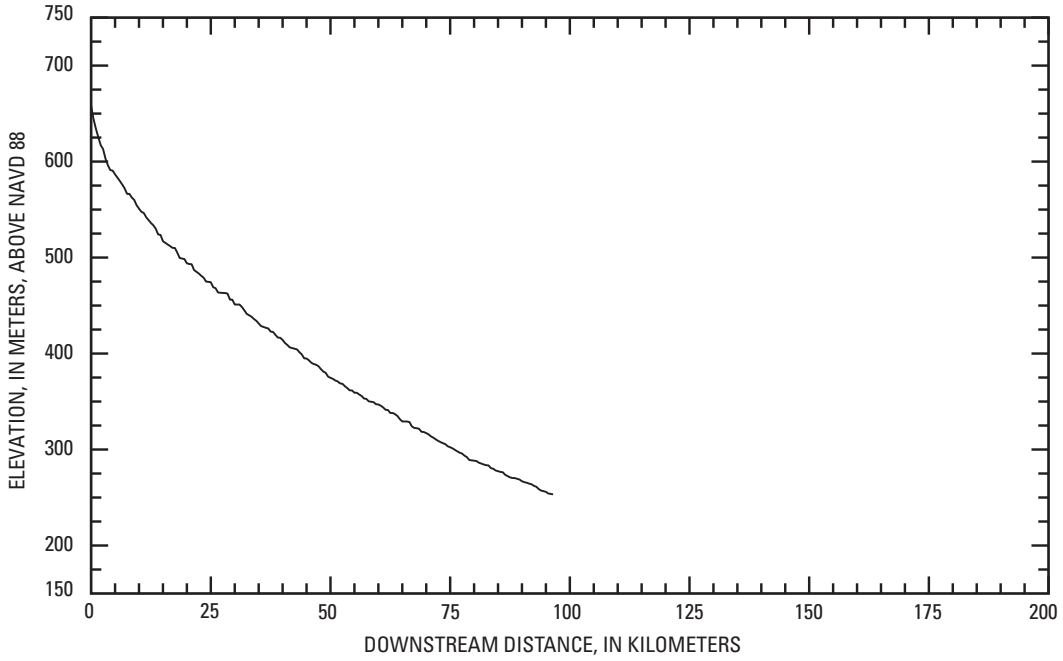

Figure 23. Longitudinal profile of Sycamore Creek, Edwards County, Texas, and vicinity.

a recent decrease in base discharge. Additionally, water-data reports for Texas since the 2001 water year only publish the annual peak discharge, and other peaks above the base discharge are not available. LCRA data were used to fill the recent gap for gaging stations in the Llano River Basin. The partial-duration flood-frequency analyses in this study used the entire period of record for all streamflow-gaging stations because the periods with missing peaks are short. The periods with missing peaks are not expected to greatly influence flood-frequency analyses, because the periods of record are sufficiently long (table 2).

Partial-duration flood peaks were entered into spreadsheets, ranked according to magnitude and recurrence intervals for the period of record were computed. The flood peak discharges and recurrence intervals were read into the R environment for statistical computing (R Development Core Team, 2004) (fig. 24) and the four-parameter kappa distribution curve fit the L-moments (Hosking and Wallis, 1997) of observed data. Computations of arrival rates and return periods of the partial-duration series are given in Stedinger and others (1993), and the techniques described therein were used to transform average arrival rates into annual exceedance probabilities. Flood magnitudes for the 1-, 1.5-, 2-, 5-year, 10-, 25-, 50-, and 100-year return periods (table 2) were calculated from the kappa distribution. Flood magnitude estimates have less accuracy for gaging stations with short periods of record.

Flood frequency also was estimated for (ungaged) study sites not coincident with streamflow-gaging stations using regional regression equations (Asquith and Slade, 1997). Regional regression equations are available for the 2-, 5-, 10-, 25-, 50-, and 100-year return periods (table 3). For ungaged study sites in the Llano River Basin, equations for Texas hydrologic region 4 (based on drainage area and channel slope) were used; and for sites in the Nueces River Basin, equations for Texas hydrologic region 5 (based on drainage area and a basin shape factor) were used.

The estimated flood magnitudes for ungaged sites in the Llano River Basin are considerably less than flood magnitudes computed from partial-duration flood-frequency analyses at USGS gaging stations 08148500 (North Llano River near Junction) and 08150000 (Llano River near Junction) (table 2).

Site Reconnaissance

Site reconnaissance trips were made to the study area from September 2003 to July 2004. Most trips were guided by TxDOT personnel familiar with LWC problems in the study area. The reconnaissance trips were necessary to (1) identify sites appropriate for field research, (2) qualitatively examine channel-bed morphology and sediment, (3) devise appropriate methods for field research, (4) examine the design of LWCs relative to the channel bed, and (5) document the condition of channels and LWCs following the June 2004 flood. Appendix 1 contains photographs of streams and LWCs made during site reconnaissance and survey trips to the study area.

Field Surveys

Field surveys at selected sites in the study area were done to (1) measure channel-reach geometry, (2) measure LWC geometry, and (3) measure particle size of bed material. The

Table 2. Flood magnitudes of U.S. Geological Survey and Lower Colorado River Authority gaging stations in the study area, Edwards, Kimble, and Real Counties, Texas, and vicinity, calculated by partial-duration flood-frequency analyses based on the kappa distribution.

[m^3/s, cubic meters per second; ft^3/s, cubic feet per second; LCRA, Lower Colorado River Authority]

Study site number (fig. 2)	Station number or name, or both	Period of record used	Return period							
			1-year [m^3/s (ft^3/s)]	1.5-year [m^3/s (ft^3/s)]	2-year [m^3/s (ft^3/s)]	5-year [m^3/s (ft^3/s)]	10-year [m^3/s (ft^3/s)]	25-year [m^3/s (ft^3/s)]	50-year [m^3/s (ft^3/s)]	100-year [m^3/s (ft^3/s)]
2	08148500 North Llano River near Junction, Tex.	09/14/1915–09/30/1977; 06/13/2001–09/30/2005	131 (4,610)	331 (11,700)	524 (18,500)	1,250 (44,100)	1,780 (62,700)	2,370 (83,600)	2,730 (96,400)	3,030 (107,000)
13	08150000 Llano River near Junction, Tex.	09/13/1915–01/31/2007	218 (7,690)	476 (16,800)	716 (25,300)	1,740 (61,300)	2,720 (96,000)	4,280 (151,000)	5,660 (200,000)	7,250 (256,000)
22	08150700 Llano River near Mason, Tex.	03/07/1968–01/31/2007	408 (14,400)	793 (28,000)	1,133 (40,000)	2,495 (88,100)	3,738 (132,000)	5,663 (200,000)	7,306 (258,000)	9,118 (322,000)
20	Johnson Fork near Junction (LCRA)	09/25/2000–01/31/2007	14 (510)	23 (810)	84 (2,960)	1,250 (44,300)	2,580 (91,300)	3,650 (129,000)	3,960 (140,000)	4,080 (144,000)
21	James River near Mason (LCRA)	04/15/1999–01/31/2007	29 (1,010)	101 (3,570)	189 (6,690)	592 (20,900)	920 (32,500)	1,300 (46,000)	1,540 (54,300)	1,730 (61,100)
24	08190000 Nueces River at Laguna, Tex.	10/25/1923–09/30/2005	138 (4,890)	326 (11,500)	513 (18,100)	1,400 (49,500)	2,410 (85,000)	4,300 (152,000)	6,320 (223,000)	9,010 (318,000)
23	08190500 West Nueces River near Brackettville, Tex.	10/01/1939–09/30/1950; 04/01/1956–09/30/2005	25 (900)	184 (6,490)	368 (13,000)	1,210 (42,700)	2,080 (73,500)	3,600 (127,000)	5,040 (178,000)	6,850 (242,000)
26	08195000 Frio River at Concan, Tex.	10/26/1923–09/30/1929; 10/01/1930–09/30/2005	161 (5,670)	331 (11,700)	484 (17,100)	1,110 (39,100)	1,690 (59,800)	2,580 (91,100)	3,400 (120,000)	4,280 (151,000)
25	08196000 Dry Frio River near Reagan Wells, Tex.	09/01/1952–09/30/2005	69 (2,450)	144 (5,080)	212 (7,490)	521 (18,400)	861 (30,400)	1,510 (53,200)	2,200 (77,500)	3,120 (110,000)

first field objective was accomplished at 10 sites in the study area. Channel-reach geometry was measured by surveying cross sections. These data are used to compute channel cross-sectional area and local slope, parameters required for bed-material entrainment computations. The second field objective was accomplished at four sites in the study area. One of the four sites, South Llano River at U.S. Highway 377 near Rocksprings, also has channel-reach geometry surveys. LWC cross sections, although not used in computations of bed-material entrainment in this study, permit visual comparison to natural channel cross sections in the study area. The third field objective was accomplished at 10 sites, the same locations for channel-reach geometry surveys, in the study area. Particle-size data are required for computations of bed-material entrainment potential. Field surveys were limited to the Llano River Basin because (1) most of the LWCs of interest to TxDOT are there, and (2) it was desirable to analyze systematic downstream trends in bed-material entrainment potential without introducing drainage-basin variability, specifically watershed and channel slope differences between the Llano River Basin and the Frio, Nueces, and West Nueces River Basins.

Channel Geometry

An electronic total station was used to measure elevation and horizontal distance of channel cross sections at 10 selected sites in the study area (figs. 25–34), all located in the Llano River subbasin. The total station functioned with a coaxial

```
library(lmomco)
Tp <- c(1,1.5,2,5,10,25,50,100)
myfile <- file.choose()
Q <- read.table(file=myfile, header=TRUE, sep="\t", fill=TRUE)
names(Q)
attach(Q)
lmr <- lmoms(Qcfs)
Qsort <- sort(Qcfs)
PP <- pp(Qsort)
plot(PP, log10(Qsort))
lmrdia <- lmrdia()
plotlmrdia(lmrdia, xlim=c(-0.1, 0.6), ylim=c(-0.1, 0.6))
points(lmr$ratios[3], lmr$ratios[4])
ls()
length(Qsort)
para <- parkap(lmr)
plot(PP, log10(Qsort))
lines(PP, log10(quakap(PP, para)),lwd=2)
lambda <- length(Qsort)/5.8
qe <- 1/(Tp*lambda)
G <- 1-qe
SOLUTION <- quakap(G,para)
detach(Q)
H <- list(event=SOLUTION,Tp=Tp,G=G,file=myfile)
points(H$G,log10(H$event),pch=16,col=2,cex=3)
return(H)
```

Figure 24. R-code used for partial-duration flood-frequency analyses.

phase-contrast measuring system used to triangulate position and elevation from horizontal and vertical angles and distance to the target. The data logger connected to the total station was set to alert the surveyor when any tolerances were exceeded following a shot. No tolerances were greatly exceeded during the course of any survey done for the project; therefore, reliable position and elevation measurements were acquired.

Sites selected for measurement of channel geometry range from upland headwater reaches with limited cobble- and gravel-sized bed material to main-stem river channels with considerable amounts of coarse bed material. Two sites are at USGS gaging stations and surveyed elevations were associated with the established stage datum at those stations. The remaining eight sites were assigned an arbitrary elevation datum. Horizontal coordinates were based on an arbitrary datum at all sites, and global positioning system coordinates were noted at each station setup. In this manner, potential future studies could closely follow the same cross-sectional transect.

Channel-geometry survey data were entered into spreadsheets, and channel slopes were computed for sites using elevations at edges of water (water surface), thalwegs, or floodplains, in decreasing preferential order (table 4). Channel slopes computed using measured cross-sectional data are preferable to DEM-computed slopes for reach-scale estimations of bed-material entrainment. Cross-sectional geometric data were imported into WinXSPRO Version 3.0, a free U.S. Department of Agriculture Forest Service (2005) software package, for computation of cross-sectional areas and hydraulic radiuses for different depths.

Low-Water-Crossing Geometry

An electronic total station was used to measure elevation and horizontal distance of LWC cross sections at four selected sites in the study area (figs. 28 [bridge center-line], 35), all in the Llano River Basin. The four sites were assigned an arbitrary elevation and horizontal datum. LWC cross sections enable computations of cross-sectional areas and hydraulic radiuses for different depths.

Bed-Material Particle Size

Bed material was sampled for particle size at 10 sites following the same cross-sectional transects surveyed for channel-reach geometry. Particle-size sampling was not done at cross sections where coarse bed material was not present. Samples were collected along transects to account for different geomorphic surfaces of the channel bed, including longitudinal bars, the thalweg, and riffles and pools. The technique used along transects commonly is referred to as the Wolman pebble count (Wolman, 1954).

Table 3. Flood magnitudes of ungaged sites in the study area, Edwards, Kimble, and Real Counties, Texas, and vicinity, computed by regional regression equations (Asquith and Slade, 1997).

[m^3/s, cubic meters per second; ft^3/s, cubic feet per second]

Study site number (fig. 2)	Study site	Return period					
		2-year [m^3/s (ft^3/s)]	5-year [m^3/s (ft^3/s)]	10-year [m^3/s (ft^3/s)]	25-year [m^3/s (ft^3/s)]	50-year [m^3/s (ft^3/s)]	100-year [m^3/s (ft^3/s)]
1	North Llano River near Roosevelt	95.7 (3,380)	283 (10,000)	490 (17,300)	841 (29,700)	1,170 (41,300)	1,570 (55,400)
3	South Llano River at Baker Ranch	15.6 (552)	47.9 (1,690)	86.1 (3,040)	153 (5,410)	219 (7,740)	300 (10,600)
4	South Llano River at U.S. Highway 377 near Rocksprings	48.1 (1,700)	139 (4,910)	240 (8,490)	411 (14,500)	569 (20,100)	767 (27,100)
5	South Llano River at 700 Springs Ranch	60.6 (2,140)	173 (6,120)	297 (10,500)	507 (17,900)	697 (24,600)	934 (33,000)
6	South Llano River at First Crossing	106 (3,760)	300 (10,600)	504 (17,800)	844 (29,800)	1,150 (40,600)	1,530 (54,000)
7	South Llano River at South Llano River State Park	118 (4,180)	331 (11,700)	555 (19,600)	926 (32,700)	1,260 (44,400)	1,670 (58,900)
8	South Llano River at Texas Tech University–Junction	111 (3,920)	309 (10,900)	518 (18,300)	864 (30,500)	1,170 (41,400)	1,550 (54,900)
9	South Llano River at Flatrock Crossing	116 (4,100)	323 (11,400)	544 (19,200)	903 (31,900)	1,230 (43,400)	1,630 (57,500)
12	Johnson Fork at Lowlands Crossing	123 (4,330)	382 (13,500)	674 (23,800)	1,170 (41,300)	1,650 (58,300)	2,240 (79,000)
14	Llano River near Ivy Chapel	365 (12,900)	971 (34,300)	1,570 (55,400)	2,510 (88,800)	3,310 (117,000)	4,300 (152,000)
15	Llano River at Yates Crossing	362 (12,800)	960 (33,900)	1,550 (54,700)	2,480 (87,600)	3,260 (115,000)	4,250 (150,000)
16	Nueces River at Ben Williams Crossing	158 (5,570)	620 (21,900)	1,210 (42,900)	2,460 (87,000)	3,850 (136,000)	5,720 (202,000)

The Wolman pebble count was facilitated through the use of a sampling grid and a particle-size analyzer (fig. 36). The sampling grid measures 50 by 50 centimeters and contains intersections spaced every 10 centimeters, resulting in 25 intersections per placement. The sampling grid is placed on a gravel or cobble bed, and the 25 particles that lie directly beneath each intersection are selected. The b-axis of each particle is passed through the smallest possible opening of the size analyzer. The b-axis is the short axis along the same dimensional plane as the longest axis of the particle. The diameter of the size-analyzer opening that passes the particle is noted. Occasionally by accident, slightly more or less than 25 particles are counted, but that should not reduce data quality. Using the count data, cumulative particle-size distribution curves can be constructed (figs. 37–46), and common particle-size descriptors can be computed (table 5). These descriptors are d_{16}, d_{50}, and d_{84}, and represent the diameters at which 16, 50, and 84 percent, respectively, of the sample is finer. The particle-size descriptors are required in computations of bed-material entrainment.

The Wolman pebble count technique (Wolman, 1954) differs from other methods that rely on volume or weight of particles to infer a size distribution. One disadvantage of the Wolman pebble count is that practitioners tend to select the largest particles. The sampling grid described above is used to minimize such biases, but larger particles still can be preferentially selected. Nevertheless, the consistency of the method permits acceptable comparisons between sites. An additional disadvantage of the Wolman pebble count is that only particles at the surface are accounted for. Particles buried beneath the surface are not included, although they certainly are mobilized during very high flows. A gradation in particle size with depth beneath the bed surface is not accounted for in studies relying on the pebble-count method. A further disadvantage involves the neglect of particle shape, as only the b-axis is measured. Long, narrow cobbles and gravels are represented by the shortest plane, and the assumption of a perfectly round particle effectively reduces the recorded particle size. Finally, the pebble count does not include differences in particle density, which means that particle weight is not propagated through to computations of bed-material entrainment.

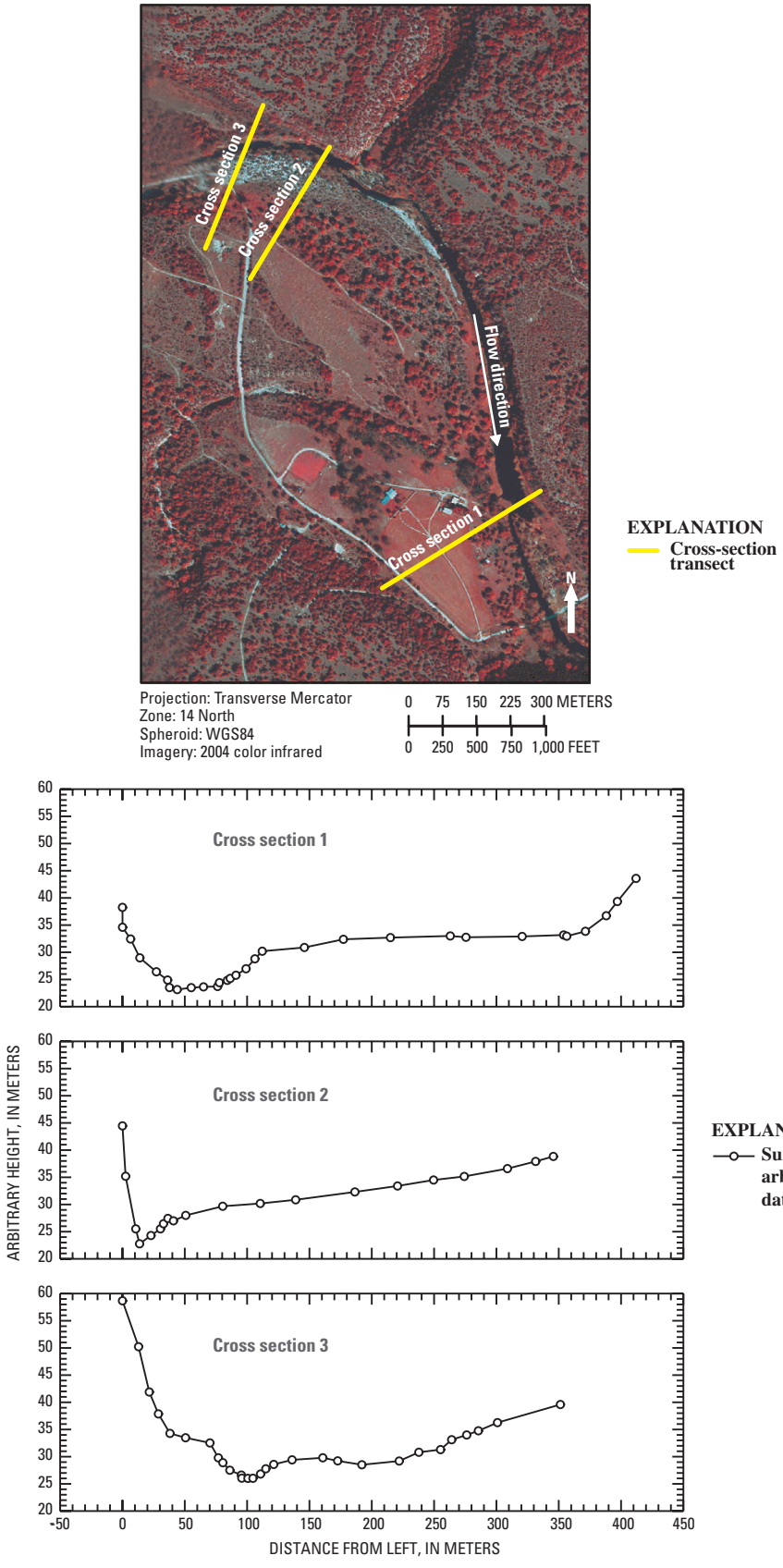

Figure 25. Map and graphs of channel cross-section transects at North Llano River near Roosevelt (see fig. 2 for site location), Kimble County, Texas.

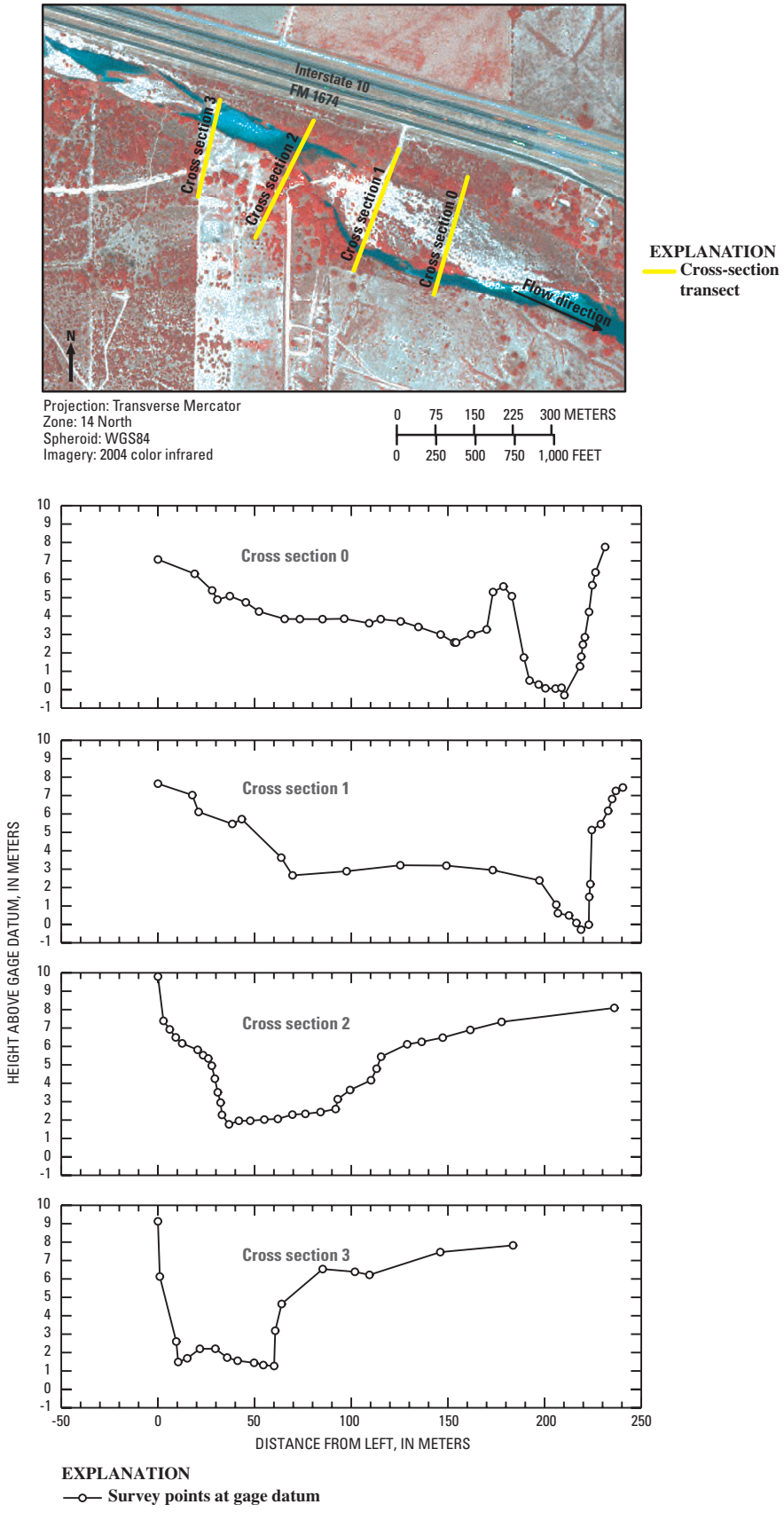

Figure 26. Map and graphs of channel cross-section transects at North Llano River near Junction (see fig. 2 for site location), Kimble County, Texas. Elevations are based on U.S. Geological Survey gage datum.

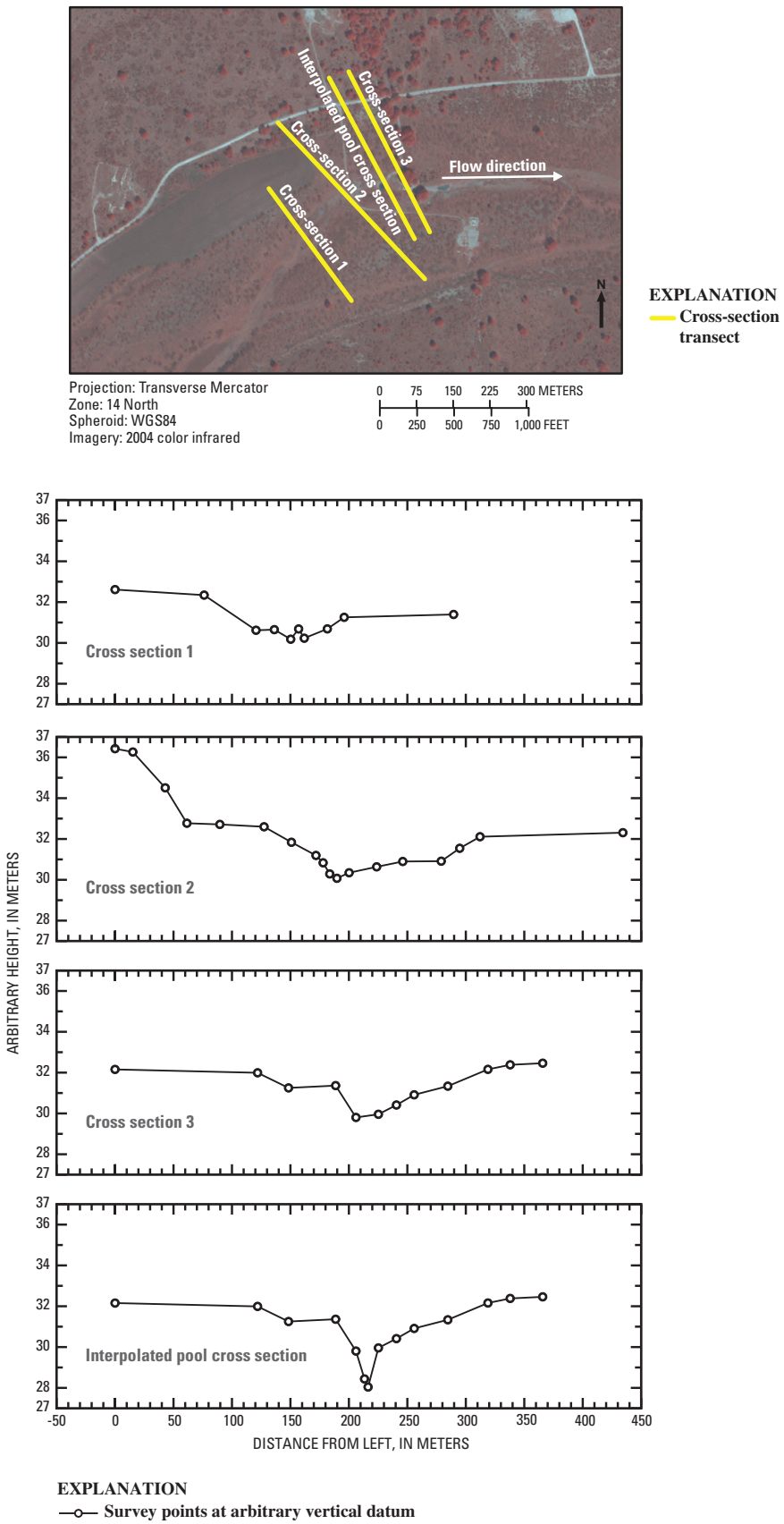

Figure 27. Map and graphs of channel cross-section transects at South Llano River at Baker Ranch (see fig. 2 for site location), Edwards County, Texas.

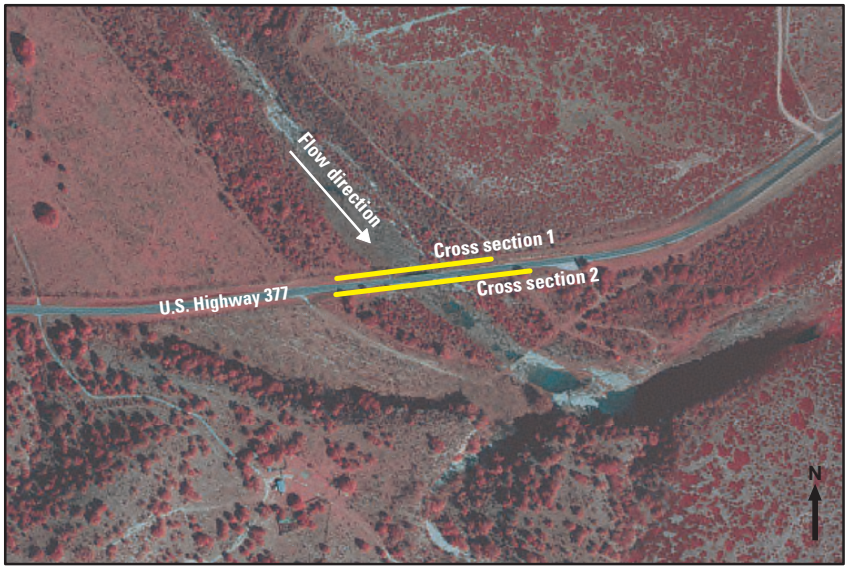

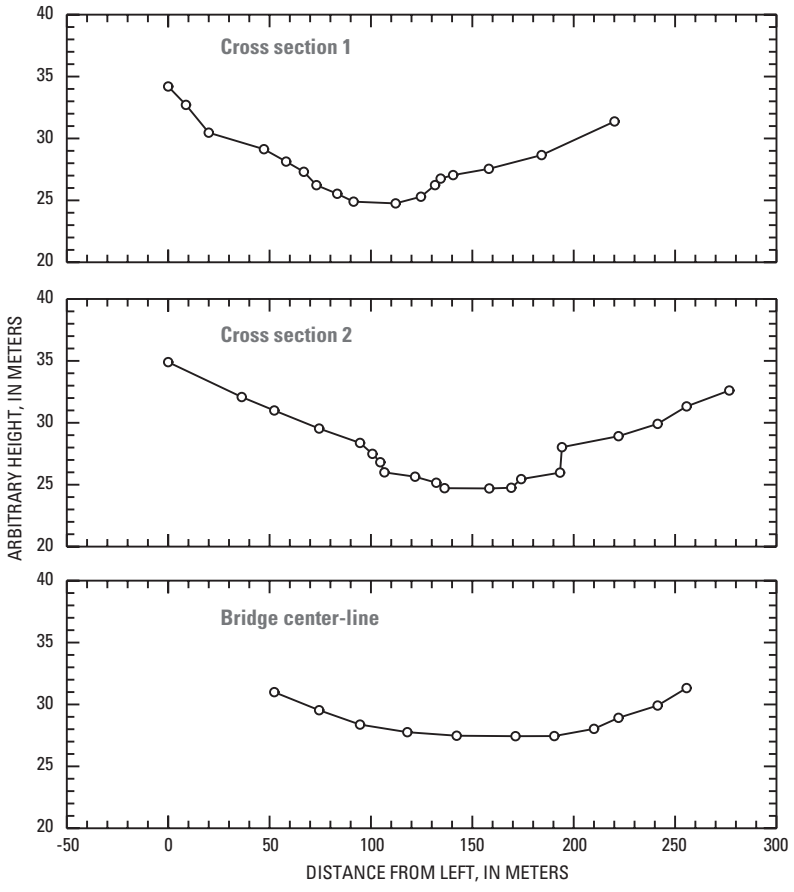

Figure 28. Map and graphs of channel cross-section transects at South Llano River at U.S. Highway 377 near Rocksprings (see fig. 2 for site location), Edwards County, Texas.

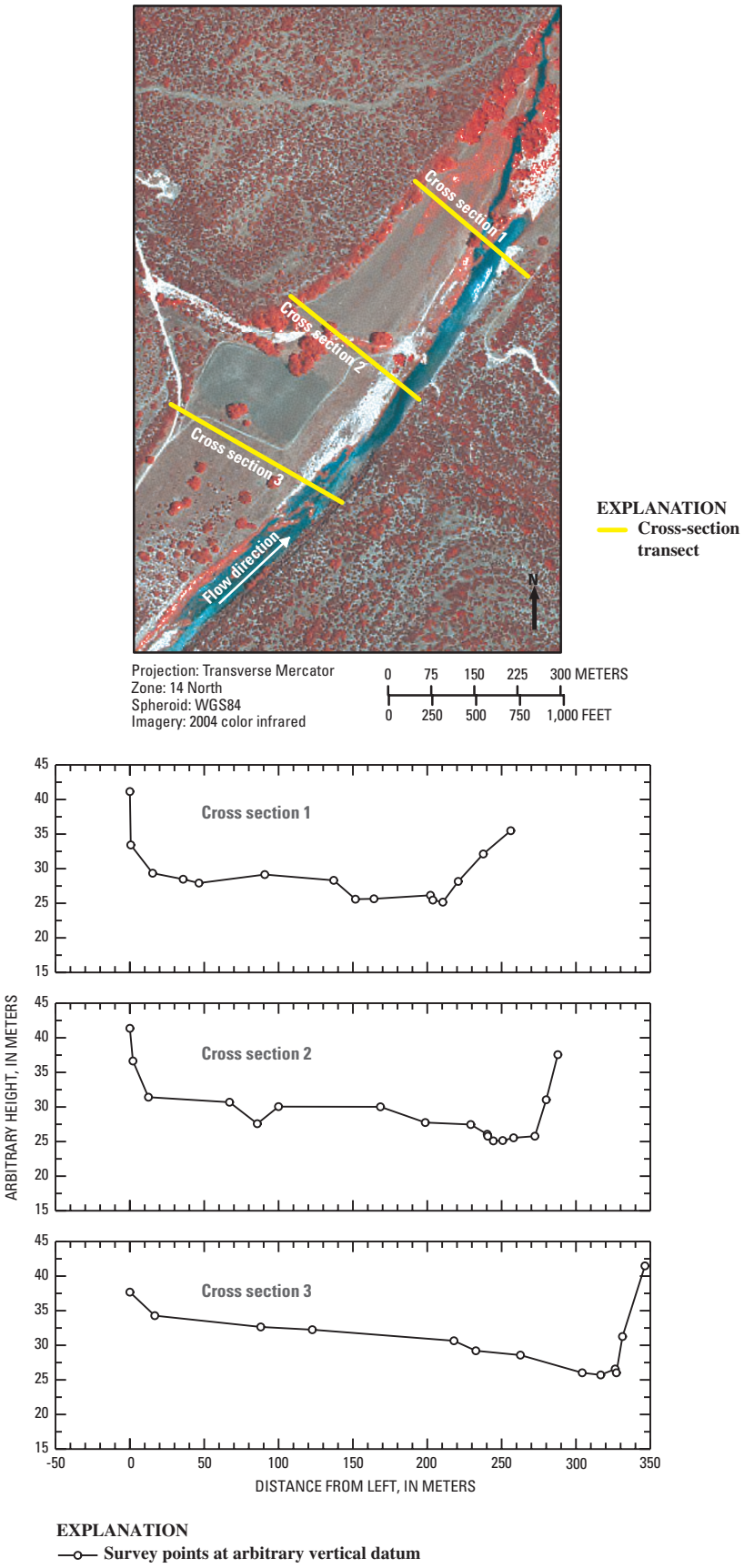

Figure 29. Map and graphs of channel cross-section transects at South Llano River at 700 Springs Ranch (see fig. 2 for site location), Edwards County, Texas.

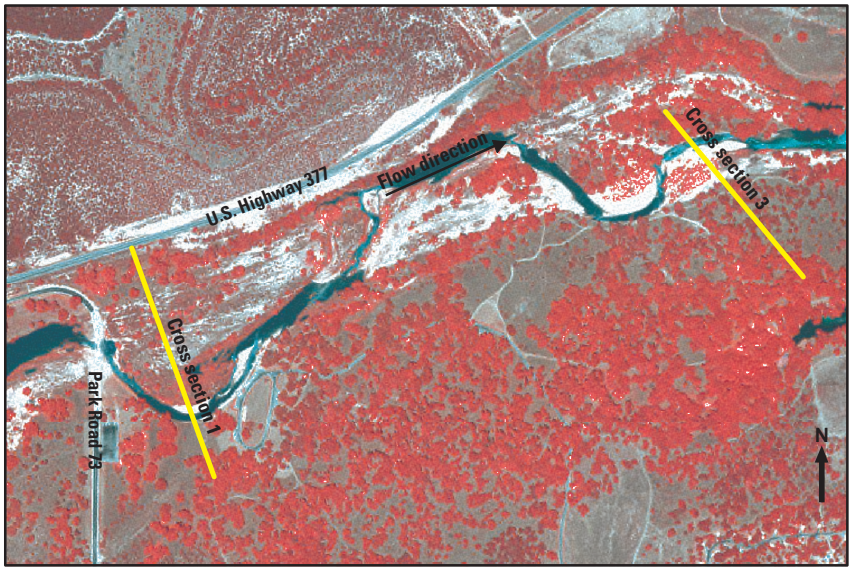

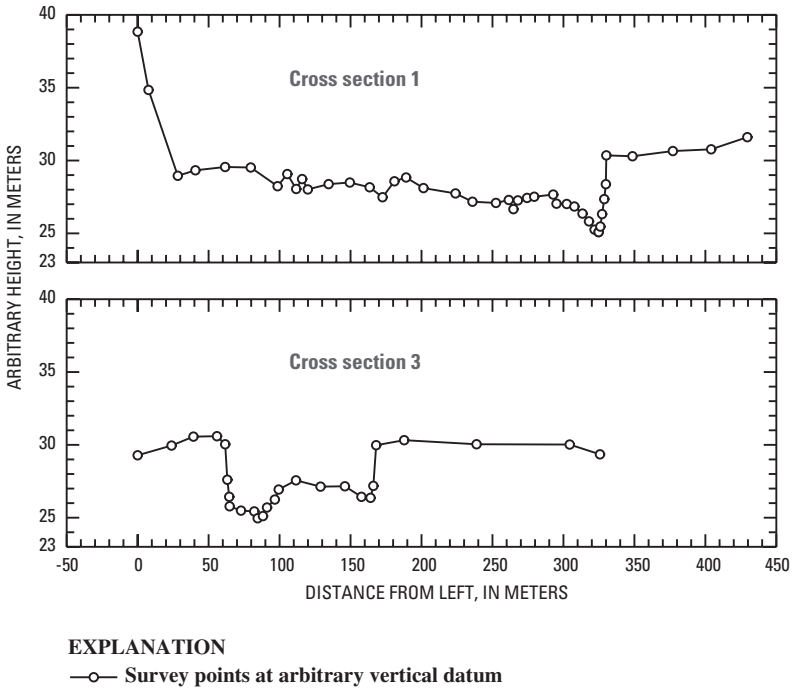

Figure 30. Map and graphs of channel cross-section transects at South Llano River at South Llano River State Park (see fig. 2 for site location), Kimble County, Texas. Cross section 1 is associated with a local elevation datum different from that of cross section 3.

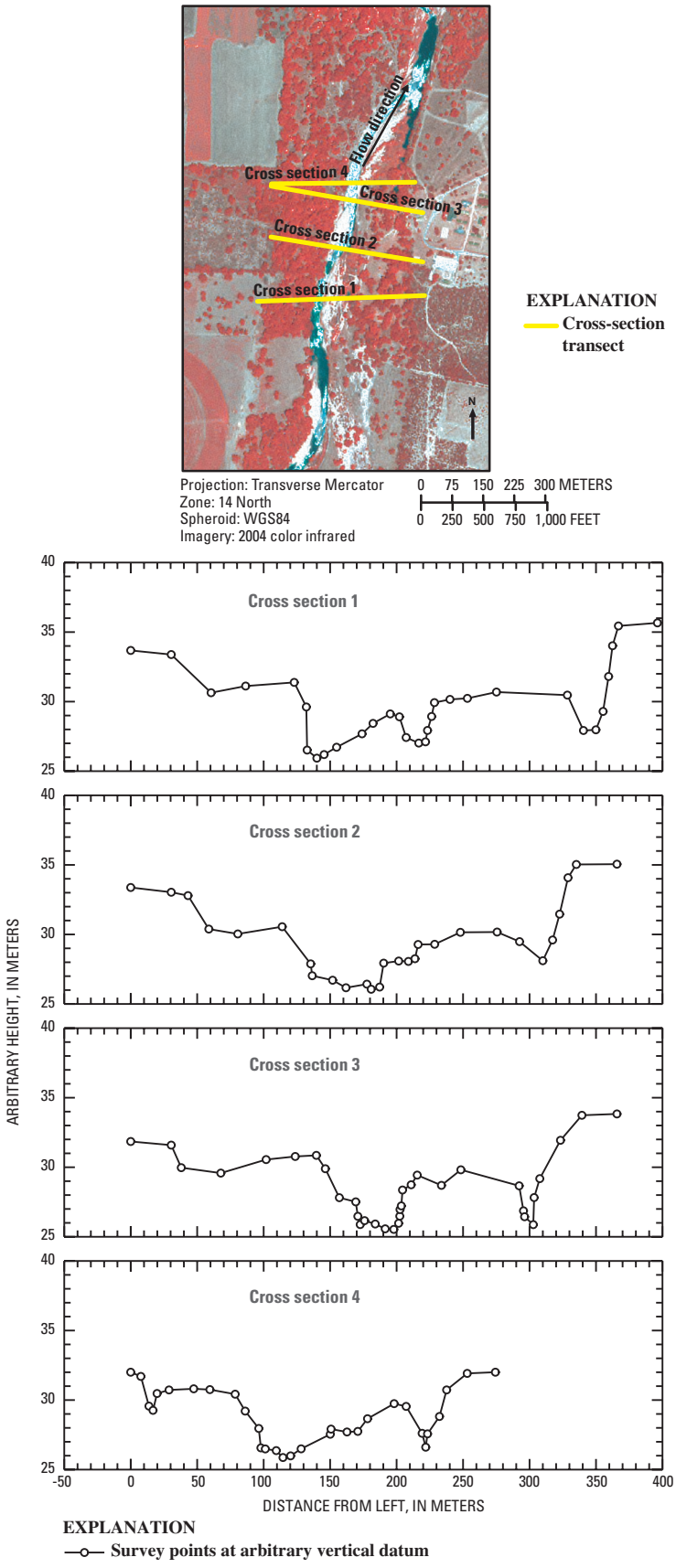

Figure 31. Map and graphs of channel cross-section transects at South Llano River at Texas Tech University–Junction (see fig. 2 for site location), Kimble County, Texas.

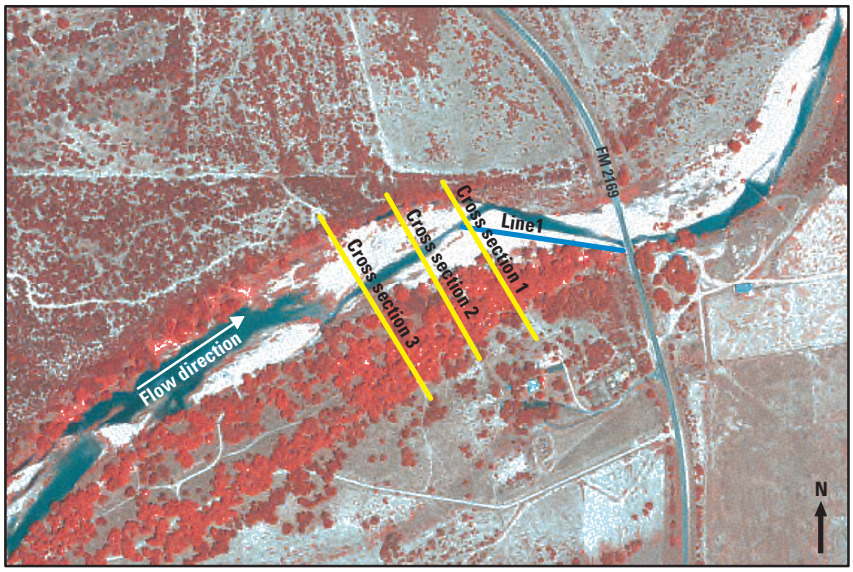

EXPLANATION
Cross-section transect
Resistivity transect

Projection: Transverse Mercator
Zone: 14 North
Spheroid: WGS84
Imagery: 2004 color infrared

0 75 150 225 300 METERS
0 250 500 750 1,000 FEET

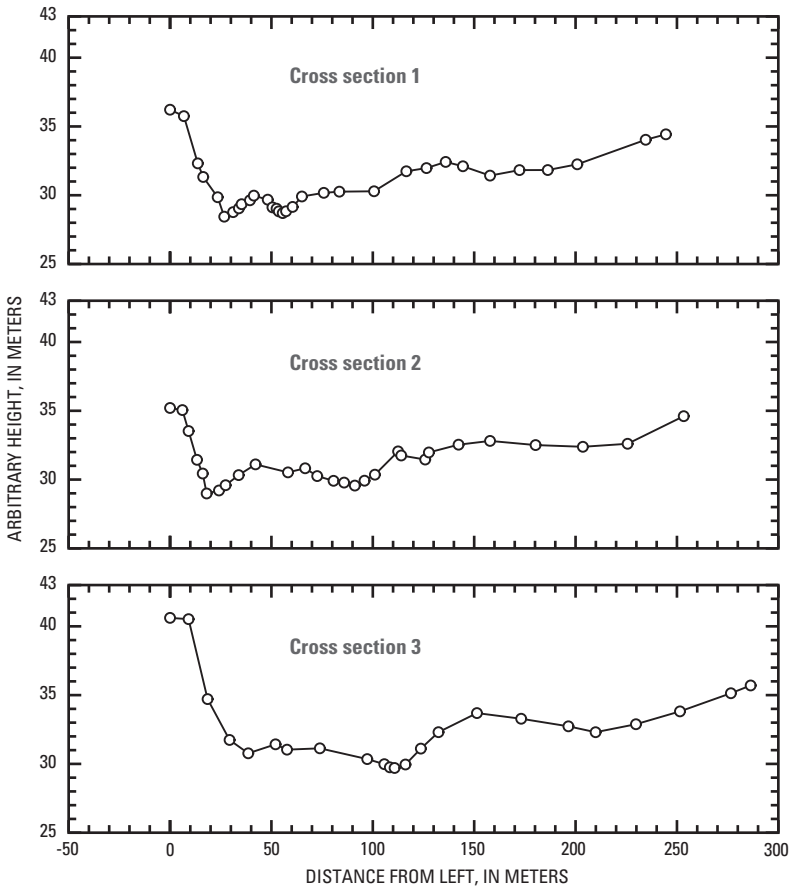

EXPLANATION
Survey points at arbitrary vertical datum

Figure 32. Map and graphs of channel cross-section transects at Johnson Fork at Lowlands Crossing (see fig. 2 for site location), Kimble County, Texas.

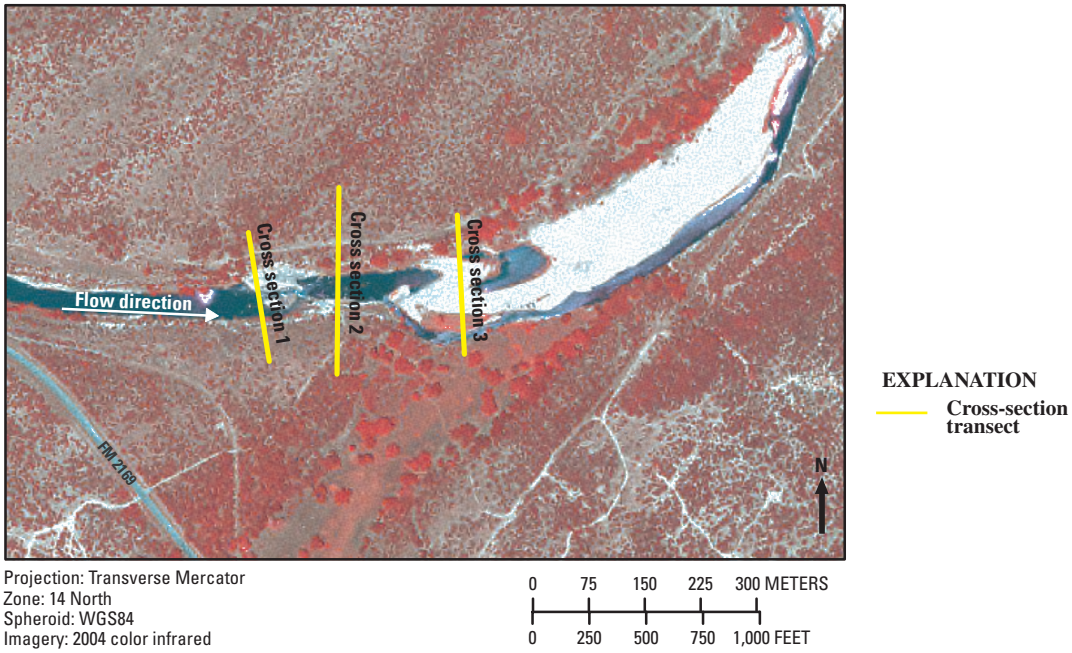

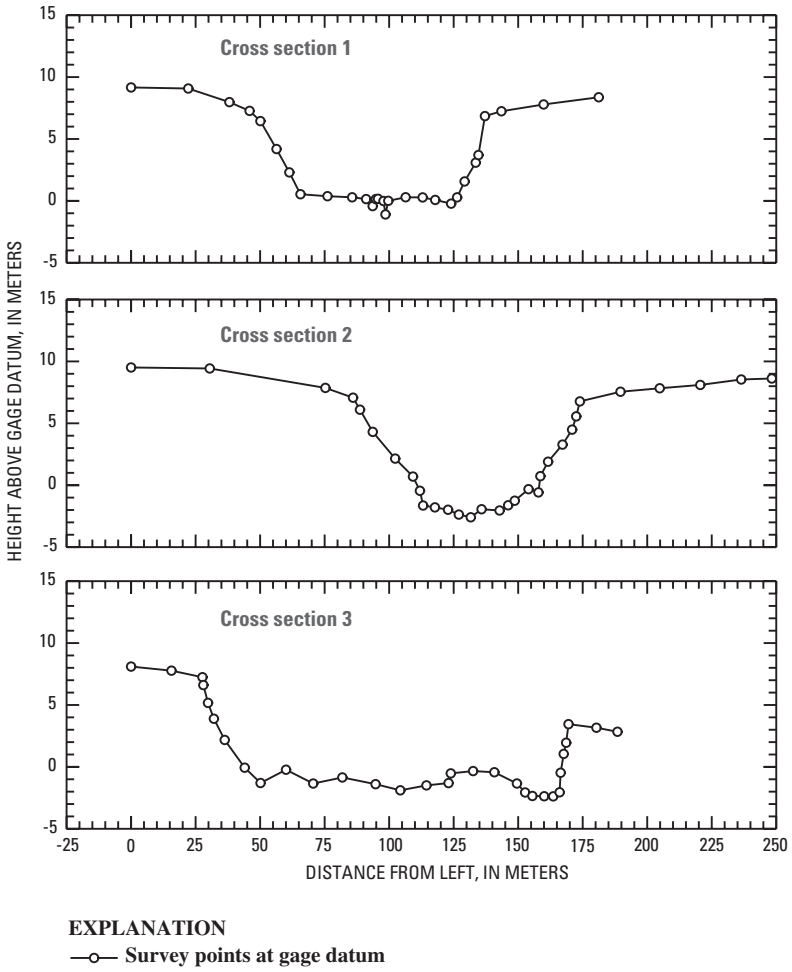

Figure 33. Map and graphs of channel cross-section transects at Llano River near Junction (see fig. 2 for site location), Kimble County, Texas. Elevations are based on U.S. Geological Survey gage datum.

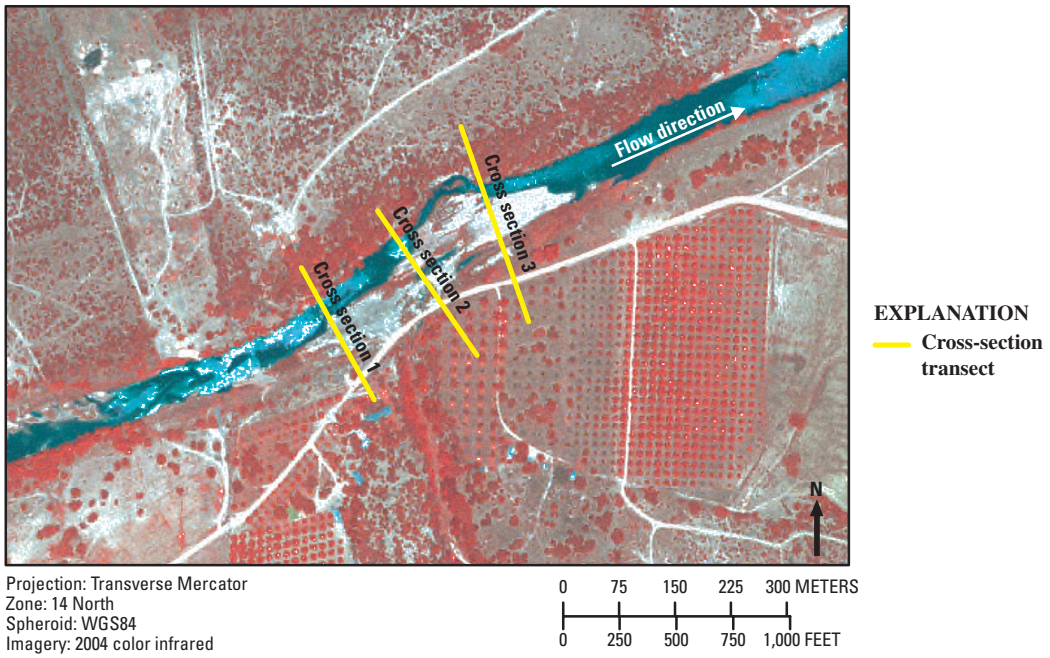

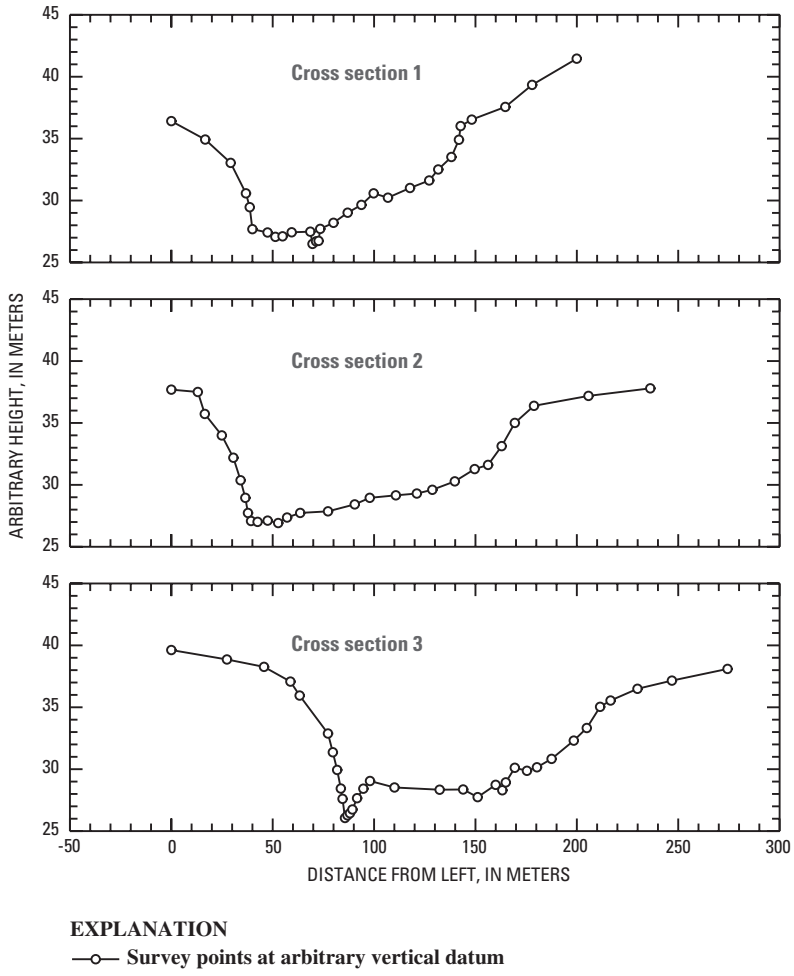

Figure 34. Map and graphs of channel cross-section transects at Llano River near Ivy Chapel (see fig. 2 for site location), Kimble County, Texas.

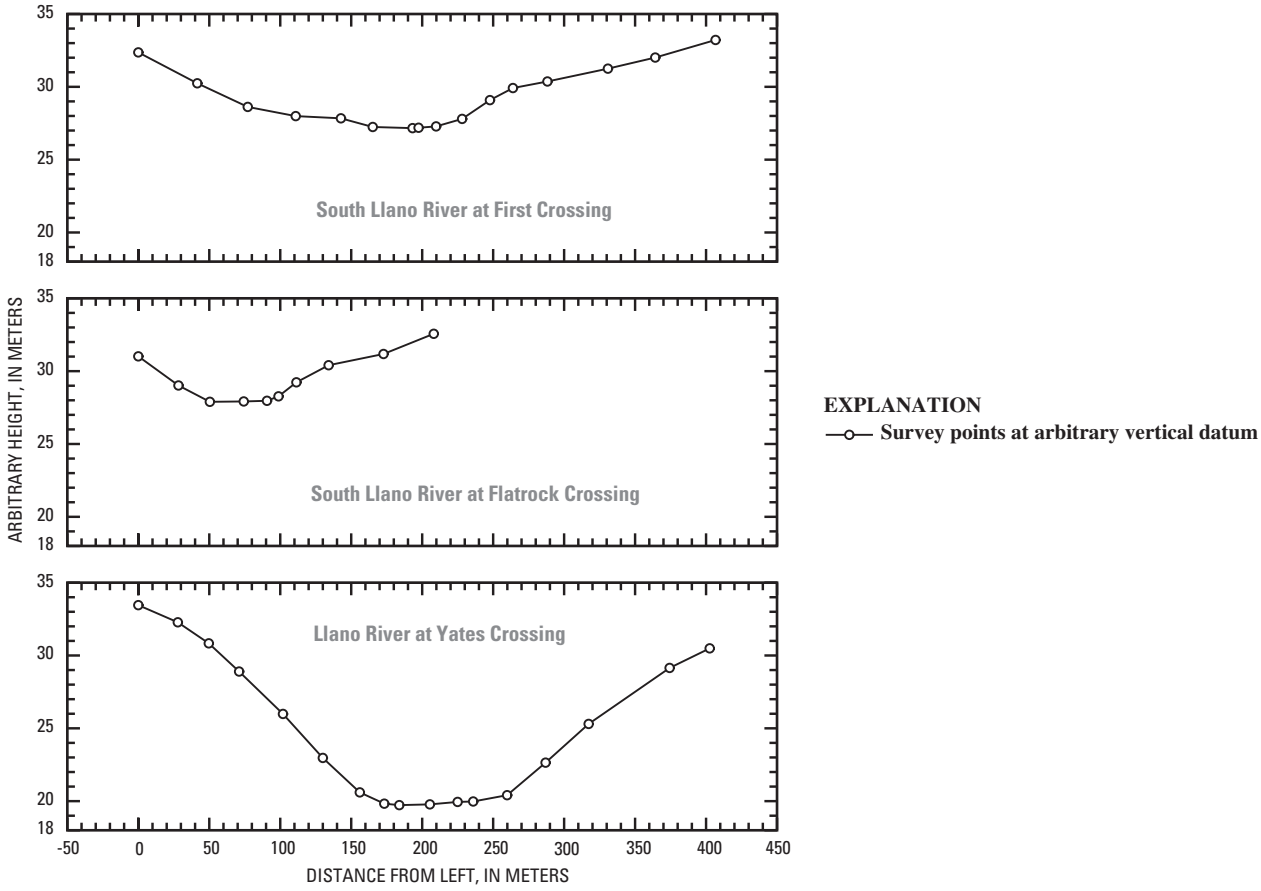

Figure 35. Cross-section graphs of selected low-water crossings in study area, Kimble County, Texas.

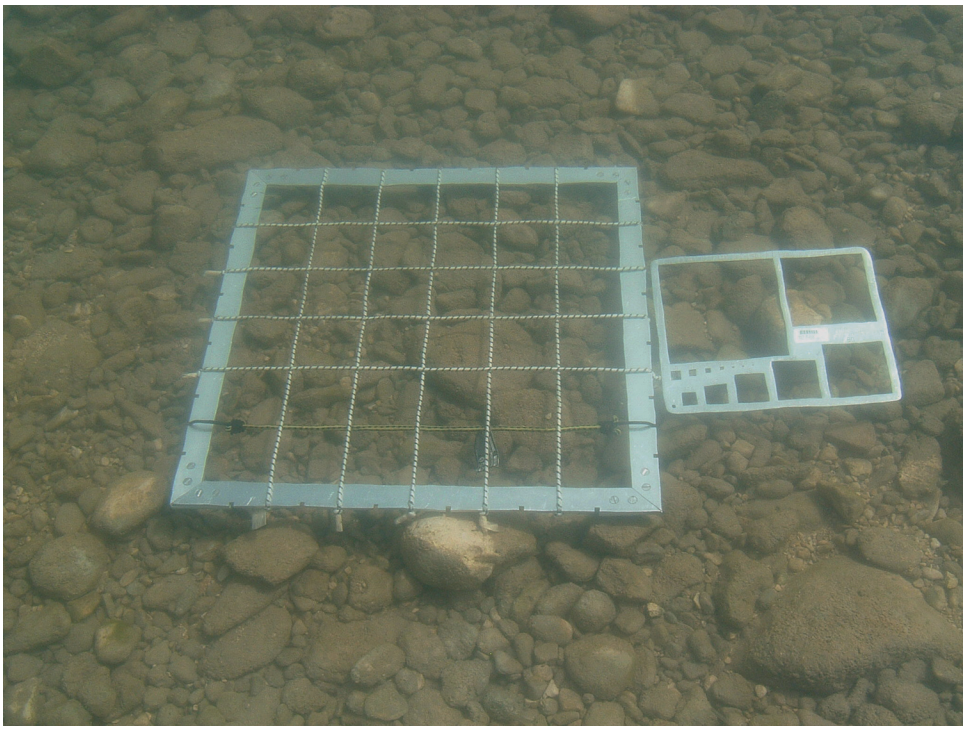

Figure 36. Underwater sampling grid and particle-size analyzer on gravel and cobble bed of South Llano River, Kimble County, Texas.

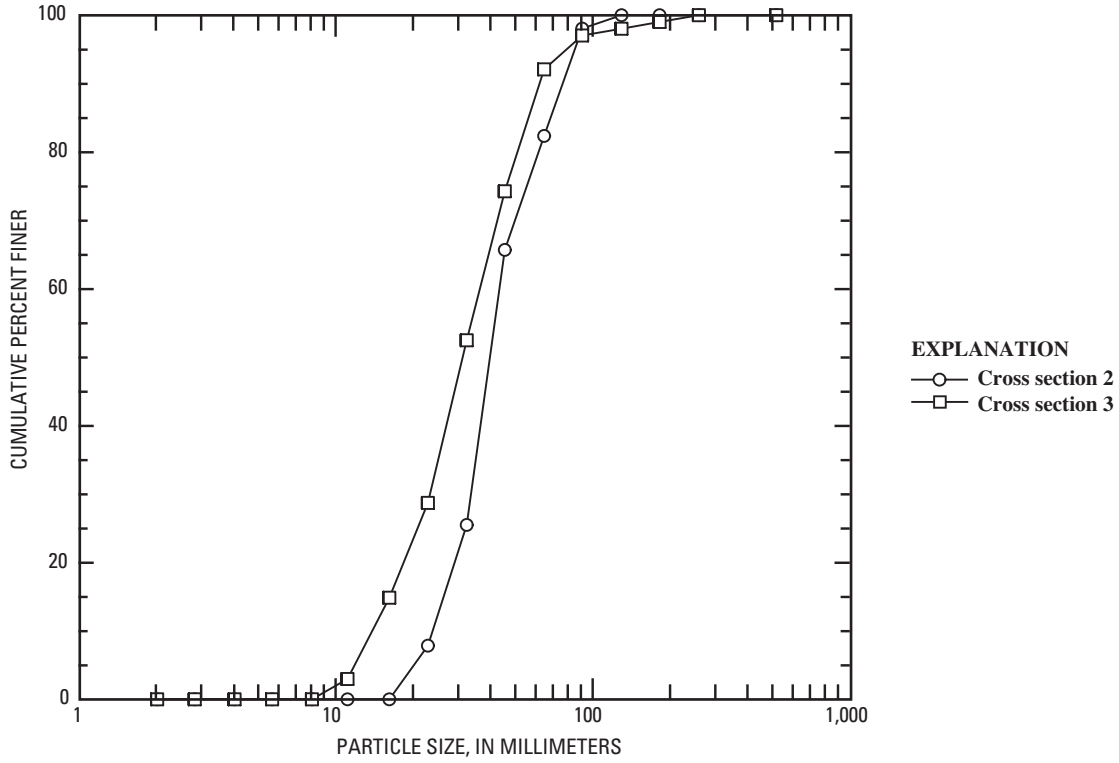

Figure 37. Bed-material particle-size distribution of North Llano River near Roosevelt, Kimble County, Texas. Most of the channel bed is bedrock. The distribution plot is for a transitional area between the channel and floodplain and one in-channel gravel bar at cross section 3.

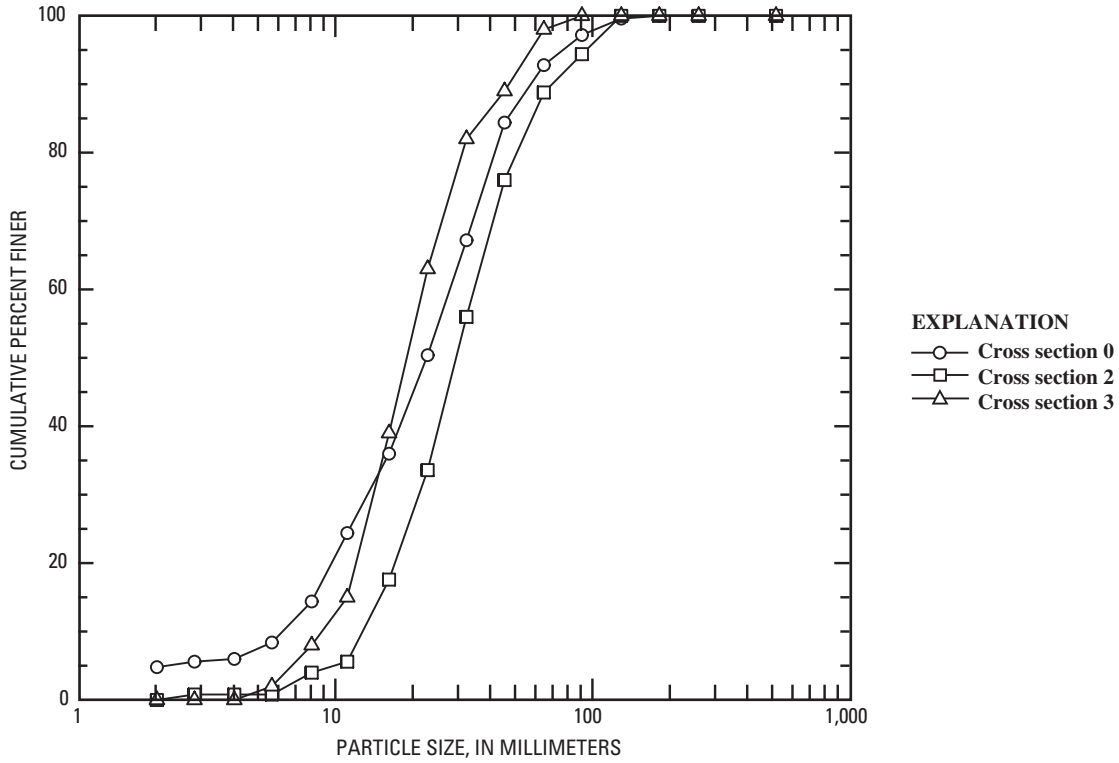

Figure 38. Bed-material particle-size distribution of North Llano River near Junction, Kimble County, Texas.

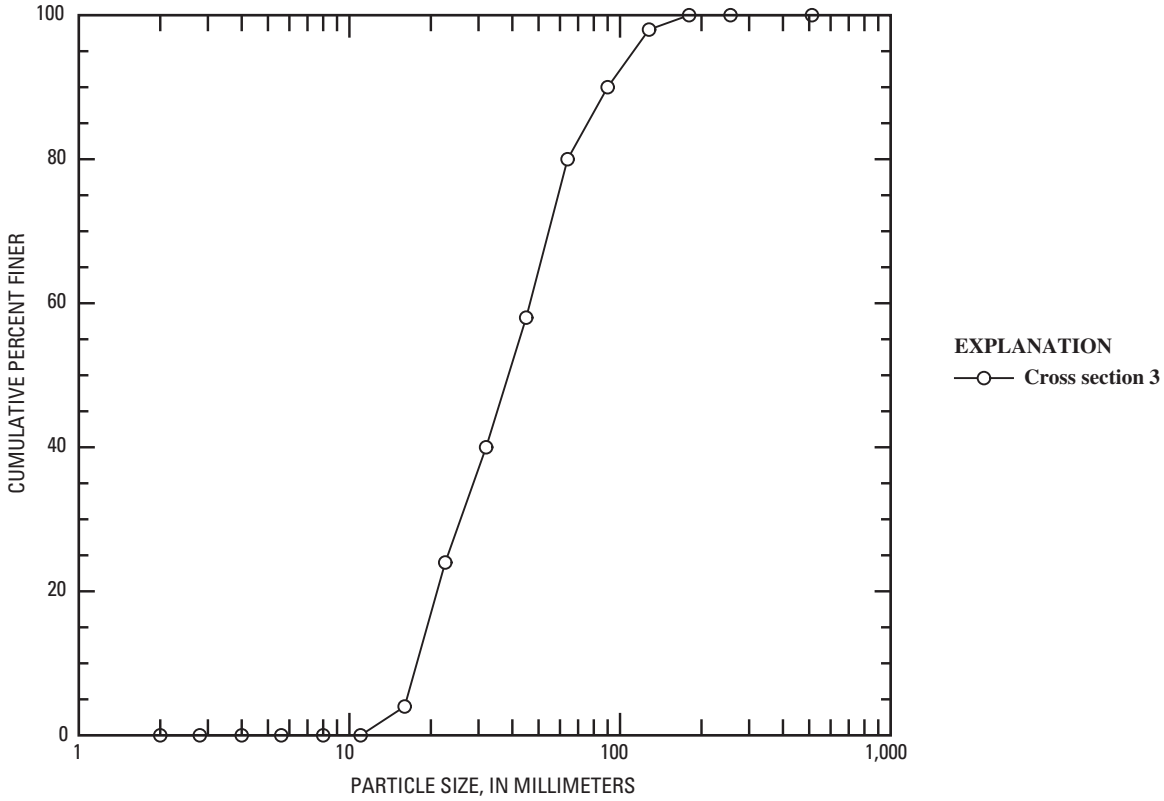

Figure 39. Bed-material particle-size distribution of South Llano River at Baker Ranch, Edwards County, Texas. Most of the bed material at the site is fine-grained (less than 2 millimeters). The distribution graph is for one isolated area of angular cobbles and gravel.

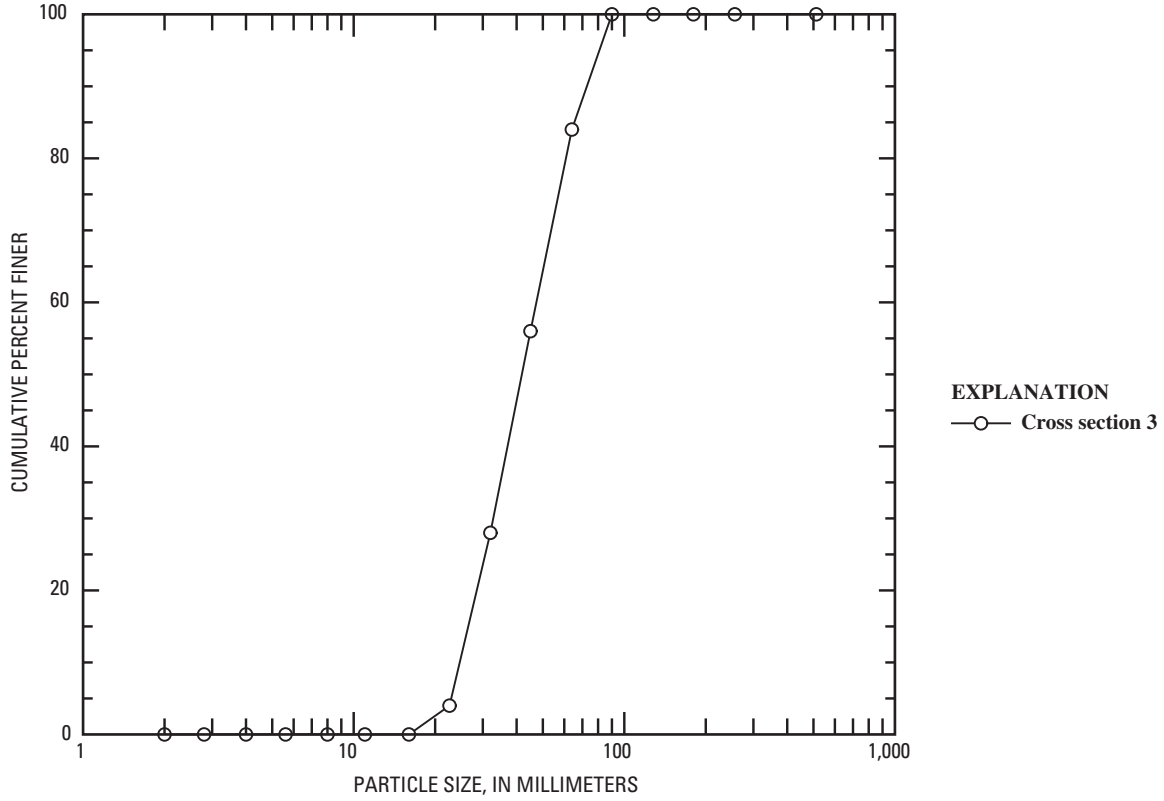

Figure 40. Bed-material particle-size distribution of South Llano River at U.S. Highway 377 near Rocksprings, Edwards County, Texas. Most of the channel bed is bedrock. The distribution plot is for one isolated area of cobbles and gravel.

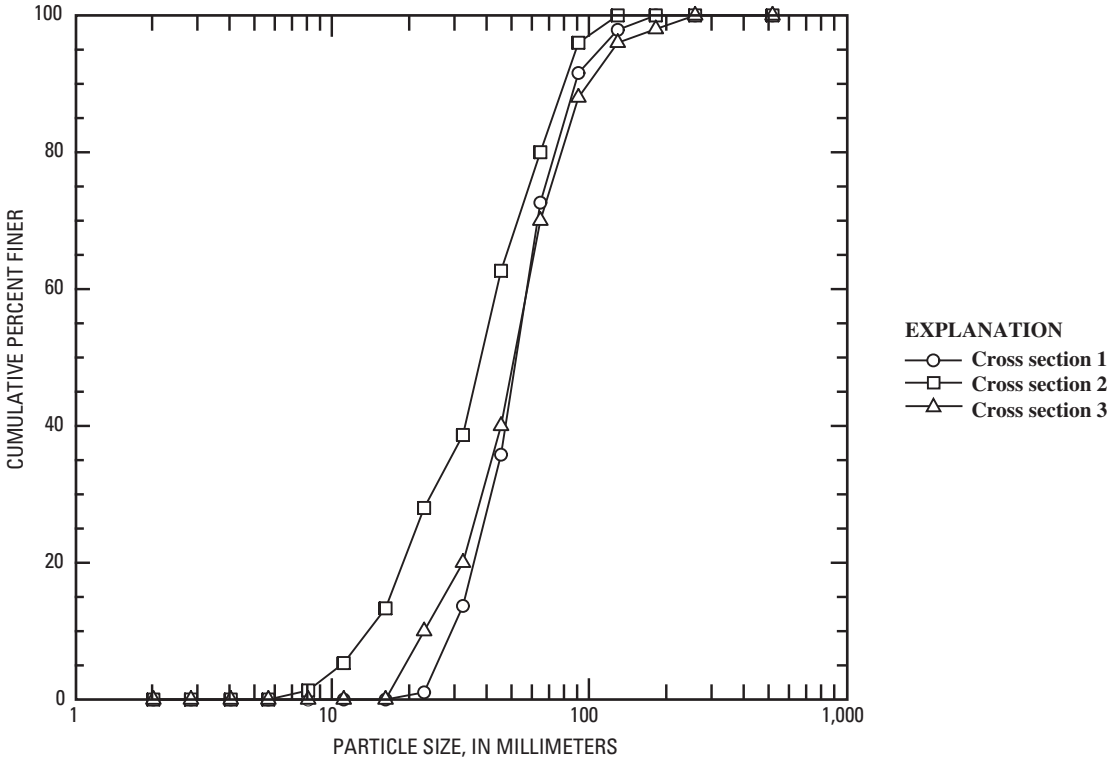

Figure 41. Bed-material particle-size distribution of South Llano River at 700 Springs Ranch, Edwards County, Texas. Most of the channel bed is bedrock. The distribution plot is for a transitional area between the channel and floodplain and one in-channel gravel bar at cross section 1.

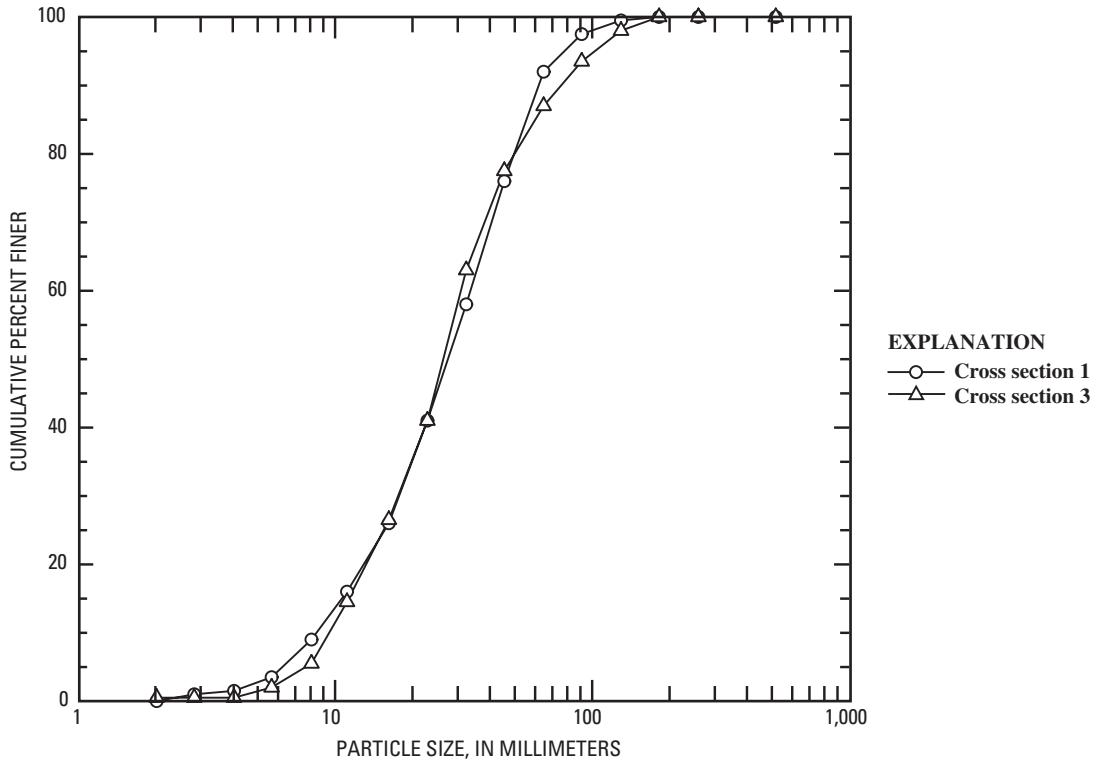

Figure 42. Bed-material particle-size distribution of South Llano River at South Llano River State Park, Kimble County, Texas.

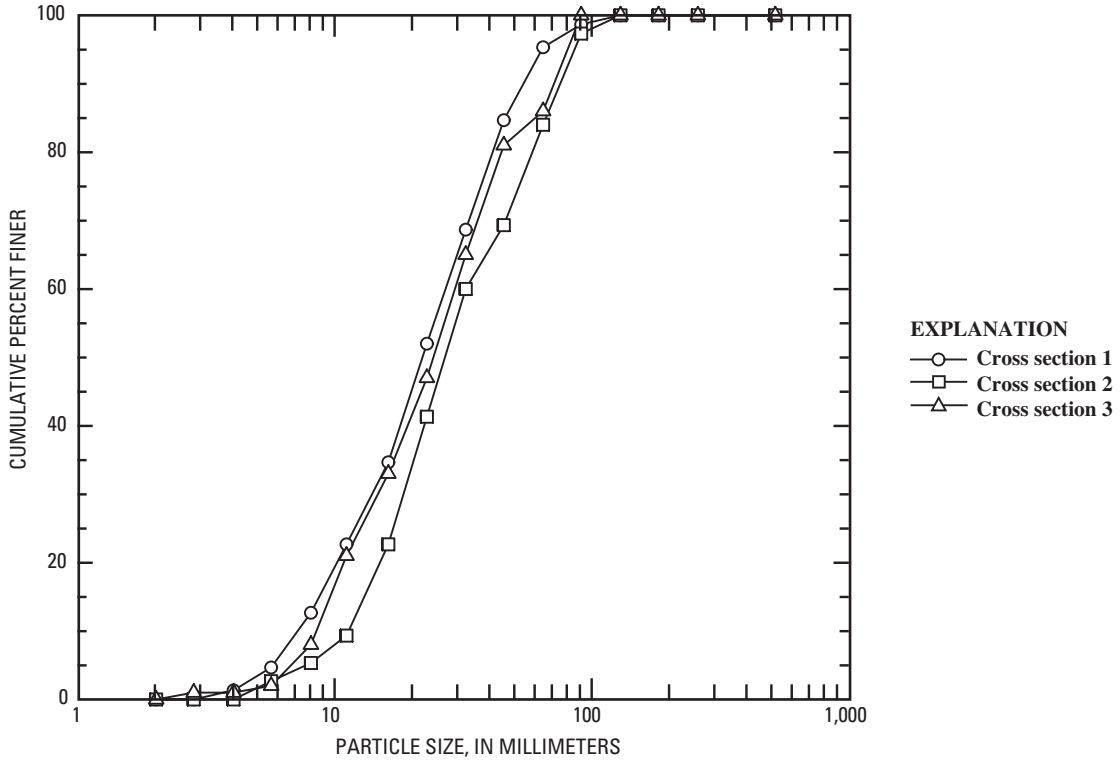

Figure 43. Bed-material particle-size distribution of South Llano River at Texas Tech University–Junction, Kimble County, Texas.

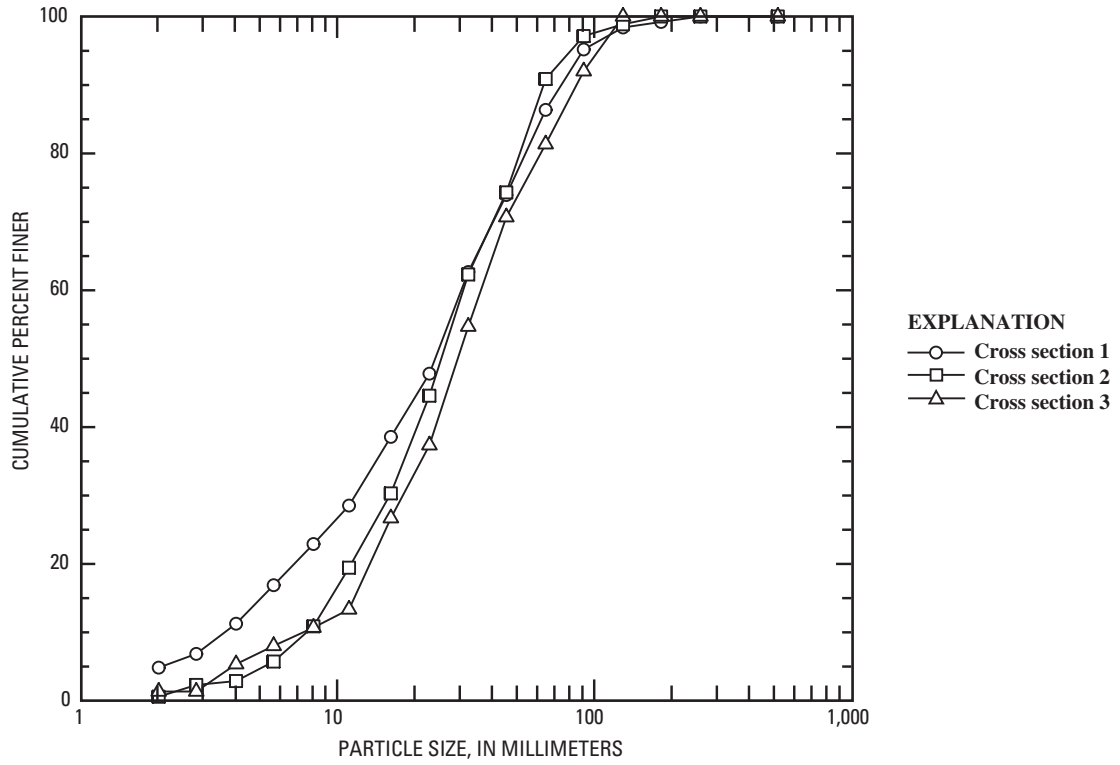

Figure 44. Bed-material particle-size distribution of Johnson Fork at Lowlands Crossing, Kimble County, Texas.

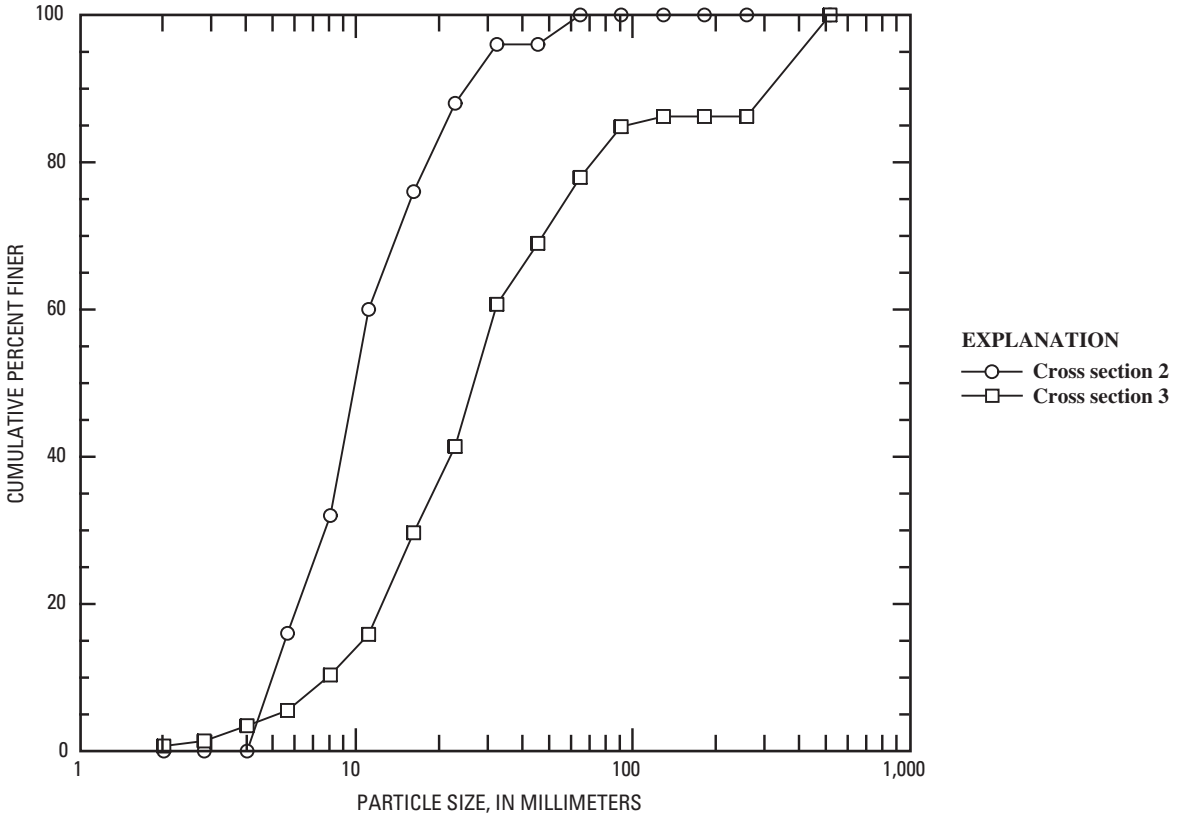

Figure 45. Bed-material particle-size distribution of Llano River near Junction, Kimble County, Texas. Most of the channel bed at cross section 2 is bedrock, except for a small side-channel bar.

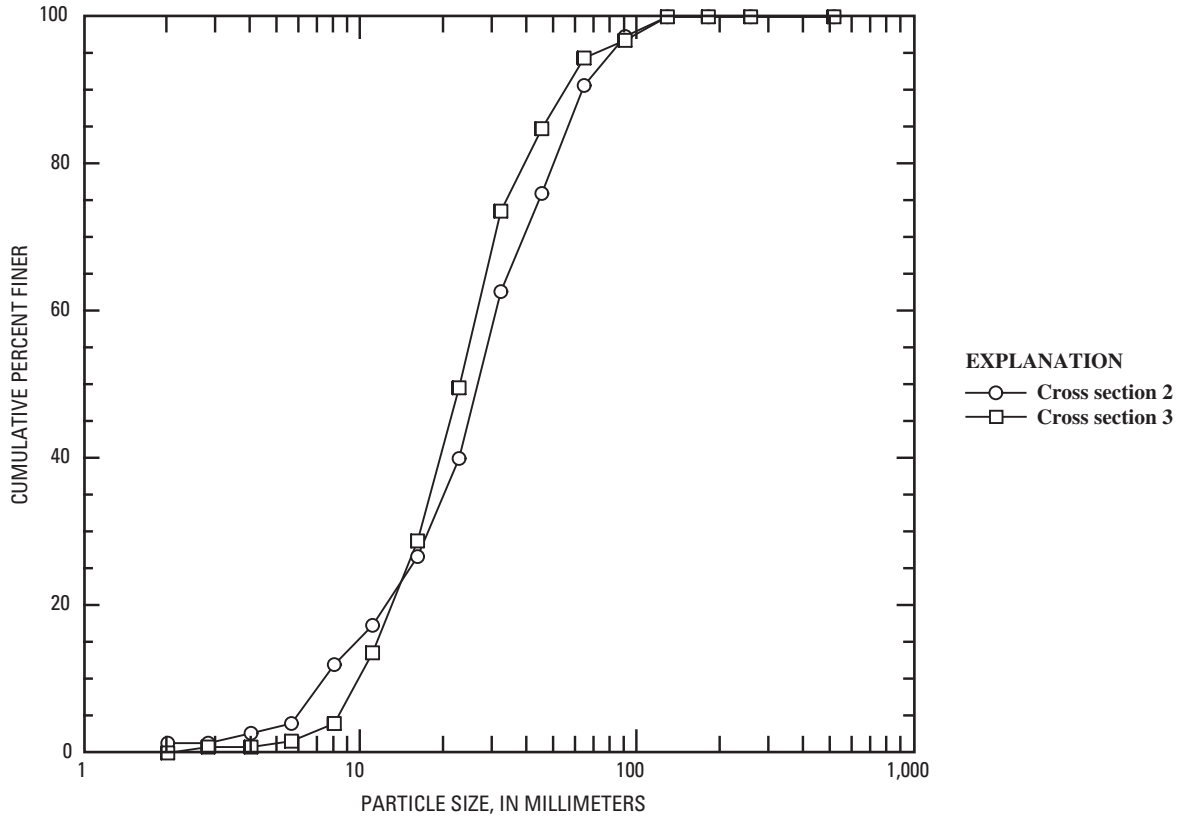

Figure 46. Bed-material particle-size distribution of Llano River near Ivy Chapel, Kimble County, Texas.

Table 4. Channel slopes computed for study sites using measured cross-sectional data, Edwards and Kimble Counties, Texas.

Study site number (fig. 2)	Study site	Channel slope (dimensionless)	Computation method
1	North Llano River near Roosevelt	0.0021	Water surface
2	North Llano River near Junction	.0029	Thalweg
3	South Llano River at Baker Ranch	.0016	Thalweg
		.0014	Floodplain
4	South Llano River at U.S. Highway 377 near Rocksprings	.0020	Thalweg
5	South Llano River at 700 Springs Ranch	.0008	Water surface
		.0012	Thalweg
7	South Llano River at South Llano River State Park	[1]0	Water surface
		.0012	Longitudinal profile
8	South Llano River at Texas Tech University–Junction	.0005	Water surface
12	Johnson Fork at Lowlands Crossing	.0053	Water surface
13	Llano River near Junction	.0071	Water surface
14	Llano River near Ivy Chapel	.0002	Water surface
		.0017	Thalweg

[1] Water surface between cross sections 1 and 2 was ponded, and no difference in elevation was detected.

Particle size generally decreases downstream, although variability is evident (fig. 47). Variability is the result of tributary inputs of coarse bed material or localized incision into older Pleistocene or Holocene terrace deposits. The generalized downstream decrease in bed-material particle size is the result of abrasion during episodes of entrainment, decreases in channel slope, and, possibly, solution of submerged particles.

Bed-Material Entrainment Potential

Bed-material entrainment refers to the incipient motion of sediment along a channel bed. During low-flow conditions in cobble- and gravel-bed rivers, coarse bed material remains in place. However, moderate- to high-flow conditions exert greater stresses on the channel bed, and coarse bed material initially mobilizes at some threshold stress, which can be associated with flow depth, flow velocity, and discharge. Computations of bed-material entrainment rely on channel-geometry and particle-size data.

The bed-material entrainment problem for TxDOT LWCs is examined at two spatial scales. First, the relative supply and abundance of cobble- and gravel-sized bed material at a site can be attributed to watershed-scale characteristics, specifically watershed slopes. Second, the stresses needed to mobilize bed material at a site can be attributed to reach-scale hydraulic factors. The two scale-dependent approaches are discussed separately below.

Relative Abundance and Activity of Bed Material

The relative abundance and activity of bed material at a site in the Edwards Plateau depends on watershed-scale factors, including lithology, historical climate patterns, land use, drainage area, and slope. For this investigation, lithology, historical climate patterns, and land use are considered approximately equal for all study sites. By default, the relative abundance and activity of bed material in the study area depends on drainage area and watershed slopes. It is expected that larger drainage areas have the potential to contribute greater amounts of sediment to downstream channel sites, and the rate at which material is supplied is controlled by watershed slopes.

During site reconnaissance trips, notes were taken to qualitatively describe the abundance and recent activity of cobble- and gravel-sized bed material at each study site (table 6). The observed channel size was considered when describing bed-material abundance, and local TxDOT personnel provided information about the activity of the bed during recent high flows. At some sites, coarse bed material dominated the channel composition, but other sites were characterized by bedrock channel beds and an absence of bed material.

Table 5. Bed-material particle-size descriptors computed for study sites, Edwards and Kimble Counties, Texas.

[d_{16}, d_{50}, and d_{84}, descriptors that represent diameters at which 16, 50, and 84 percent, respectively, of the sample is finer than; mm, millimeters]

Study site number (fig. 2)	Study site	Cross section	Total particles measured	d_{16} (mm)	d_{50} (mm)	d_{84} (mm)
1	North Llano River near Roosevelt	2	102	26.9	39.9	66.7
		3	101	16.5	31.0	55.4
2	North Llano River near Junction	0	250	8.5	22.4	44.7
		2	125	15.3	29.5	56.9
		3	100	11.2	19.0	35.7
3	South Llano River at Baker Ranch	3	50	20.0	39.2	74.4
4	South Llano River at U.S. Highway 377 near Rocksprings	1	25	27.3	42.2	64.0
5	South Llano River at 700 Springs Ranch	1	95	33.4	52.3	79.6
		2	75	17.2	38.1	70.5
		3	50	28.2	51.3	84.2
7	South Llano River at South Llano River State Park	1	200	11.0	27.6	54.5
		3	200	11.6	26.4	58.0
8	South Llano River at Texas Tech University–Junction	1	150	9.0	21.8	44.5
		2	75	13.5	27.0	64.0
		3	100	9.8	24.2	56.4
12	Johnson Fork at Lowlands Crossing	1	249	5.4	24.0	60.4
		2	175	9.8	25.5	56.1
		3	75	12.0	29.5	70.5
13	Llano River near Junction	2	25	5.6	9.9	20.4
		3	145	11.1	26.8	86.9
14	Llano River near Ivy Chapel	2	75	10.3	26.7	55.4
		3	125	11.8	22.8	44.1

As a measure of relative bed-material abundance and activity, a three-level classification was used in this investigation:

1. Level I describes channels that are clogged by bed material and undergo substantial reconfiguration during high flows (fig. 48).
2. Level II describes channels that contain individual lobes or bars of bed material that undergo some reconfiguration during high flows (fig. 49).
3. Level III describes channels that do not contain appreciable amounts of coarse bed material and do not undergo reconfiguration during high flows (fig. 50).

Mean watershed slope, computed using GIS, accounts for both drainage area and slope and is an appropriate parameter to predict relative abundance and activity of coarse bed material in the study area. The relation between mean watershed slope and the qualitative classification of coarse bed-material abundance and activity shows that steeper

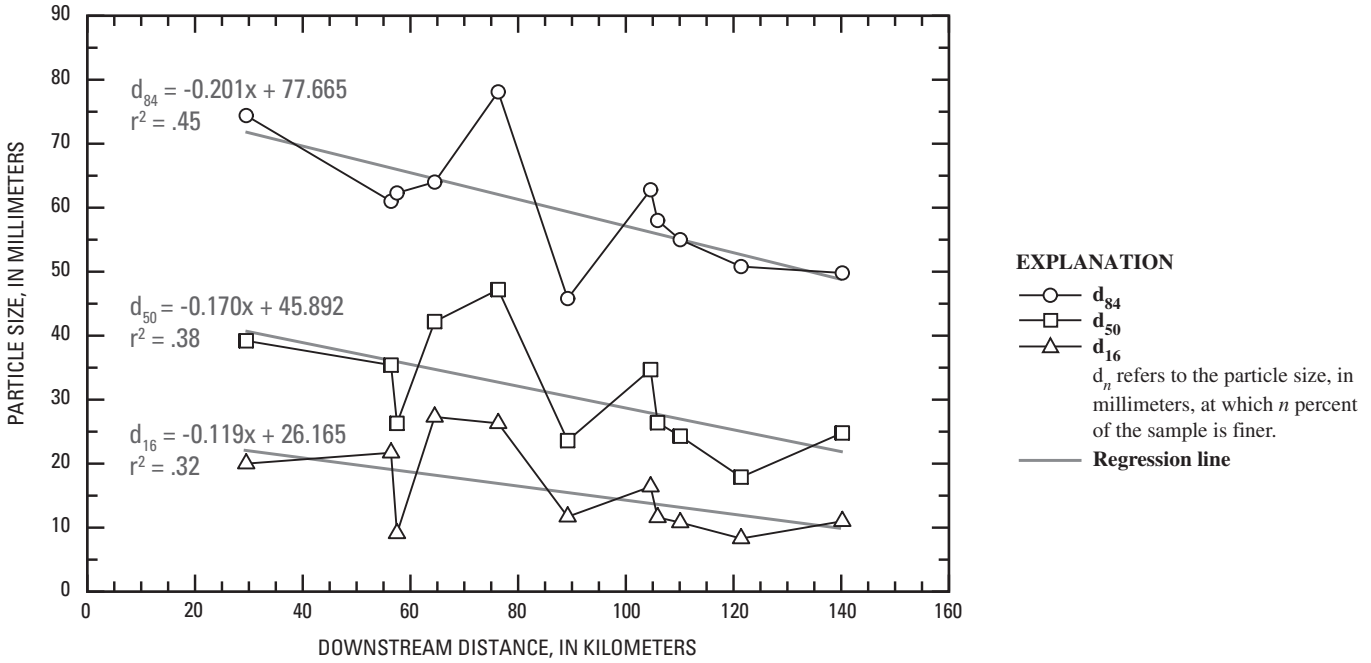

Figure 47. Mean particle size descriptors (d_{16}, d_{50}, d_{84}) and downstream distance for study sites where Wolman pebble counts were made, Edwards and Kimble Counties, Texas. Particle sizes represent the mean of all cross-sectional transects at each study site. Eleven rather than ten sites are shown because the distance between cross sections 1 and 3 at South Llano River State Park is far enough apart to consider them separate sites. Linear regression equations and r-squared values are provided.

Figure 48. Nueces River at Vance Crossing, Edwards-Real County line, Texas. Cobble- and gravel-sized bed material clogs the channel and undergoes substantial reconfiguration during high flows.

Figure 49. South Llano River at South Llano River State Park, Kimble County, Texas. Cobble- and gravel-sized bed material form longitudinal channel bars and undergo some reconfiguration during high flows.

Figure 50. South Llano River at Baker Ranch, Edwards County, Texas. The channel bed is composed of fine-grained (diameter less than 2 millimeters) bed material mixed with isolated angular cobbles and gravel.

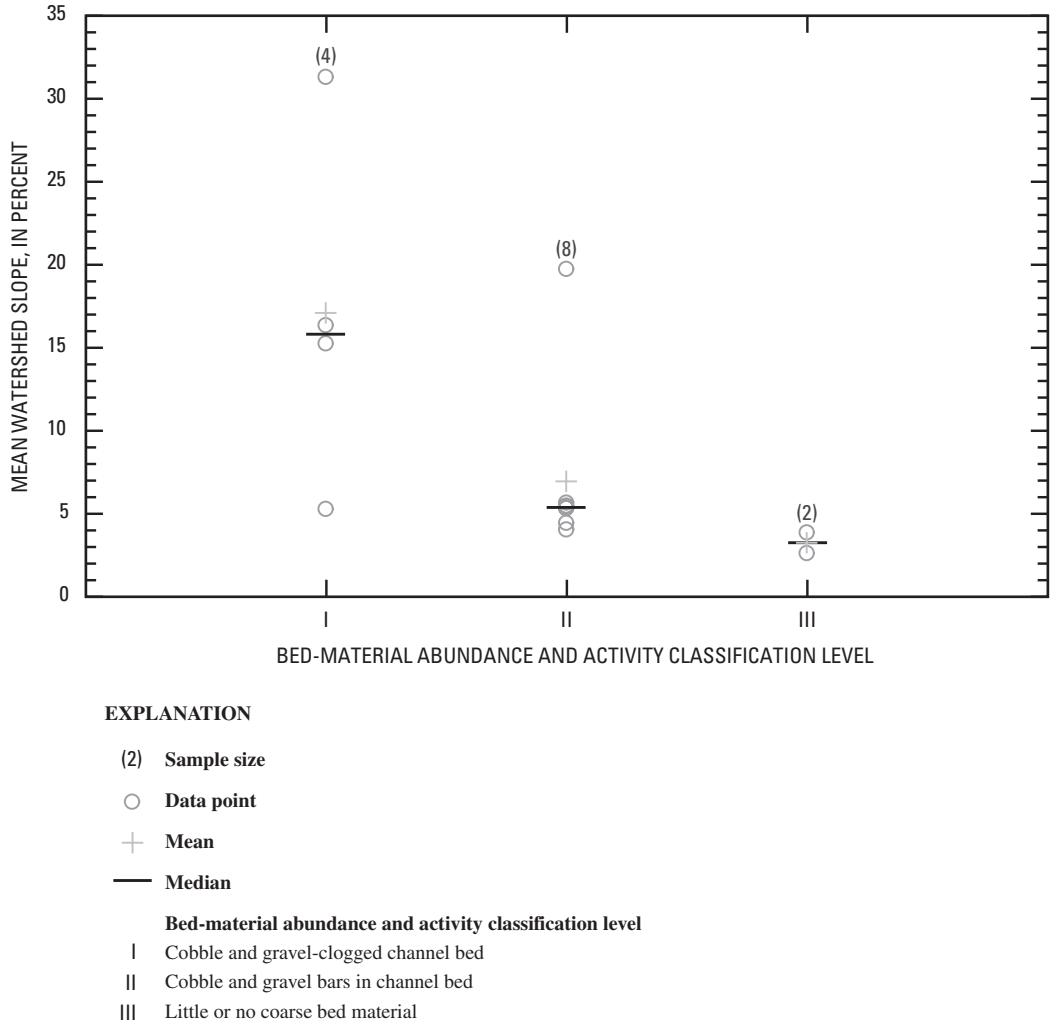

Figure 51. Distribution of mean watershed slope and qualitative bed-material abundance index and activity classification level. The statistical visualization represents mean watershed slopes, in percent, of sites classified by bed-material abundance and activity. Level I describes channels that are clogged by bed material and undergo substantial reconfiguration during high flows. Level II describes channels that contain individual lobes or bars of bed material that undergo some reconfiguration during high flows. Level III describes channels that do not contain appreciable amounts of coarse bed material and do not undergo reconfiguration during high flows.

watershed slopes contribute to the increased availability and frequent reconfiguration of cobble- and gravel-sized bed material (fig. 51).

One exception to the relation between mean watershed slope and the qualitative classification previously described is Johnson Fork at Lowlands Crossing. This site has a channel that is known for considerable quantities of coarse bed material and reconfiguration. Although overall mean watershed slope is not relatively high (5.3 percent), the site is in the lower part of the watershed, characterized by increasing numbers of steep tributaries. The site shows that exceptions to the relation of mean watershed slope to bed-material abundance and activity can be explained by proximity to the highest slopes of the watershed.

Stresses Needed to Mobilize (Entrain) Bed Material

Site-specific computations of bed-material entrainment are based on the relation between the critical shear stress (τ_c) required to initially mobilize sediment and the boundary shear stress (τ_o) exerted by a given flow. Boundary shear stress (Elliott, 2002) can be computed from:

$$\tau_o = \gamma R S, \quad (1)$$

where

τ_o is the boundary shear stress, in newtons per square meter;
γ is the specific weight of water at 20 degrees Celsius (9,789 newtons per cubic meter);

Table 6. Qualitative observations and classification of coarse bed-material abundance and activity at selected study sites, Edwards, Kimble, and Real Counties, Texas.

[I, cobble- and gravel-choked channel bed, substantial reconfiguration during high flows; II, cobble and gravel bars in channel bed, moderate reconfiguration during high flows; III, little or no coarse bed material, little to no reconfiguration during high flows]

Study site number (fig. 2)	Study site	Qualitative bed-material abundance and activity classification level
1	North Llano River near Roosevelt	II
2	North Llano River near Junction	II
3	South Llano River at Baker Ranch	III
4	South Llano River at U.S. Highway 377 near Rocksprings	III
5	South Llano River at 700 Springs Ranch	II
7	South Llano River at South Llano River State Park	II
8	South Llano River at Texas Tech University–Junction	II
12	Johnson Fork at Lowlands Crossing	I
13	Llano River near Junction	II
14	Llano River near Ivy Chapel	II
16	Nueces River at Ben Williams Crossing	I
17	Nueces River at Vance Crossing	I
18	Cedar Creek at Ranch Road 336	I
19	Frio River at Upper Ranch Road 1120 Crossing	II

R is the hydraulic radius, in meters; mean depth commonly is used as a substitute; and

S is the energy gradient, in meters per meter; channel slope commonly is used as a substitute.

Critical shear stress (Elliott, 2002) can be computed from:

$$\tau_c = \tau^* (\gamma_s - \gamma) d_n, \quad (2)$$

where

τ_c is the critical shear stress, in newtons per square meter;

τ^* is the dimensionless shear stress or Shields parameter (0.045);

γ_s is the specific weight of the calcite sediment (26,430 newtons per cubic meter); and

d_n is the particle size, in meters, at which n percent of the sediment is finer.

The dimensionless shear stress (τ^*) (Shields, 1936) can be modified according to bed-material particle size and bed roughness. Elliott (2002) uses a τ^* value of 0.030 for channel beds composed of coarse material, appropriate for hazard-mitigation investigations because shallow flow depths and lesser discharges will result in bed-material entrainment (Shen and Julien, 1993). Others have found that a τ^* value of 0.030 is a minimum associated with sand-sized beds (Knighton, 1998), and surfaces with a relatively greater roughness height commonly attain a τ^* value of 0.045 (Komar, 1988; Robert, 2003). For purposes of this investigation, a τ^* value of 0.045 is used in computations of critical shear stress because cobble- and gravel-sized beds support hydraulically rough conditions at moderate to high flows. The particle size (d_n) used in computations of critical shear stress depends on the purpose of the investigation. For a variety of applications, d_{50}, the median particle size, is used in computations of bed-material entrainment (see Elliott, 2002).

The critical shear stress represents the hydraulic conditions at which incipient motion of bed particles of size n occur, but mobilization is limited to a few particles. Elliott (2002) also computes a complete entrainment threshold at which the boundary shear stress is twice the critical shear stress for the given particle size. The complete entrainment threshold describes the conditions at which widespread mobilization of bed sediment occurs. Factors other than shear stress have been linked to bed-material entrainment, including turbulence and channel size (Knighton, 1998), but this investigation did not consider those factors.

For this investigation, critical shear stress values were computed (tables 7 and 8) using equation 2 for all cross sections in the study area that have particle-size data (see

Table 7. Computations for initial bed-material entrainment at sites with particle-size data, Edwards and Kimble Counties, Texas.

[d_{16}, d_{50}, and d_{84}, descriptors that represent diameters at which 16, 50, and 84 percent, respectively, of the sample is finer than; τ_c, critical shear stress; N/m^2, newtons per square meter; Q, discharge; m^3/s, cubic meters per second; ft^3/s, cubic feet per second; --, not computed]

Study site number (fig. 2)	Study site	Cross section	d_{16} τ_c (N/m^2)	d_{50} τ_c (N/m^2)	d_{84} τ_c (N/m^2)	Manning's *n*	d_{16} Q [m^3/s (ft^3/s)]	d_{50} Q [m^3/s (ft^3/s)]	d_{84} Q [m^3/s (ft^3/s)]
1	North Llano River near Roosevelt	2	20.14	29.88	49.95	0.040	18.1 (639)	54.4 (1,920)	162 (5,700)
		3	12.36	23.21	41.49	.035	10.7 (379)	47.6 (1,680)	684 (24,100)
2	North Llano River near Junction	0	6.37	16.77	33.47	.040	1.74 (61.4)	14.2 (502)	53.3 (1,880)
		2	11.46	22.09	42.61	.035	18.9 (668)	63.8 (2,250)	234 (8,260)
		3	8.39	14.23	26.73	.035	6.48 (229)	19.4 (686)	69.5 (2,450)
3	South Llano River at Baker Ranch	3	14.98	29.36	55.72	.027	105 (3,710)	626 (22,100)	-- (--)
4	South Llano River at U.S. Highway 377 near Rocksprings	1	20.44	31.60	47.93	.027	98.9 (3,490)	242 (8,530)	542 (19,100)
5	South Llano River at 700 Springs Ranch	1	25.01	39.17	59.61	.035	292 (10,300)	923 (32,600)	2,680 (94,800)
		2	12.88	28.53	52.79	.030	52.8 (1,860)	568 (20,000)	2,490 (88,000)
		3	21.12	38.42	63.05	.030	309 (10,900)	1,000 (35,300)	3,200 (113,000)
7	South Llano River at South Llano River State Park	1	8.24	20.67	40.81	.040	7.18 (253)	202 (7,130)	1,330 (46,900)
		3	8.69	19.77	43.43	.040	15.9 (563)	222 (7,830)	1,090 (38,600)
8	South Llano River at Texas Tech University–Junction	1	6.74	16.33	33.32	.035	86.2 (3,040)	733 (25,900)	3,970 (140,000)
		2	10.11	20.22	47.93	.035	220 (7,760)	1,180 (41,800)	-- (--)
		3	7.34	18.12	42.24	.035	54.4 (1,920)	864 (30,500)	-- (--)
12	Johnson Fork at Lowlands Crossing	1	4.04	17.97	45.23	.035	.11 (4.0)	5.95 (210)	146 (5,160)
		2	7.34	19.10	42.01	.035	.34 (12.0)	14.4 (509)	126 (4,470)
		3	8.99	22.09	52.79	.035	1.62 (57.1)	11.8 (416)	210 (7,430)
13	Llano River near Junction	2	4.19	7.41	15.28	.035	.2 (7.2)	.3 (10.5)	1.58 (55.7)
		3	8.31	20.07	65.08	.035	.58 (20.6)	4.42 (156)	253 (8,950)
14	Llano River near Ivy Chapel	2	7.71	19.99	41.49	.035	8.82 (311)	140 (4,940)	637 (22,500)
		3	8.84	17.07	33.02	.035	2.24 (79.1)	103 (3,640)	402 (14,200)

Table 8. Computations for complete bed-material entrainment at sites with particle-size data, Edwards and Kimble Counties, Texas.

[d_{16}, d_{50}, and d_{84}, descriptors that represent diameters at which 16, 50, and 84 percent, respectively, of the sample is finer than; τ_c, critical shear stress; N/m^2, newtons per square meter; Q, discharge; m^3/s, cubic meters per second; ft^3/s, cubic feet per second; --, not computed]

Study site number (fig. 2)	Study site	Cross section	d_{16} τ_c (N/m^2)	d_{50} τ_c (N/m^2)	d_{84} τ_c (N/m^2)	Manning's *n*	d_{16} Q [m^3/s (ft^3/s)]	d_{50} Q [m^3/s (ft^3/s)]	d_{84} Q [m^3/s (ft^3/s)]
1	North Llano River near Roosevelt	2	40.29	59.76	99.90	0.040	104 (3,670)	243 (8,570)	1,090 (38,500)
		3	24.71	46.43	82.97	.035	271 (9,570)	859 (30,300)	2,370 (83,800)
2	North Llano River near Junction	0	12.73	33.55	66.95	.040	7.34 (259)	53.4 (1,890)	224 (7,920)
		2	22.92	44.18	85.22	.035	65.4 (2,310)	269 (9,490)	877 (31,000)
		3	16.77	28.46	53.47	.035	33.6 (1,190)	81.7 (2,880)	258 (9,120)
3	South Llano River at Baker Ranch	3	29.95	58.71	111.43	.027	635 (22,400)	-- (--)	-- (--)
4	South Llano River at U.S. Highway 377 near Rocksprings	1	40.89	63.20	95.85	.027	403 (14,200)	988 (34,900)	2,580 (91,100)
5	South Llano River at 700 Springs Ranch	1	50.02	78.33	119.22	.035	1,790 (63,100)	5,180 (183,000)	-- (--)
		2	25.76	57.06	105.59	.030	456 (16,100)	3,020 (107,000)	-- (--)
		3	42.24	76.83	126.11	.030	1,200 (42,500)	5,220 (184,000)	-- (--)
7	South Llano River at South Llano River State Park	1	16.47	41.34	81.63	.040	103 (3,640)	1,340 (47,300)	6,740 (238,000)
		3	17.37	39.54	86.87	.040	179 (6,310)	813 (28,700)	-- (--)
8	South Llano River at Texas Tech University–Junction	1	13.48	32.65	66.65	.035	454 (16,000)	3,840 (136,000)	-- (--)
		2	20.22	40.44	95.85	.035	1,180 (41,800)	-- (--)	-- (--)
		3	14.68	36.24	84.47	.035	411 (14,500)	-- (--)	-- (--)
12	Johnson Fork at Lowlands Crossing	1	8.09	35.95	90.46	.035	1.51 (53.2)	57.8 (2,040)	521 (18,400)
		2	14.68	38.19	84.02	.035	2.42 (85.5)	91.6 (3,230)	539 (19,000)
		3	17.97	44.18	105.59	.035	5.64 (199)	164 (5,810)	858 (30,300)
13	Llano River near Junction	2	8.39	14.83	30.55	.035	.35 (12.5)	1.55 (54.6)	17.4 (614)
		3	16.62	40.14	130.15	.035	2.32 (81.9)	85.1 (3,010)	892 (31,500)
14	Llano River near Ivy Chapel	2	15.43	39.99	82.97	.035	56.0 (1,980)	585 (20,700)	2,540 (89,700)
		3	17.67	34.15	66.05	.035	116 (4,110)	439 (15,500)	1,580 (55,900)

table 5). Critical shear stress values were computed for three particle-size descriptors: d_{16}, d_{50}, and d_{84}. Complete entrainment thresholds were computed by doubling the critical shear stress values. Hydraulic radius (R) values were back-computed by equating the critical shear stress to the boundary shear stress in equation 1. For sites with cross-sectional geometric data, hydraulic radius (R) values were associated with channel cross-sectional areas (A) by using output files from cross-sectional analyses in WinXSPro. Manning's n roughness coefficients, based on suggestions in Arcement and Schneider (1989) and the authors' judgment, were assigned to individual cross sections. Flow velocity (U) values for combinations of critical shear stress, complete entrainment, and particle-size descriptors at each cross section were computed from (Shen and Julien, 1993):

$$U = (1/n) R^{2/3} S^{1/2}, \quad (3)$$

where

U is flow velocity in meters per second;
n is Manning's roughness coefficient;
R is the hydraulic radius, in meters; and
S is channel slope, in meters per meter.

Next, discharge (Q) values for combinations of critical shear stress, complete entrainment, and particle-size descriptors at each cross section were computed from:

$$Q = UA, \quad (4)$$

where

Q is discharge in cubic meters per second; and
A is cross-sectional area in square meters.

Finally, the Froude number, a dimensionless number quantifying the resistance of an object moving through water, was computed for combinations of critical shear stress, complete entrainment, and particle-size descriptors at each cross section. The Froude number is computed from Sturm (2001):

$$F = U/(g R)^{1/2}, \quad (5)$$

where

F is the dimensionless Froude number; and
g is the gravitational constant (9.80 meters per square second).

For convenience, the hydraulic radius (R) substitutes for depth (D).

Critical shear stress values show variation from site to site as a result of differences in particle-size descriptors (d_{16}, d_{50}, and d_{84}). Greater variability becomes evident in back-computations of hydraulic radiuses necessary for initial or complete entrainment as a result of differences in channel slope. Finally, further variability in the cross-sectional areas associated with computed hydraulic radiuses lead to considerably different discharges responsible for bed-material entrainment. The results in tables 7 and 8 show that site-by-site assessments probably cannot support broad regional interpretations of bed-material entrainment frequency, especially when data are collected at sites that might not reflect the average condition of most channel reaches.

An alternative to the site-by-site approach is using an average- or expected-condition approach. Parameters that can be generalized in computations of bed-material entrainment are channel slope and particle size. The median channel slope of all study sites is 0.0017, appropriate for main channels in the study area because of relatively straight or linear longitudinal profiles (figs. 11–14). Linear regression models were applied to predict the particle-size descriptors d_{16}, d_{50}, and d_{84}, for a given downstream distance from the headwater source. Figure 47 shows a general downstream decrease in particle size for the study sites, described by the following regression-fitted equations:

$$d_{16} = -0.119x + 26.165, \quad (6)$$

$$d_{50} = -0.170x + 45.892, \text{ and} \quad (7)$$

$$d_{84} = -0.201x + 77.665, \quad (8)$$

where

d_n is the particle size, in millimeters, at which n percent of sediment is finer; and
x is downstream distance, in kilometers.

R-squared values of .32 apply to equation 6, .38 to equation 7, and .45 to equation 8.

The median channel slope, 0.0017, and the particle-size descriptors computed from equations 6 to 8 are used in equations 2 and 3. A median n of 0.035 is used to compute flow velocity in equation 3. Finally, equation 4 is used to compute the discharges required to entrain the expected particle size for a given downstream distance.

The average- or expected-condition approach limits the variability inherent in site-by-site analysis and represents general downstream conditions. In general, the average-condition approach slightly reduced the discharges required to entrain bed material in upper channel reaches and slightly increased the discharges required to entrain bed material in lower channel reaches. The results are desirable, because the site-by-site approach overestimated discharges required for bed-material entrainment in upper channel reaches and underestimated discharges required for bed-material entrainment in lower channel reaches. The average-condition approach should only be applied along channel reaches that have slopes within one magnitude and a relatively consistent downstream reduction of bed-material particle size. The results from application of the average-condition approach are presented in tables 9 and 10.

Table 9. Computations for initial bed-material entrainment at sites with particle-size data, Edwards and Kimble Counties, Texas, using average-condition approach based on median channel slope, downstream decrease of particle size, and median Manning's *n*.

[d_{16}, d_{50}, and d_{84}, descriptors that represent diameters at which 16, 50, and 84 percent, respectively, of the sample is finer than; τ_c, critical shear stress; N/m^2, newtons per square meter; Q, discharge; m^3/s, cubic meters per second; ft^3/s, cubic feet per second; --, not computed]

Study site number (fig. 2)	Study site	Cross section	d_{16} τ_c (N/m^2)	d_{50} τ_c (N/m^2)	d_{84} τ_c (N/m^2)	d_{16} Q [m^3/s (ft^3/s)]	d_{50} Q [m^3/s (ft^3/s)]	d_{84} Q [m^3/s (ft^3/s)]
1	North Llano River near Roosevelt	2	14.60	27.18	49.65	17.3 (610)	60.5 (2,130)	190 (6,730)
		3	14.60	27.18	49.65	12.4 (439)	54.7 (1,930)	798 (28,200)
2	North Llano River near Junction	0	11.68	22.99	44.71	3.26 (115)	21.9 (774)	80.8 (2,850)
		2	11.68	22.99	44.71	20.9 (739)	71.6 (2,530)	264 (9,330)
		3	11.68	22.99	44.71	8.84 (312)	29.2 (1,030)	107 (3,780)
3	South Llano River at Baker Ranch	3	17.00	30.63	53.69	86.4 (3,050)	380 (13,400)	-- (--)
4	South Llano River at U.S. Highway 377 near Rocksprings	1	13.85	26.14	48.45	42.7 (1,510)	169 (5,960)	567 (20,000)
5	South Llano River at 700 Springs Ranch	1	12.81	24.64	46.65	176 (6,220)	640 (22,600)	2,150 (75,900)
		2	12.81	24.64	46.65	42.5 (1,500)	416 (14,700)	1,860 (65,500)
		3	12.81	24.64	46.65	179 (6,320)	601 (21,200)	2,120 (74,800)
7	South Llano River at South Llano River State Park	1	10.26	21.04	42.39	8.96 (316)	220 (7,780)	1,470 (51,800)
		3	10.18	20.82	42.16	19.1 (675)	248 (8,740)	1,160 (40,800)
8	South Llano River at Texas Tech University–Junction	1	9.81	20.29	41.56	90.3 (3,190)	691 (24,400)	3,760 (133,000)
		2	9.81	20.29	41.56	176 (6,200)	968 (34,200)	-- (--)
		3	9.81	20.29	41.56	53.8 (1,900)	760 (26,800)	-- (--)
12	Johnson Fork at Lowlands Crossing	1	14.45	27.03	49.50	.32 (11.4)	9.44 (333)	188 (6,630)
		2	14.45	27.03	49.50	.64 (22.7)	22.0 (776)	171 (6,020)
		3	14.45	27.03	49.50	2.68 (94.7)	16.3 (575)	244 (8,600)
13	Llano River near Junction	2	8.76	18.87	39.84	.42 (14.9)	.7 (24.9)	3.79 (134)
		3	8.76	18.87	39.84	.77 (27.1)	5.38 (190)	232 (8,190)
14	Llano River near Ivy Chapel	2	7.11	16.47	36.99	8.36 (295)	123 (4,340)	590 (20,800)
		3	7.11	16.47	36.99	1.94 (68.5)	101 (3,550)	433 (15,300)

Table 10. Computations for complete bed-material entrainment at sites with particle-size data, Edwards and Kimble Counties, Texas, using average-condition approach based on median channel slope, downstream decrease of particle size, and median Manning's *n*.

[d_{16}, d_{50}, and d_{84}, descriptors that represent diameters at which 16, 50, and 84 percent, respectively, of the sample is finer than; τ_c, critical shear stress; N/m^2, newtons per square meter; Q, discharge; m^3/s, cubic meters per second; ft^3/s, cubic feet per second; --, not computed]

Study site number (fig. 2)	Study site	Cross section	$d_{16}\ \tau_c$ (N/m^2)	$d_{50}\ \tau_c$ (N/m^2)	$d_{84}\ \tau_c$ (N/m^2)	d_{16} Q [m^3/s (ft^3/s)]	d_{50} Q [m^3/s (ft^3/s)]	d_{84} Q [m^3/s (ft^3/s)]
1	North Llano River near Roosevelt	2	29.21	54.37	99.30	99.4 (3,510)	270 (9,530)	1,290 (45,400)
		3	29.21	54.37	99.30	314 (11,100)	988 (34,900)	2,770 (97,900)
2	North Llano River near Junction	0	23.36	45.98	89.41	13.7 (485)	82.3 (2,910)	340 (12,000)
		2	23.36	45.98	89.41	72.4 (2,560)	302 (10,600)	990 (35,000)
		3	23.36	45.98	89.41	45.8 (1,620)	123 (4,340)	398 (14,000)
3	South Llano River at Baker Ranch	3	34.00	61.26	107.39	527 (18,600)	-- (--)	-- (--)
4	South Llano River at U.S. Highway 377 near Rocksprings	1	27.71	52.27	96.90	189 (6,660)	659 (23,300)	2,720 (96,100)
5	South Llano River at 700 Springs Ranch	1	25.61	49.27	93.31	1,080 (38,100)	3,590 (127,000)	-- (--)
		2	25.61	49.27	93.31	367 (13,000)	2,220 (78,200)	-- (--)
		3	25.61	49.27	93.31	697 (24,600)	3,140 (111,000)	-- (--)
7	South Llano River at South Llano River State Park	1	20.52	42.09	84.77	129 (4,540)	1,460 (51,600)	7,450 (263,000)
		3	20.37	41.64	84.32	214 (7,570)	908 (32,000)	-- (--)
8	South Llano River at Texas Tech University–Junction	1	19.62	40.59	83.12	476 (16,800)	3,620 (128,000)	-- (--)
		2	19.62	40.59	83.12	947 (33,400)	-- (--)	-- (--)
		3	19.62	40.59	83.12	406 (14,300)	-- (--)	-- (--)
12	Johnson Fork at Lowlands Crossing	1	28.91	54.07	99.00	4.26 (150)	91.7 (3,240)	669 (23,600)
		2	28.91	54.07	99.00	4.60 (162)	140 (4,930)	727 (25,700)
		3	28.91	54.07	99.00	9.36 (331)	227 (8,030)	994 (35,100)
13	Llano River near Junction	2	17.52	37.74	79.68	.73 (25.8)	3.66 (129)	41.8 (1,480)
		3	17.52	37.74	79.68	3.05 (108)	104 (3,660)	817 (28,800)
14	Llano River near Ivy Chapel	2	14.23	32.95	73.99	53.1 (1,870)	515 (18,200)	2,350 (83,100)
		3	14.23	32.95	73.99	101 (3,560)	429 (15,200)	1,710 (60,300)

The parameter showing the least variability for interpretation of bed-material entrainment is the Froude number. The Froude numbers computed for all combinations of critical shear stress, complete entrainment, and particle-size descriptors at each cross section (tables 11 and 12) are less than 1, implying that subcritical flows are responsible for bed-material entrainment in the study area. Variability in the Froude number is greater for the site-by-site analysis, but is greatly reduced for the average-condition approach. Using the average-condition approach, Froude numbers of 0.40 and 0.45 are associated with initial and complete entrainment, respectively, of bed material as large as the median particle size (d_{50}). For culvert or LWC design, use of the Froude number at which bed material is mobilized is advantageous because structures can be designed to accommodate certain flow velocities at depth.

Risk-Oriented Interpretation Using Flood Frequency

Discharges necessary to initially or completely entrain bed material at study sites (tables 7–10) can be associated with flood-frequency analyses to estimate the potential for bed-material entrainment in the study area. Partial-duration flood-frequency analyses of gaging-station data and regional regression flood-frequency analyses are used as appropriate for estimating entrainment potential at individual sites.

- Three sites, North Llano River near Junction, Johnson Fork at Lowlands Crossing, and Llano River near Junction, are at or very close to gaging stations and, therefore, are appropriate for use of partial-duration flood-frequency analyses.

- Two sites, South Llano River at South Llano River State Park and South Llano River at Texas Tech University–Junction, have drainage areas and watershed slopes similar to North Llano River near Junction, thus the partial-duration flood-frequency analysis for the North Llano River near Junction gage is applicable for those sites.

- One site, Llano River near Ivy Chapel, occurs between the Llano River near Junction and the Llano River near Mason. For that site, a drainage-area ratio of the Llano River near Junction and Llano River near Mason gages is used to estimate flood frequency.

- Four sites, South Llano River at Baker Ranch, South Llano River at U.S. Highway 377 near Rocksprings, South Llano River at 700 Springs Ranch, and North Llano River near Roosevelt, have drainage areas or watershed slopes that are not similar to those of available gaging stations and, therefore, are appropriate for use of regional regression flood-frequency analyses.

Tables 13 and 14 show the return periods of the discharges responsible for initial and complete entrainment of bed material, based on site-by-site assessments and generalized channel slope and particle size, respectively. No values indicate that the hydraulic radius necessary to entrain bed material exceeded the vertical extent of the available cross-sectional geometric data.

The return periods for initial and complete bed-material entrainment vary greatly. In general, the return period for entrainment decreases with downstream distance, both as a function of particle size and the method used to compute flood frequency. As particle size gradually decreases with downstream distance, the shear stress necessary to entrain bed material decreases. The most influential factor in the observed decrease, however, is the method used to determine flood frequency. As mentioned previously, the regional regression method underestimates peak streamflow in the study area and, therefore, the streamflow necessary to entrain material is predicted to occur less frequently than at sites for which flood frequency was computed using the partial-duration series. The most accurate estimates of return periods for bed-material entrainment are for sites that use the partial-duration flood-frequency analyses.

It is emphasized that the computation of critical shear stress, streamflow, and return periods for bed-material entrainment only serve as a predictive model for bed-material entrainment in the study area. The model indicates that bed material is more likely to be entrained as particle size decreases and channel slope and hydraulic radius increase, essentially as resistance decreases and hydraulic energy increases. The applicability of the model is increased, at the expense of a reduction in accuracy, by associating hydraulic radius with a measured cross-sectional area and a user-defined Manning's n to compute the streamflow necessary for bed-material entrainment, and then by associating that streamflow with a flood-frequency model. The final results provide limited guidance in prediction of bed-material entrainment in the study area, but some interpretations can be gleaned.

First, the frequency of bed-material entrainment generally increases with downstream distance as a result of decreasing particle size and increased flood magnitudes. Second, an average of 1 year occurs between flows that initially entrain bed material as large as the median particle size, and an average of 1.5 years occurs between flows that completely entrain bed material as large as the median particle size. The return periods tend to match qualitative observations in the study area. Floods and bed-material entrainment are not uniformly distributed through time. Floods and associated bed-material entrainment frequently occur with decreased intervals of time between them during wet periods; and they occur less frequently during relatively normal to dry periods. The frequent entrainment of cobble- and gravel-sized bed material underscores the difficulties TxDOT faces with maintenance of LWCs in the study area.

Table 11. Froude numbers of initial and complete bed-material entrainment at sites with particle-size data, Edwards and Kimble Counties, Texas, for site-by-site analyses.

[F, Froude number; d_{16}, d_{50}, and d_{84}, descriptors that represent diameters at which 16, 50, and 84 percent, respectively, of the sample is finer than; initial, initial entrainment; complete, complete entrainment]

Study site number (fig. 2)	Study site	Cross section	F (initial d_{16})	F (initial d_{50})	F (initial d_{84})	F (complete d_{16})	F (complete d_{50})	F (complete d_{84})
1	North Llano River near Roosevelt	2	0.36	0.39	0.42	0.41	0.44	0.48
		3	.38	.43	.47	.43	.48	.53
2	North Llano River near Junction	0	.34	.39	.44	.38	.44	.50
		2	.42	.47	.53	.47	.53	.59
		3	.40	.44	.49	.45	.49	.55
3	South Llano River at Baker Ranch	3	.46	.51	.57	.52	.58	.64
4	South Llano River at U.S. Highway 377 near Rocksprings	1	.53	.57	.61	.60	.64	.69
5	South Llano River at 700 Springs Ranch	1	.36	.39	.41	.40	.43	.47
		2	.37	.43	.47	.42	.48	.53
		3	.41	.45	.49	.46	.50	.55
7	South Llano River at South Llano River State Park	1	.26	.30	.34	.29	.34	.38
		3	.26	.30	.34	.30	.34	.39
8	South Llano River at Texas Tech University–Junction	1	.22	.25	.28	.24	.28	.32
		2	.23	.26	.30	.26	.29	.34
		3	.22	.25	.29	.25	.28	.33
12	Johnson Fork at Lowlands Crossing	1	.43	.56	.65	.49	.63	.73
		2	.48	.56	.64	.54	.63	.72
		3	.50	.58	.67	.56	.65	.75
13	Llano River near Junction	2	.48	.53	.60	.54	.59	.67
		3	.54	.63	.76	.61	.70	.85
14	Llano River near Ivy Chapel	2	.33	.39	.44	.37	.44	.49
		3	.34	.38	.42	.38	.42	.47

Table 12. Froude numbers of initial and complete bed-material entrainment at sites with particle-size data, Edwards and Kimble Counties, Texas, using average-condition approach based on median channel slope, downstream decrease of particle size, and median Manning's *n*.

[F, Froude number; d_{16}, d_{50}, and d_{84}, descriptors that represent diameters at which 16, 50, and 84 percent, respectively, of the sample is finer than; initial, initial entrainment; complete, complete entrainment]

Study site number (fig. 2)	Study site	Cross section	F (initial d_{16})	F (initial d_{50})	F (initial d_{84})	F (complete d_{16})	F (complete d_{50})	F (complete d_{84})
1	North Llano River near Roosevelt	2	0.37	0.41	0.45	0.41	0.46	0.51
		3	.37	.41	.45	.41	.46	.51
2	North Llano River near Junction	0	.35	.40	.44	.40	.45	.50
		2	.35	.40	.44	.40	.45	.50
		3	.35	.40	.44	.40	.45	.50
3	South Llano River at Baker Ranch	3	.38	.42	.46	.42	.47	.51
4	South Llano River at U.S. Highway 377 near Rocksprings	1	.36	.41	.45	.41	.46	.50
5	South Llano River at 700 Springs Ranch	1	.36	.40	.45	.40	.45	.50
		2	.36	.40	.45	.40	.45	.50
		3	.36	.40	.45	.40	.45	.50
7	South Llano River at South Llano River State Park	1	.35	.39	.44	.39	.44	.49
		3	.35	.39	.44	.39	.44	.49
8	South Llano River at Texas Tech University–Junction	1	.34	.39	.44	.39	.44	.49
		2	.34	.39	.44	.39	.44	.49
		3	.34	.39	.44	.39	.44	.49
12	Johnson Fork at Lowlands Crossing	1	.37	.41	.45	.41	.46	.51
		2	.37	.41	.45	.41	.46	.51
		3	.37	.41	.45	.41	.46	.51
13	Llano River near Junction	2	.34	.38	.44	.38	.43	.49
		3	.34	.38	.44	.38	.43	.49
14	Llano River near Ivy Chapel	2	.33	.38	.43	.37	.42	.48
		3	.33	.38	.43	.37	.42	.48

Table 13. Approximate return periods for initial and complete bed-material entrainment at sites with particle-size data, Edwards and Kimble Counties, Texas, based on site-by-site individual measurements or estimates.

[d_{16}, d_{50}, and d_{84}, descriptors that represent diameters at which 16, 50, and 84 percent, respectively, of the sample is finer than; yr, years; >, greater than; --, cross-sectional area not possible to compute with available geometric data; <, less than]

Study site number (fig. 2)	Study site	Cross section	Return period for initial entrainment of d_{16} (yr)	Return period for initial entrainment of d_{50} (yr)	Return period for initial entrainment of d_{84} (yr)	Return period for complete entrainment of d_{16} (yr)	Return period for complete entrainment of d_{50} (yr)	Return period for complete entrainment of d_{84} (yr)
1	North Llano River near Roosevelt	2	<1	<1.5	3.1	2.1	4.4	44
		3	<1	<1.5	18	4.8	26	>100
2	North Llano River near Junction[a]	0	<1	<1	<1	<1	<1	1.2
		2	<1	<1	1.3	<1	1.3	3.5
		3	<1	<1	<1	<1	<1	1.3
3	South Llano River at Baker Ranch	3	14	>100	--	>100	--	--
4	South Llano River at U.S. Highway 377 near Rocksprings	1	3.7	10	46	24	>100	>100
5	South Llano River at 700 Springs Ranch	1	9.8	98	>100	>100	>100	--
		2	1.8	33	>100	21	>100	--
		3	11	>100	>100	>100	>100	--
7	South Llano River at South Llano River State Park	1	<1	1.2	5.7	<1	5.8	>100
		3	<1	1.2	4.4	1.1	3.2	--
8	South Llano River at Texas Tech University–Junction	1	<1	2.9	>100	1.8	>100	--
		2	1.2	4.7	--	4.7	--	--
		3	<1	3.4	--	1.7	--	--
12	Johnson Fork at Lowlands Crossing	1	<1	<1	2.2	<1	1.8	3.1
		2	<1	1.0	2.1	<1	2.0	3.2
		3	<1	<1	2.3	<1	2.2	4.0
13	Llano River near Junction[1]	2	<1	<1	<1	<1	<1	<1
		3	<1	<1	1.1	<1	<1	2.5
14	Llano River near Ivy Chapel	2	<1	<1	1.5	<1	1.4	6.6
		3	<1	<1	1.1	<1	1.2	3.5

[1] Partial-duration flood-frequency site.

Table 14. Approximate return periods for initial and complete bed-material entrainment at sites with particle-size data, Edwards and Kimble Counties, Texas, based on median channel slope, downstream decrease of particle size, and median Manning's *n*.

[d_{16}, d_{50}, and d_{84}, descriptors that represent diameters at which 16, 50, and 84 percent, respectively, of the sample is finer than; yr, years; >, greater than; --, cross-sectional area not possible to compute with available geometric data; <, less than]

Study site number (fig. 2)	Study site	Cross section	Return period for initial entrainment of d_{16} (yr)	Return period for initial entrainment of d_{50} (yr)	Return period for initial entrainment of d_{84} (yr)	Return period for complete entrainment of d_{16} (yr)	Return period for complete entrainment of d_{50} (yr)	Return period for complete entrainment of d_{84} yr)
1	North Llano River near Roosevelt	2	<1	<1.5	3.5	2.1	4.8	65
		3	<1	<1.5	23	5.7	36	>100
2	North Llano River near Junction[1]	0	<1	<1	<1	<1	<1	1.5
		2	<1	<1	1.3	<1	1.4	3.9
		3	<1	<1	<1	<1	<1	1.7
3	South Llano River at Baker Ranch	3	10	>100	>100	>100	--	--
4	South Llano River at U.S. Highway 377 near Rocksprings	1	1.8	6.5	50	7.5	73	>100
5	South Llano River at 700 Springs Ranch	1	5.1	42	>100	>100	>100	--
		2	1.5	18	>100	15	>100	--
		3	5.2	37	>100	50	>100	--
7	South Llano River at South Llano River State Park	1	<1	1.2	7.1	<1	7.0	>100
		3	<1	1.3	4.6	1.2	3.6	--
8	South Llano River at Texas Tech University–Junction	1	<1	2.7	>100	1.9	>100	--
		2	1.1	3.8	--	3.7	--	--
		3	<1	3.0	--	1.7	--	--
12	Johnson Fork at Lowlands Crossing	1	<1	<1	2.3	<1	2.0	3.5
		2	<1	1.5	2.2	<1	2.2	3.7
		3	<1	1.1	2.4	<1	2.4	4.3
13	Llano River near Junction[1]	2	<1	<1	<1	<1	<1	<1
		3	<1	<1	1.0	<1	<1	2.3
14	Llano River near Ivy Chapel	2	<1	<1	1.4	<1	1.3	5.7
		3	<1	<1	1.2	<1	1.2	3.8

[1] Partial-duration flood-frequency site.

Summary

The Texas Department of Transportation (TxDOT) spends considerable money for maintenance and replacement of low-water crossings (LWCs) of streams in the Edwards Plateau in Central Texas as a result of the transport of cobble- and gravel-sized bed material. TxDOT Research Project 0–4695 is focused on research of bed-material entrainment as related to LWC maintenance issues in the Edwards Plateau. This study was done by the U.S. Geological Survey (USGS), in cooperation with TxDOT, and in collaboration with Texas Tech University, Lamar University, and the University of Houston, to quantify the potential for bed-material entrainment in selected streams of the plateau in a study area comprising Edwards, Kimble, and Real Counties, Texas, and vicinity.

The study area contains a number of streams appropriate for bed-material entrainment research, including the Llano River, Frio River, Nueces River, and tributaries. The streams originate in relatively western and southern parts of the Edwards Plateau, an elevated lower-Cretaceous limestone and dolomite tableland. The streams in the study area are incised into the plateau, resulting in removal of considerable amounts of lower-Cretaceous carbonate rock. Climatic fluctuations during the last 20,000 years have resulted in periods of variable streamflow and associated sediment transport rates. Currently (2007), much of the alluvial material occurs as valley fill and bed material in the streams of the plateau.

The study sites primarily were chosen to characterize downstream changes in channel geometry and bed-material entrainment potential. For this reason, all detailed study sites are in the Llano River Basin, chosen because (1) most of the problematic LWCs identified by TxDOT personnel are located there and (2) it was desirable to analyze systematic downstream trends in bed-material entrainment potential without introducing drainage-basin variability.

Study sites range from ephemeral, bedrock, upper headwater channels to relatively wide, perennial channels occurring within Pleistocene and Holocene alluvial terraces and active floodplains. Other sites in the Frio and Nueces River Basins were visited and qualitatively examined for problems related to bed-material entrainment.

A variety of methods were used to obtain data necessary for computation of bed-material entrainment potential and included:

- GIS mapping software was used to delineate watersheds, determine drainage areas, and model watershed and channel slopes.
- Partial-duration flood-frequency analyses were done to determine the return periods of floods for USGS and Lower Colorado River Authority gaging stations in the study area. Regional regression equations were used to estimate flood frequency at ungaged study sites.
- Site reconnaissance was done with assistance from TxDOT personnel knowledgeable about the locations of sites with extreme bed-material mobility and damage to transportation infrastructure.
- Field surveys were designed to obtain the parameters needed to apply equations to compute bed-material entrainment potential. Field surveys included measurements of channel geometry, LWC geometry, and bed-material particle sizes.

Results indicate that the bed-material entrainment problem for TxDOT LWCs occurs at two spatial scales—watershed scale and channel-reach scale.

First, the relative abundance and activity of cobble- and gravel-sized bed material at a site can be attributed to watershed characteristics, specifically watershed slope. The relative abundance and activity of bed material along a given channel reach becomes greater with increasingly steeper watershed slopes, based on analyses of digital elevation models and qualitative observations made during field-reconnaissance trips to the study area.

Second, the stresses needed to mobilize bed material at a site can be attributed to reach-scale hydraulic factors. The propensity for initial and complete entrainment of bed material depends on cross-sectional geometry and particle size. Flood-frequency analyses are associated with computations of bed-material entrainment to estimate the frequency of bed-material entrainment. In general, the frequency of entrainment increases with downstream distance, as a result of decreasing particle size and increased flood magnitudes. An average of 1 year occurs between flows that initially entrain bed material as large as the median particle size (d_{50} [diameter at which 50 percent of the sample is finer]), and an average of 1.5 years occurs between flows that completely entrain bed material up to the median particle size (d_{50}). The Froude numbers associated with initial and complete entrainment of bed material as large as the median particle size (d_{50}) are about 0.40 and 0.45, respectively.

References Cited

Arcement, Jr., G.J., and Schneider, V.R., 1989, Guide for selecting Manning's roughness coefficients for natural channels and flood plains: U.S. Geological Survey Water-Supply Paper 2339, 38 p.

Asquith, W.H., and Slade, Jr., R.M., 1997, Regional equations for estimation of peak-streamflow frequency for natural basins in Texas: U.S. Geological Survey Water-Resources Investigations Report 96–4307, 68 p.

Baker, V.R., 1977, Stream-channel response to floods, with examples from central Texas: Geological Society of America Bulletin, v. 88, p. 1,057–1,071.

Beard, L.R., 1975, Generalized evaluation of flash-flood potential: University of Texas at Austin Center for Research in Water Resources Report CRWR–124, 95 p.

Blum, M.D., Toomey, R.S., III, and Valastro, Salvatore, Jr., 1994, Fluvial response to late Quaternary climatic and

environmental change, Edwards Plateau, Texas: Palaeogeography, Palaeoclimatology, Palaeoecology, v. 108, p. 1–21.

Blum, M.D., and Valastro, Salvatore, Jr., 1989, Response of the Pedernales River of Central Texas to late Holocene climatic change: Annals of the Association of American Geographers, v. 79, p. 435–456.

Blum, M.D., and Valastro, Salvatore, Jr., 1992, Quaternary stratigraphy and geoarchaeology of the Colorado and Concho Rivers, West Texas: Geoarchaeology, v. 7, p. 419–448.

Caran, S.C., and Baker, V.R., 1986, Flooding along the Balcones Escarpment, Central Texas, *in* Abbott, P.L., and Woodruff, Jr., C.M., eds., The Balcones Escarpment—Geology, hydrology, ecology, and social development in central Texas: Austin, Tex., Earth Enterprises, Inc., p. 1–14.

Cooke, M.J., Stern, L.A., Banner, J.L., Mack, L.E., Stafford, Jr., T.W., and Toomey, R.S., III, 2003, Precise timing and rate of massive late Quaternary soil denudation: Geology, v. 31, p. 853–856.

Elliott, J.G., 2002, Bed-material entrainment potential, Roaring Fork River at Basalt, Colorado: U.S. Geological Survey Water-Resources Investigations Report 02–4223, 33 p.

Geometrics, 2005, OhmMapper TR1—Operation manual: San Jose, Calif., 125 p.

Griffith, G.E., Bryce, S.A., Omernik, J.M., Comstock, J.A., Rogers, A.C., Harrison, B., Hatch, S.L., and Bezanson, D., 2004, Ecoregions of Texas [color poster]: Reston, Va., U.S. Geological Survey, map scale 1:2,500,000.

Gustavson, T.C., 1978, Bed forms and stratification types of modern gravel meander lobes, Nueces River, Texas: Sedimentology, v. 25, p. 401–426.

Heitmuller, F.T., Asquith, W.H., Fang, Xing, Thompson, D.B., and Wang, Keh-Han, 2005, Literature review for Texas Department of Transportation Research Project 0-4695—Guidance for design in areas of extreme bed-load mobility, Edwards Plateau, Texas: U.S. Geological Survey Open-File Report 2005–1234, 40 p.

Hosking, J.R.M., and Wallis, J.R., 1997, Regional frequency analysis: Cambridge, Cambridge University Press, 224 p.

Knighton, D., 1998, Fluvial forms and processes: London, Arnold, 383 p.

Komar, P.D., 1988, Sediment transport by floods, *in* Baker, V.R., Kochel, R.C., and Patton, P.C., eds., Flood geomorphology: New York, Wiley, p. 97–111.

Larkin, T.J., and Bomar, G.W., 1983, Climatic atlas of Texas: Austin, Tex., Texas Department of Water Resources, 151 p.

Lucius, J.E., Langer, W.H., and Ellefsen, K.J., 2007, An introduction to using surface geophysics to characterize sand and gravel deposits: U.S. Geological Survey Circular 1310, 33 p.

Maidment, D.R., ed., 2002, Arc Hydro—GIS for water resources: Redlands, Calif., ESRI Press, 203 p.

Mear, C.E., 1995, Quaternary geology of the upper Sabinal River valley, Uvalde and Bandera Counties, Texas: Geoarchaeology, v. 10, p. 457–480.

Powers, C.J., Wilson, J., Haeni, F.P., and Johnson, C.D., 1999, Surface-geophysical investigation of the University of Connecticut landfill, Storrs, Connecticut: U.S. Geological Survey Water-Resources Investigations Report 99–4211, 34 p.

R Development Core Team, 2004, R—A language and environment for statistical computing: Vienna, Austria, R Foundation for Statistical Computing, ISBN 3–900051–07–0, at *http://www.R-project.org*

Robert, A., 2003, River processes: London, Arnold, 214 p.

Shah, S.D., and Stanton, G.P., 2006, Two-dimensional resistivity investigation along West Fork Trinity River, Naval Air Station-Joint Reserve Base Carswell Field, Fort Worth, Texas, October 2004: U.S. Geological Survey Data Series 178, 24 p.

Shen, H.W., and Julien, P.Y., 1993, Erosion and sediment transport, *in* Maidment, D.A., ed., Handbook of hydrology, chap. 12: New York, McGraw-Hill, p. 12.1–61.

Shields, A., 1936, Application of similarity principles and turbulence research to bedload movement, *translated from* Anwendung der Aehnlichkeitsmechanik und der Turbulenzforschung auf die Geschiebewegung: Mitteilung Preussischen Versuchanstalt für Wasserbau und Schiffbau, Berlin, No. 26, by W.P. Ott and J.C. van Uchelen, California Institute of Technology Hydrodynamics, Pasadena, Calif., Report No. 167, 43 p.

Soong, D.T., Ishii, A.L., Sharpe, J.B., and Avery, C.F., 2004, Estimating flood-peak discharge magnitudes and frequencies for rural streams in Illinois: U.S. Geological Survey Scientific Investigations Report 2004–5103, 158 p.

Stedinger, J.R., Vogel, R.M., and Foufoula-Georgiou, Efi, 1993, Frequency analysis of extreme events, *in* Maidment, D.A., ed., Handbook of hydrology, chap. 18: New York, McGraw-Hill, p. 18.1–66.

Sturm, T.W., 2001, Open channel hydraulics: New York, McGraw-Hill, 493 p.

U.S. Army Corps of Engineers, 1995, Engineering and design, geophysical exploration for engineering and environmental investigations—Electrical and electromagnetic methods: Engineering Manual 1110–1–1802, chap. 4, 57 p.

U.S. Department of Agriculture Forest Service, 2005, WinXSPRO version 3.0: at *http://www.stream.fs.fed.us/publications/winxspro.html*

U.S. Geological Survey, 2005, Earth Resources Observation and Science (EROS), Seamless Data Distribution System, accessed September 19, 2005, a *http://seamless.usgs.gov*

U.S. Geological Survey, 2006, National Hydrography Dataset, accessed May 2, 2006, at *http://nhd.usgs.gov*

U.S. Geological Survey, 2007, Water resources data for the United States, water year 2006: U.S. Geological Survey Water-Data Report WDR–US–2006: at *http://wdr.water.usgs.gov/wy2006/search.jsp*

Wolman, M.G., 1954, A method for sampling coarse bed material: Transactions of the American Geophysical Union, v. 35, p. 951–956.

Appendix 1—Selected Photographs of Sites and Low-Water Crossings in Edwards, Kimble, and Real Counties, Texas

Blank Page

Figure 1.1. Downstream end of culvert pipes at Ben Williams Crossing of the Nueces River on Ranch Road 335. Many of the culverts are clogged with cobbles and gravel.

Figure 1.2. Ben Williams Crossing of the Nueces River on Ranch Road 335.

Figure 1.3. View downstream from damaged low-water crossing of Cedar Creek at Ranch Road 336 following June 2004 flood.

Figure 1.4. Upper Ranch Road 1120 crossing of the Frio River following the peak of the June 2004 flood.

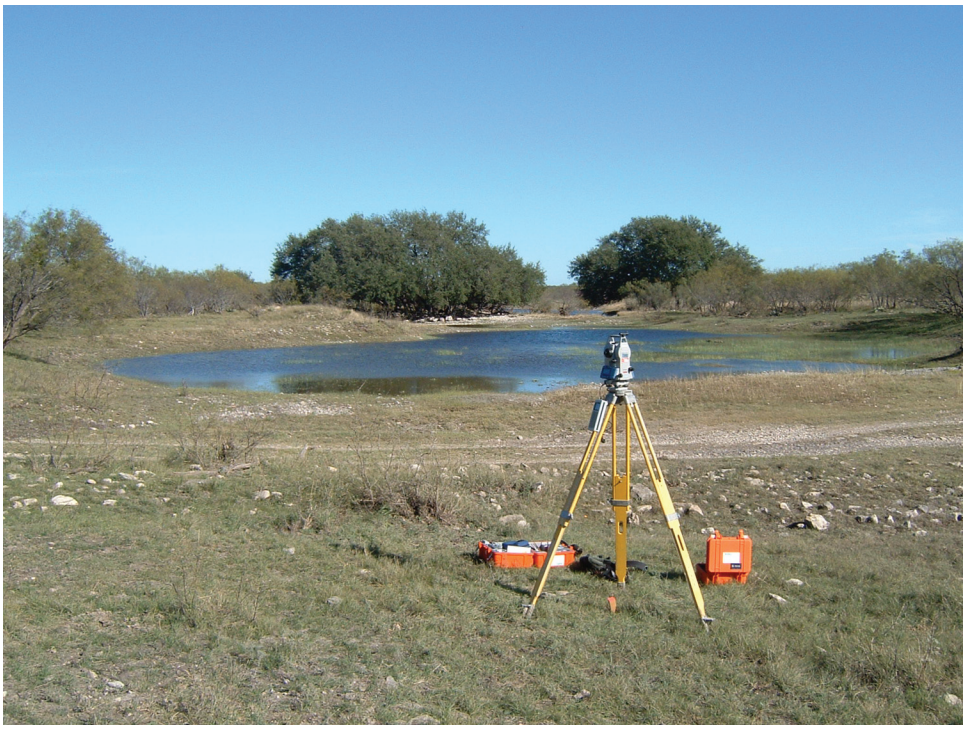

Figure 1.5. View downstream from cross section 2 of South Llano River at Baker Ranch.

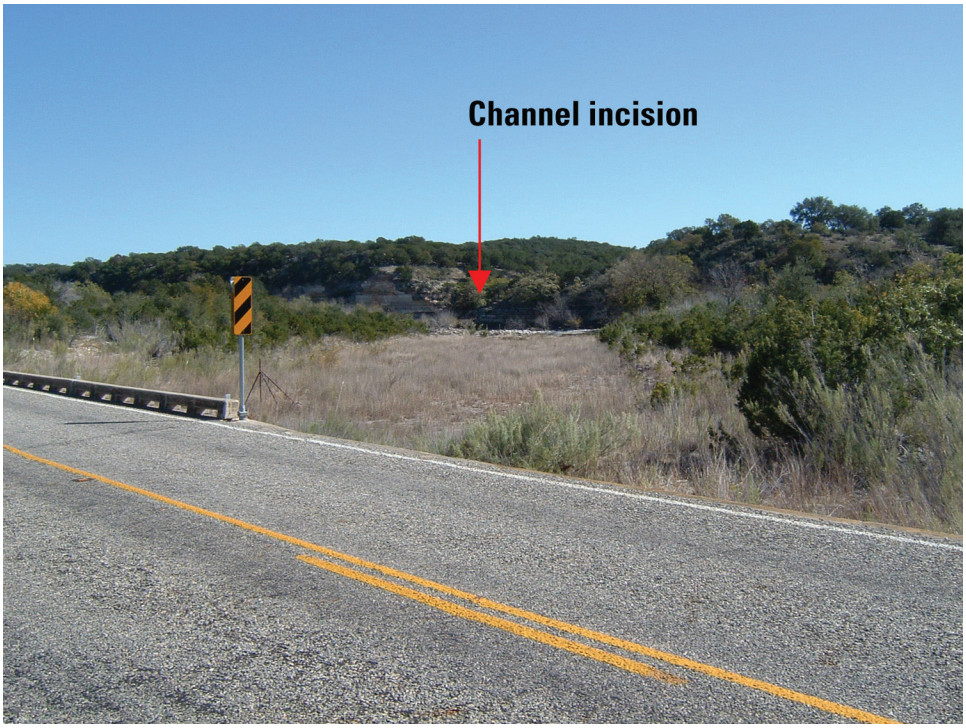

Figure 1.6. View downstream from the South Llano River at U.S. Highway 377 near Rocksprings. Notice the depth of channel incision into the Edwards Plateau on the right bank.

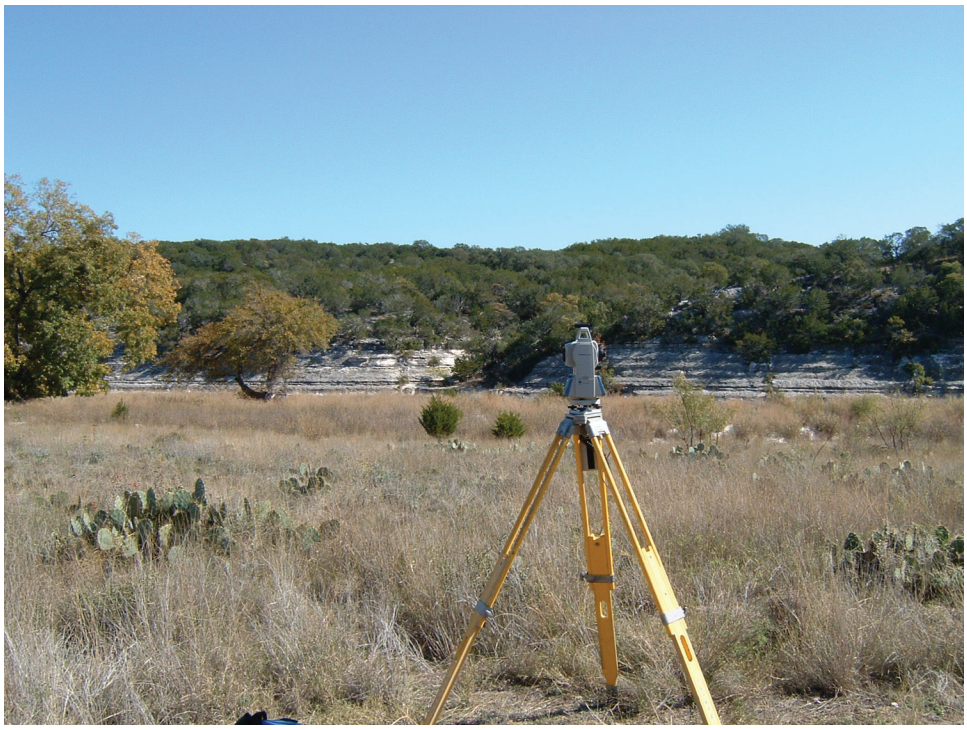

Figure 1.7. View across the floodplain of the South Llano River at 700 Springs Ranch at cross section 2. The depth of incision into the Edwards Plateau is greater than that at South Llano River at U.S. Highway 377 near Rocksprings.

Figure 1.8. First Crossing of the South Llano River along U.S. Highway 377 in Kimble County.

Figure 1.9. View upstream from the South Llano River at South Llano River State Park near cross section 1.

Figure 1.10. View across the channel and channel bar of South Llano River at Texas Tech University–Junction at cross section 3.

Figure 1.11. Cobble and gravel lenses within relatively fine-grained Holocene floodplain deposits in bank of South Llano River at Texas Tech University–Junction.

Figure 1.12. View across the South Llano River at Texas Tech University–Junction toward vegetated Holocene floodplain.

Figure 1.13. View across a gravel bar and floodplain of North Llano River near Roosevelt at cross section 3.

Figure 1.14. View across a cobble and gravel bar of North Llano River near Junction at cross section 1.

Figure 1.15. View upstream from Johnson Fork at Lowlands Crossing at cross section 2.

Figure 1.16. View across the channel and low-water crossing of Johnson Fork at Guzman Crossing.

Figure 1.17. View upstream from Johnson Fork at Paks Crossing.

Figure 1.18. View of the bedrock channel bed of Llano River near Junction at cross section 1.

Figure 1.19. View across Llano River near Junction at cross section 3. Notice the downstream imbrication of boulders of the channel bar deposit.

Figure 1.20. View across Llano River near Junction at cross section 2.

Figure 1.21. View downstream from Llano River near Ivy Chapel at cross section 2.

Figure 1.22. View upstream from Llano River near Ivy Chapel at cross section 3.

Figure 1.23. Reconstruction of Ranch Road 337 low-water crossing of the Frio River near Leakey, December 2004.

Appendix 2—Two-Dimensional Geophysical Resistivity Investigation

Blank Page

Two-dimensional (2-D) geophysical resistivity investigations were made at Johnson Fork at Lowlands Crossing and Nueces River at Ben Williams Crossing. The resistivity surveys were done to understand the composition of bed material with depth beneath the surface, but results were limited and not directly applicable to computations of bed-material entrainment.

2D resistivity surveys were made at Ben Williams Crossing of the Nueces River on the Edwards and Real County line and Lowlands Crossing of Johnson Fork in Kimble County. Surface and geophysical methods provide a relatively fast and inexpensive means to characterize the subsurface of channel beds (Powers and others, 1999). Electrical surface-geophysical methods can be used to detect variations in the electrical properties of the subsurface. The electrical properties of soil and rock are controlled by water content, salt content, porosity, and the presence of metallic minerals. Variations in the electrical properties of soils and rocks, either vertically or horizontally, produce variations in the electrical signatures measured by surface geophysical tools (Shah and Stanton, 2006). Changes in the received signal can be related to changes in the composition, extent, and physical properties of subsurface soil and rock, to the extent that differences in lithology or rock type are accompanied by differences in resistivity (U.S. Army Corps of Engineers, 1995). According to Lucius and others (2007), dry sand- and gravel-deposits have high resistivity (200 ohm-meters [ohm-m] or more), and saturated sand- and gravel-deposits are characterized by low resistivity (50 ohm-m or less). Carbonate bedrock also is characterized by high resistivity, and commonly is greater than 1,000 ohm-m. Specifically, the Geometrics OhmMapper TR5, a mobile resistivity measuring system, was used to complete the survey. The OhmMapper TR5 is a capacitively coupled instrument that measures apparent resistivity of the earth using antennas in a dipole-dipole array (Geometrics, 2005).

The data for two resistivity profiles traversing Johnson Fork at Lowlands Crossing (fig. 32) and Nueces River at Ben Williams Crossing (fig. 2.1) are described and graphically presented in the form of 2D sections that show contoured resistivity in gradational colors (fig. 2.2). The two resistivity sections are shown in figure 2.2 at a common resistivity scale.

Line 1 (fig. 2.2A), at Johnson Fork, traverses northwest to southeast toward Ranch Road 2169, aligned roughly parallel to the channel. Line 1 shows five distinct pockets of higher resistivity throughout the section at similar depths. At the mid-to-western end of the line are three pockets of relatively high resistivity (1,500 to 2,000 ohm-m) that extend to about 0.9 to 1.8 meters (3 to 6 feet) below the surface. The remaining two pockets of high resistivity range from about 1,000 to 1,300 ohm-m. The remainder of the section shows a relatively lower resistivity (higher conductivity) range from about 100 to 800 ohm-m.

Line 2 (fig. 2.2B) is perpendicular to the Nueces River at Ben Williams Crossing. The capacitively-coupled data were collected at a shallower depth than in line 1 probably because of a more conductive environment. Line 2 shows a pattern of high resistivity (greater than 1,000 ohm-m) close to the surface throughout the section. Most of these resistivity zones start at the surface and extend to a depth of approximately 1.5 meters (5 feet). Highest resistivity occurs in two small zones about 0.5 to 0.9 meters (1.5 to 3 feet) below the surface near the southeastern end of the line.

To accurately interpret these data, more ground-truthing data, such as well construction, lithologic, or borehole geophysical logs are needed. Also, additional surface-geophysical methods such as direct-current resistivity or time-domain electromagnetic techniques (Lucius and others, 2007) could penetrate deeper below land surface. The minimal variations in the sections were not sufficient to identify the content of the interstitial space between coarse alluvial particles. With appropriate verification using complementary methods, high conductivity (low resistivity) at the surveyed crossings could indicate the presence of either clay or water in the interstitial space, as opposed to sand or air, which can affect channel-substrate stability at low-water crossings.

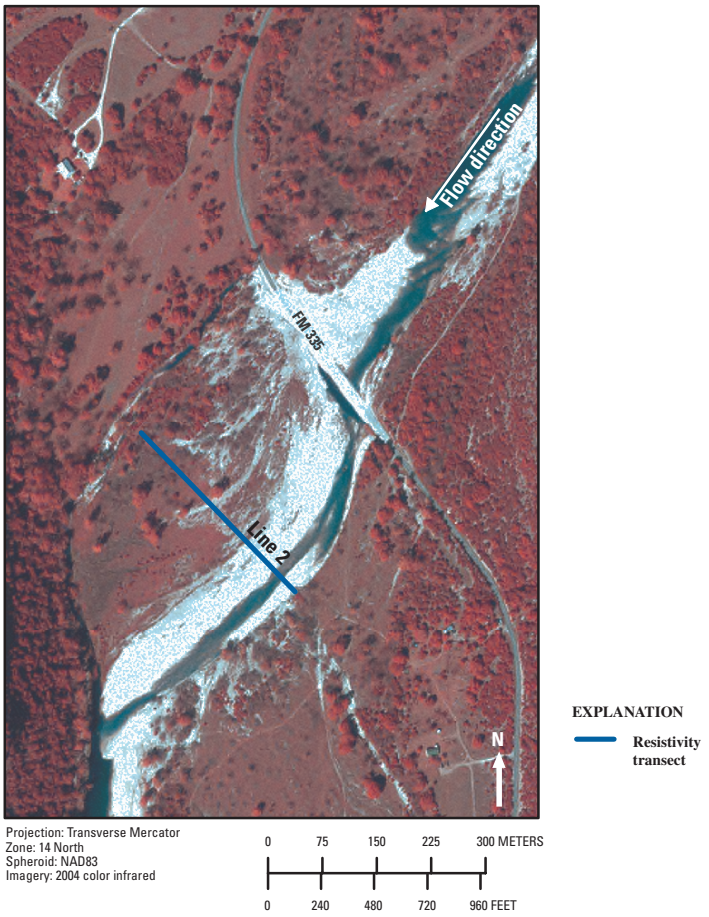

Figure 2.1. Channel resistivity transect at Nueces River at Ben Williams Crossing (see fig. 2 for site location), Edwards-Real County line, Texas.

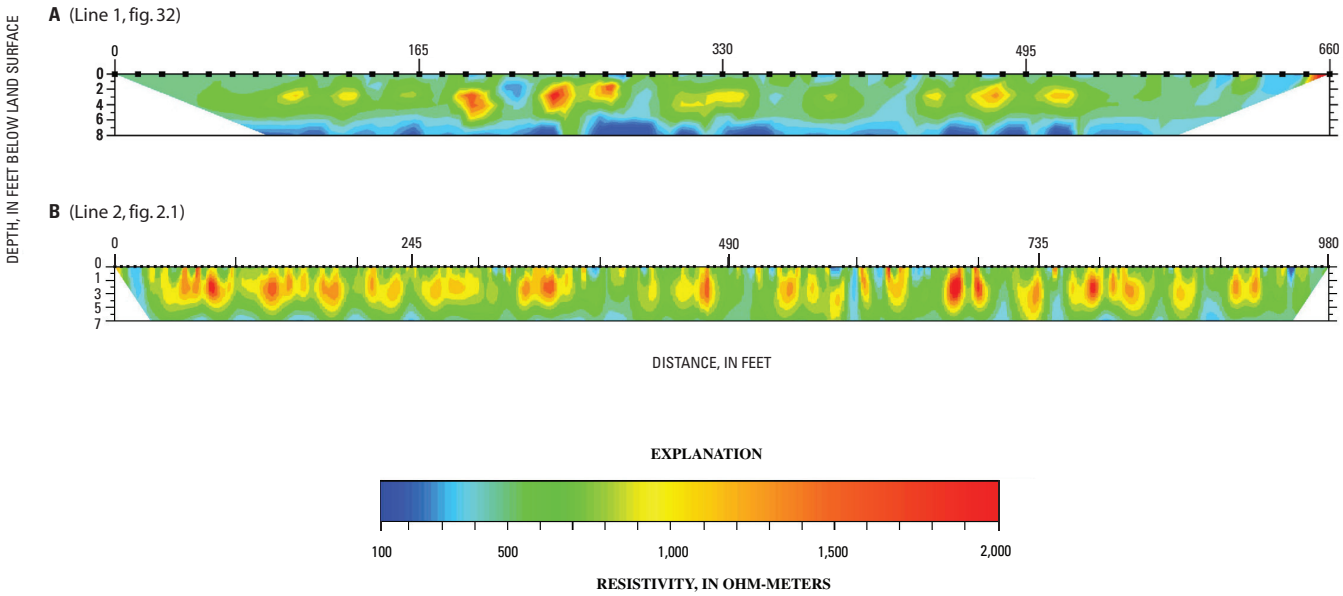

Figure 2.2. Field results of capacitively-coupled data (actual resistivity) at common resistivity scale for (A) Johnson Fork at Lowlands Crossing and (B) Nueces River at Ben Williams Crossing.

Publishing support provided by
Lafayette Publishing Service Center

Information regarding water resources in Texas is available at
http: //tx.usgs.gov/